

**Design, Development, and Evaluation of Wearable Length
Fastening Devices for Use with Twisted Coiled Actuators**

**A THESIS
SUBMITTED TO THE FACULTY OF THE GRADUATE SCHOOL
OF THE UNIVERSITY OF MINNESOTA
BY**

Timothy Dorn

**IN PARTIAL FULFILLMENT OF THE REQUIREMENTS
FOR THE DEGREE OF
MASTER OF SCIENCE**

Advisor: Prof. Brad Holschuh

April, 2023

© Timothy Dorn 2023
ALL RIGHTS RESERVED

Acknowledgements

The author would like to thank Doctor Brad Halschuh for advising on this project. Additionally, the author would like to thank Doctor Lucy Dunne and Doctor William Durfee for serving as committee members and providing their insights.

Abstract

Artificial muscles and compliant, large stroke linear actuators have enabled new classes of wearable robotics. However, these actuators are inefficient, needing constant power to maintain force and displacement, decreasing their utility in wearable systems. Variable length latching mechanisms alleviate this problem, matching actuator displacement, and holding force and displacement constant when the actuator is powered off. However, most existing latching designs are either not wearable, or must be disengaged manually, limiting their robotic applications. In this research, three wearable and remotely releasable latching mechanisms were designed for use in wearable robotic systems: a stepper motor with a belt and pulley; a linear ratchet; and a cam cleat. The designs were manufactured and tested, with all three designs maintaining force and displacement values up to 15N of cable tension and releasable up to 5N of cable tension. These results demonstrate the viability of integrating latches into soft wearable robotic systems.

Contents

Acknowledgements	i
Abstract	ii
List of Tables	vi
List of Figures	viii
1 Introduction	1
1.1 Background	2
1.2 Problem Formulation	3
2 Related Works	5
2.1 Soft Robotics	5
2.2 Wearable Robotics	6
2.3 Wearable Soft Actuators	6
2.3.1 Cable or Tendon Actuators	7
2.3.2 Fluidic Actuators	8
2.3.3 Shape Changing Actuators	8
2.4 Twisted Coiled Actuators	9
2.5 Latching Devices	10
2.5.1 Buckles	10
2.5.2 Motors and Disk Brakes	11
2.5.3 Ratchets and Cable Ties	11
2.5.4 Rope Traversal	12

2.6 State of the Art	14
3 Design	15
3.1 Latch Wearability and Integration	15
3.2 Latch Designs	19
3.2.1 Motor Brake Design	19
3.2.2 Linear Ratchet Design	22
3.2.3 Toothed Cam Design	24
3.3 Latch Dimensions Summary	28
4 Methods	29
4.1 Objective	29
4.2 Apparatus	29
4.3 Experimental Setup	30
4.3.1 Tightening Latch Speed and Drag	32
4.3.2 Static Hold	33
4.3.3 Latch Release Under Tension	33
4.3.4 Displacement Characterization of Ratchet	34
4.3.5 Characterization of Latch Release Forces For Ratchet and Cam Designs	34
4.3.6 Cable Characterization	35
4.4 Experimental Parameters	37
5 Experimental Results	39
5.1 Latch Tightening and Engagement	39
5.1.1 Causes of Strain	41
5.2 Latch Holding	49
5.3 Latching Release	66
5.4 Cable Friction	71
6 Discussion	73
6.1 Latch Tightening and Engagement	73
6.2 Latch Holding	76

6.2.1	Motor Latch	77
6.2.2	Ratchet Latch	77
6.2.3	Cam Latch	78
6.2.4	Hoop Pressure	79
6.3	Latching Release	79
6.4	Wearability	80
6.4.1	Ratchet Latch	81
6.4.2	Cam Latch	82
6.4.3	Dynamic Systems	83
6.5	Manufacturability and Cost	84
6.5.1	Motor Latch	84
6.5.2	Ratchet Latch	84
6.5.3	Cam Latch	85
6.6	Summary	85
6.7	Potential Improvements and Limitations	89
7	Conclusion and Future Work	91
References		94
Appendix A.	Motor Latch Design Schematics	103
Appendix B.	Ratchet Latch Design Schematics	113
Appendix C.	Cam Latch Design Schematics	120

List of Tables

3.1	Latch dimensions and masses.	28
3.2	Cable cross sectional areas, widths, and minimum bend radii.	28
4.1	Power characteristics of the stepper motor and linear actuator. Charge and time were calculated using a 9V Energizer Industrial battery [68]. . .	38
4.2	Average circumferences of various body parts likely to be used as mounting locations for wearable applications [69, 70].	38
5.1	Velocity and drag forces for each latch. Drag force is positive in the direction opposite to the direction of cable displacement.	40
5.2	Cable yield stress in megapascals.	48
5.3	Results of 10 minute tensioned hold experiment for the unpowered motor configuration. Measured values of tensile force as measured by the tensile testing machine are shown for values of peak force, force measured six (6) seconds after peak force, 60 seconds after peak force, and the final force measured at ten minutes (600 seconds) after peak force. The percent of force lost relative to the peak force measured is also shown.	53
5.4	Unpowered motor configuration cable stress measurements for six (6) seconds after peak stress, 60 seconds after peak stress, and the final stress measured at ten minutes (600 seconds) after peak stress.	54
5.5	Results of 10 minute tensioned hold experiment for the powered motor configuration. Measured values of tensile force as measured by the tensile testing machine are shown for values of peak force, force measured six (6) seconds after peak force, 60 seconds after peak force, and the final force measured at ten minutes (600 seconds) after peak force. The percent of force lost relative to the peak force measured is also shown.	56

5.6	Powered motor configuration cable stress measurements for six (6) seconds after peak stress, 60 seconds after peak stress, and the final stress measured at ten minutes (600 seconds) after peak stress.	57
5.7	Results of 10 minute tensioned hold experiment for the ratchet design. Measured values of tensile force as measured by the tensile testing machine are shown for values of peak force, force measured six (6) seconds after peak force, 60 seconds after peak force, and the final force measured at ten minutes (600 seconds) after peak force. The percent of force lost relative to the peak force measured is also shown.	59
5.8	Ratchet design cable stress measurements for six (6) seconds after peak stress, 60 seconds after peak stress, and the final stress measured at ten minutes (600 seconds) after peak stress.	59
5.9	Results of 10 minute tensioned hold experiment for the cam design. Measured values of tensile force as measured by the tensile testing machine are shown for values of peak force, force measured six (6) seconds after peak force, 60 seconds after peak force, and the final force measured at ten minutes (600 seconds) after peak force. The percent of force lost relative to the peak force measured is also shown.	60
5.10	Cam design cable stress measurements for six (6) seconds after peak stress, 60 seconds after peak stress, and the final stress measured at ten minutes (600 seconds) after peak stress.	60
5.11	Time taken for each latch to reduce cable tension to below 10% of initial tension.	70
5.12	Static friction of each cable against a polyester fabric sheet.	72

List of Figures

2.1	Various soft actuator actuation methods. a) Actuation displacement of twisted spring system [28]. Adapted from Palli, G. et al. b) McKibben pneumatic artificial muscle [29]. c) Schematic of linear multi-chamber pneumatic artificial muscles. d) Schematic of dielectric elastomer membrane before and after voltage activation [30]. Adapted from Novelli, G. et al. e) Monolithic stacked dielectric elastomer schematic. Adapted from Shintake, J et al [31]. f) Molecular diagram of Austenite-Martensite phase transformation. Adapted from Jackson, C et al [32].	7
2.2	Diagram of the actuation mechanics of TCAs.	9
2.3	A variety of latching methods and mechanisms. a) Schematic of a buckle, commonly seen on backpacks and luggage [47]. b) Chain and sprocket linear system [48]. c) Bidirectional circular ratchet used in a wrench [49].	11
2.4	A variety of latching methods and mechanisms. a) Motorized rope ascender [52]. b) Cam cleat with dual directional latching [53]. c) Uni-directional cam cleat [54]. d) Manual rope ascender with spring-loaded toothed cam [55]. e) Cable tie with hinged locking arm [56].	12
2.5	Existing wearable latching research and designs. a) Wearable, self-locking SMA actuated latch. Reproduced with permission from Holschuh, B [46]. b) Wearable latching mechanism for use with active compression garments. Reproduced with permission from C. Hansen et al [58]. c) Automatic lacing system for use in athletic footwear [50]. d) Reproduced with permission from M. Clarke et al [57]. e) Watch with dynamic fit adjustable wristband [60].	13
3.1	The metal snap fasteners used for attaching each latch.	16

3.2	Latch and TCA in a serial integration configuration.	17
3.3	Latch and TCA in a parallel integration configuration.	18
3.4	Overview of motor design operational concepts. a) Model of full motor latch design with motor cable. b) Model of motor latch design with transparent latch body. Individual components and their interactions can be seen. c) Simplified motor model with only the stepper motor, belt, and pulley visible. d) Diagram of interactions between the stepper motor, belt, and pulley. The rotation of the stepper motor axle causes the pulley to rotate. The teeth of the pulley then engage with the teeth of the belt causing a linear movement of the belt.	20
3.5	Motor design exploded view.	21
3.6	Completed motor design assembly.	21
3.7	Chloroprene rubber with fiberglass reinforcements toothed belt.	21
3.8	Overview of ratchet design operational concepts. a) Model of latch body with cable in the latch. b) Diagram of ratchet teeth while in the latched position. The cable is prevented from moving to the left due to the ratchet teeth engaging with the grooves of the cable. c) Diagram of ratchet teeth in the tightening position. The teeth are partially depressed by the cable as the cable moves to the right. d) Diagram of ratchet teeth when fully depressed by the cable during tightening as the cable moves further to the right. e) Model of linear actuator placed in the latch body. The actuator is in its passive state and not applying pressure to the lever release arm. f) Model of interaction between the linear actuator and the lever release arm during disengagement. The active linear actuator is pressing the lever arm into the disengaged position which moves the teeth down and out of the way of the cable.	23
3.9	Ratchet design exploded view.	24
3.10	Completed ratchet latch assembly.	25
3.11	Nylon-66 grooved cable tie cable.	25

3.12 Overview of cam design operational concepts. a) Model of latch body with cover removed. b) Model of cam latch with cable in the tightening position. c) Model of cam latch in the latched position. The teeth of the cam are engaged with the rope preventing it from moving. d) Model of cam latch with the linear actuator pressing against the lever arm of the cam to disengage the cam teeth from the cable.	26
3.13 Cam design exploded view.	27
3.14 Completed cam latch assembly.	27
3.15 Polypropylene rope used with cam latch design.	27
4.1 Ratchet latch clamped into tensile testing machine.	30
4.2 Experimental setup diagram of latch and cable configuration within the tensile testing machine.	30
4.3 Overview of the different experiments performed on each latch and the range of forces that were used for each experiment. The colored squares indicate whether a latch was tested in an experiment and for what force.	31
4.4 The forces on an inclined plane which can be used to derive the coefficient of static friction.	35
4.5 Diagram of the relevant parameters for calculating circumferential pressure on a cylinder.	36
5.1 Relationship between strain and force for each latch configuration.	41
5.2 Relationship between strain and force for each latch configuration for 1 to 15 N.	42
5.3 Relationship between strain and stress for each latch configuration.	42
5.4 Characterization of teeth engagement for the ratchet design. The green Instron machine measurements represent the theoretical perfect displacement response, while the gray line represents the ratchet designs actual engagement response	44
5.5 Comparison of cam rotations before and after cable engagement for the cam latch design.	45
5.6 The difference in displacement measurements taken above and below each latch for a range of target forces.	46

5.7	The difference in displacement measurements taken above and below each latch for a range of cable stresses.	47
5.8	Stress versus strain for each latch cable. The motor cable was a chloroprene rubber toothed timing belt with fiberglass reinforcements; the ratchet cable was a Nylon-66 grooved cable tie cable; the cam cable was a polypropylene braided yarn.	47
5.9	Failure characteristics of the unpowered configuration of the motor design represented by the blue data points. The green data points represent a similar test conducted with a target force of 50 N where the design did not exhibit any failure modes.	49
5.10	Failure characteristics of the ratchet design represented by the gray data points. The green data points represent a similar test conducted with a target force of 15 N where the design did not exhibit any failure modes.	50
5.11	Failure characteristics of the cam design represented by the yellow data points. The green data points represent a similar test conducted with a target force of 10 N where the design did not exhibit any failure modes.	51
5.12	Measurements of tensile force taken over 10 minutes for the unpowered motor latch (target forces between 1 and 15 Newtons).	52
5.13	Measurements of tensile force taken over 10 minutes for the unpowered motor latch (target forces between 20 and 60 Newtons).	52
5.14	Measurements of tensile force taken over 10 minutes for the powered motor latch (target forces between 1 and 15 Newtons).	55
5.15	Measurements of tensile force taken over 10 minutes for the powered motor latch (target forces between 20 and 60 Newtons).	55
5.16	Measurements of tensile force taken over 10 minutes for the ratchet latch (target forces between 1 and 15 Newtons).	58
5.17	Measurements of tensile force taken over 10 minutes for the cam latch (target forces between 1 and 15 Newtons).	58
5.18	The final tensile force measured after 10 minutes for each latch for target forces between 1 and 60 Newtons.	61
5.19	The final tensile force measured after 10 minutes for each latch for target forces between 1 and 15 Newtons.	62

5.20 The final tensile stress measured after 10 minutes for each latch for a range of stresses.	62
5.21 Measured difference between peak force and final tensile force measured after 10 minutes for each latch for target forces between 1 and 60 Newtons.	63
5.22 Measured difference between peak force and final tensile force measured after 10 minutes for each latch for target forces between 1 and 15 Newtons.	63
5.23 Percent difference between peak force and final tensile force measured after 10 minutes for each latch for target forces between 1 and 60 Newtons.	64
5.24 Percent difference between peak force and final tensile force measured after 10 minutes for each latch for target forces between 1 and 15 Newtons.	64
5.25 Measured difference between peak cable stress and final cable stress measured after 10 minutes for each latch.	65
5.26 Percent difference between peak cable stress and final cable stress measured after 10 minutes for each latch.	66
5.27 Hoop pressure applied by the the unpowered motor latch, calculated for a variety of latch locations on the body.	67
5.28 Hoop pressure applied by the the powered motor latch, calculated for a variety of latch locations on the body.	67
5.29 Hoop pressure applied by the the ratchet latch, calculated for a variety of latch locations on the body.	68
5.30 Hoop pressure applied by the the cam latch, calculated for a variety of latch locations on the body.	68
5.31 Calculated value of hoop pressure on an average human thigh for each latch for target forces between 1 and 60 Newtons.	69
5.32 Calculated value of hoop pressure on an average human thigh for each latch for target forces between 1 and 15 Newtons.	69
5.33 Time taken for each latch to release cable tension, with linear trend lines indicating the relationship between release time and cable tension.	71
5.34 Measured force applied to ratchet and cam release levers required to disengage each latch. The measured force output of the linear actuator is shown for reference.	72
6.1 Radar plot showing the characteristics of the three latch designs.	86

6.2	Motor design characterization summary.	87
6.3	Ratchet design characterization summary.	87
6.4	Cam design characterization summary.	88

Chapter 1

Introduction

Robotic systems are defined by their methods of actuation. Rigid actuators like motors, hard pneumatics (pistons and compressors), and hydraulics have been the building blocks of traditional robotic systems, including wearable robotic systems e.g. rigid exoskeletons. However, these systems are poorly suited for soft, compliant, wearable applications. The desire for robotic systems, and specifically actuators, to be deformable, lightweight, and low energy, while continuing to provide the strength and reliability of traditional rigid actuators is one of the major challenges in the field of soft, wearable robotics. Linear actuators, for instance, are nearly ubiquitous in modern machinery as pistons and pneumatic, hydraulic, and electric linear actuators, however none of these classes of actuators lend themselves well to use in soft systems [1], necessitating the development of entirely new classes of linear actuators for use in soft, wearable systems.

Where these existing linear actuator technologies fail to be soft, deformable, and light weight, human and animal muscles excel. Biological muscles have several admirable properties, such as high specific work, power, and efficiency [2][3]. Additionally, biological muscles have intrinsic material properties that provide adaptive impedance control without requiring sensory feedback [4], energy storage and recovery during cycling [5], and embedded sensors and power sources [6][7]. A major goal of soft, wearable robotics is to develop materials and systems that simulate these advantageous qualities.

Drawing inspiration from these biological systems, research has increasingly begun to focus on a class of biomimetic linear actuators known as artificial muscles. While this research has shown promise, contemporary artificial muscles have a variety of drawbacks,

such as the need for high voltage, high current, or high fluidic pressures, depending on the class of artificial muscle [8]. These drawbacks result in large power requirements, and consequently either large battery packs or short term usage, reducing the wearability or mechanical utility of the artificial muscles.

The research presented in this paper will attempt to mitigate some of these drawbacks through the development of wearable latching devices designed to be integrated into existing artificial muscle systems. Such latching devices do not change the intrinsic properties of contemporary artificial muscles, but serves as a complimentary technology to increase the utility of artificial muscles in wearable systems. Specifically, latching devices enable the short term use of artificial muscles in applying a desired actuation force and displacement, then allows said artificial muscle to be powered off without loss of applied force or displacement. Such a system decreases the long term energy requirements of wearable actuators, provided high frequency actuation is not required. This paper will explore the design, evaluation, and implications of wearable latching devices for use with artificial muscle systems.

1.1 Background

Modern linear actuators trace their development to the industrial revolution. From steam pistons and hydraulics to modern electric linear actuators, these devices all share similar attributes. Conventional linear actuators are excellent at applying consistent forces and accelerations, and doing so dependably over numerous cycles. Various classes of these linear actuator are capable of passive static loading, high energy efficiency, smooth motion control, high speed, large duty cycle, and large stroke length. However, they also are relatively heavy, large, hard, and rigid. These attributes of conventional linear actuators makes them a challenge to integrate into biomimetic, biocompatible, and soft robotic systems. Such systems emphasize compliant materials and safety over strength and rigidity, thus a new class of linear actuator is required for use in these systems [9].

Advances in material science have lead to the development of multiple soft linear actuator designs [10][11][12]. One of the most promising actuation domains has been in twisted coiled actuators (TCAs) which are coiled fibers or wires in the shape of a spring

that can be made to contract, often through thermal loading. TCAs are lightweight, flexible, and inexpensive, and have been demonstrated to have a large stroke length and be capable of repeated loading under high tension [13]. However, they also have high energy requirements [14], are electrically inefficient, difficult to control [15], and require constant heating to maintain force and displacement [16]. These limitations have hindered the wider use of TCAs in soft robotic systems.

A potential solution to these limitations is an electronically controlled soft latching system, which would lock the displacement of the TCA into place on command. Such a system would allow the TCA to contract as normal, then allow the latch to take over the load from the TCA once a desired force or displacement has been reached. The TCA would then be powered off until a new displacement is desired. Additionally, making the latching system remotely releasable preserves the hands-off nature of existing TCA systems and enables complex robotic operations without direct human interaction.

1.2 Problem Formulation

For this research, several wearable latching systems will be designed, constructed, and comparatively assessed, with the goal of enabling future artificial muscle systems that will require less power, have increased displacement precision, and that will be more easily controlled. This will be accomplished while maintaining the compact size, flexibility, and variable displacement capabilities that make TCAs well suited for soft, wearable robotic systems. To achieve this goal, the latching mechanisms will be designed to be able to lock the length of soft linear actuators into place on command, allowing TCAs to remain at a fixed length even while the power to the TCAs has been stopped. The latching mechanisms will be able to achieve this position lock while continuing to support the valuable properties of TCAs such as their high stroke length, flexibility, light weight, small form factor, and biocompatibility. To this end, the fastening devices will be designed with and evaluated against a set of performance requirements:

1. Maintain the displacement and force of a TCA while the TCA is powered off. Latches should be able to maintain 90% of displacement and force to be considered reliable.

2. Achieve (1.) for any arbitrary displacement values within the displacement envelope of the TCA. Displacement should be accurate and precise to within 5 mm to enable use anywhere on the body.
3. Be able to release tensile forces on command, allowing for a TCA to return to its relaxed length. This should be achievable up to systems stresses of 1 MPa, consistent with existing artificial muscle capabilities [3].
4. Fit within a small form factor, be integratable with human garments, and allow multiple TCAs to operate in parallel close to one other. Latches should mass less than 20 grams (e.g. the mass of a watch [17]) to enable use anywhere on the body.

Beyond these requirements, the latches developed for this research will also be designed to maximally explore the design space of soft latching actuators, providing insights into the benefits and drawbacks of each latching design as they pertain to soft, wearable robotic systems.

Chapter 2

Related Works

2.1 Soft Robotics

Whereas traditional hard robots are composed of rigid links, soft robots are designed to be flexible and compliant, allowing for technologies and solutions that would not be possible otherwise. One advantage of this design is the relative safety of a soft robot over a hard one. Most existing hard robots consist of metal structures attached to powerful and fast actuators, which can injure or kill people or animals that come into contact with a robot while it is operating [18]. Consequently, many industries that rely on robotic processes, such as robotic assembly lines, must invest heavily in safety devices and protocols, and must limit human-robot interactions to meet regulatory requirements [19, 20, 21, 22, 23]. This significantly hinders the potential of robots as a technology if the people using the robots must either stay far away from them or abide by a strict set of safety standards that requires specialized, customized robots [24]. Soft robotics significantly decreases this danger. The inherently soft and compliant nature of a soft robot means that even if the robot does run into a person the individual is unlikely to be harmed [1]. This improved safety allows for much closer interactions between robots and humans for technologies like biomedical applications and wearable robotics.

The other great advantage of soft robotics is the potential for biomimicry and the theorized improved efficiencies that come with it. Biological systems, such as plants and animals, are composed almost entirely of soft and compliant actuators. While hard actuators and hard robots have had, and continue to have many valuable applications,

they struggle to imitate biological systems, which limit their potential applications and the potential of robots as a whole. Soft actuators that imitate muscles are particularly useful for biomimicry, as muscle tissue is the primary biological actuator in most animal species. The design of humanoid robots, exoskeletons, and other animal inspired designs have the potential to be greatly improved by incorporating soft, biomimetic actuators into their designs.

2.2 Wearable Robotics

Wearable robotics, as the name suggests, is the application of robotic technologies onto the human body. Full-body force amplifying exoskeletons are perhaps the most ambitious application, but many smaller applications also exist that aide people with medical disabilities, carry loads for camera operators, and create more immersive video games [25, 26, 27]. Existing wearable robots have largely used traditional hard actuators like motors and pistons, which makes them heavy, large, and potentially dangerous for human wearers. They can also be relatively inefficient, as many traditional actuators are more efficient at larger sizes but must be shrunk down to be usable at human scales. These limitations have restricted the widespread adoption of wearable robots to very specific fields and applications.

Soft robotics offers a potential improvement over traditional wearable robotic designs. The value of soft robotics being relatively safe, in combination with biomimetic, form-fitting actuators that are lighter and more space efficient are particularly valuable traits for wearable robotics. Even relatively inefficient soft actuators can have benefits over hard actuators due to their smaller size and more efficient designs requiring less energy overall.

2.3 Wearable Soft Actuators

For soft wearable robotic systems to function, a variety of wearable soft actuators have been developed. Today, three broad classes of such actuators exist. These are cable or tendon driven actuators, fluidic actuators, and shape changing actuators [8].

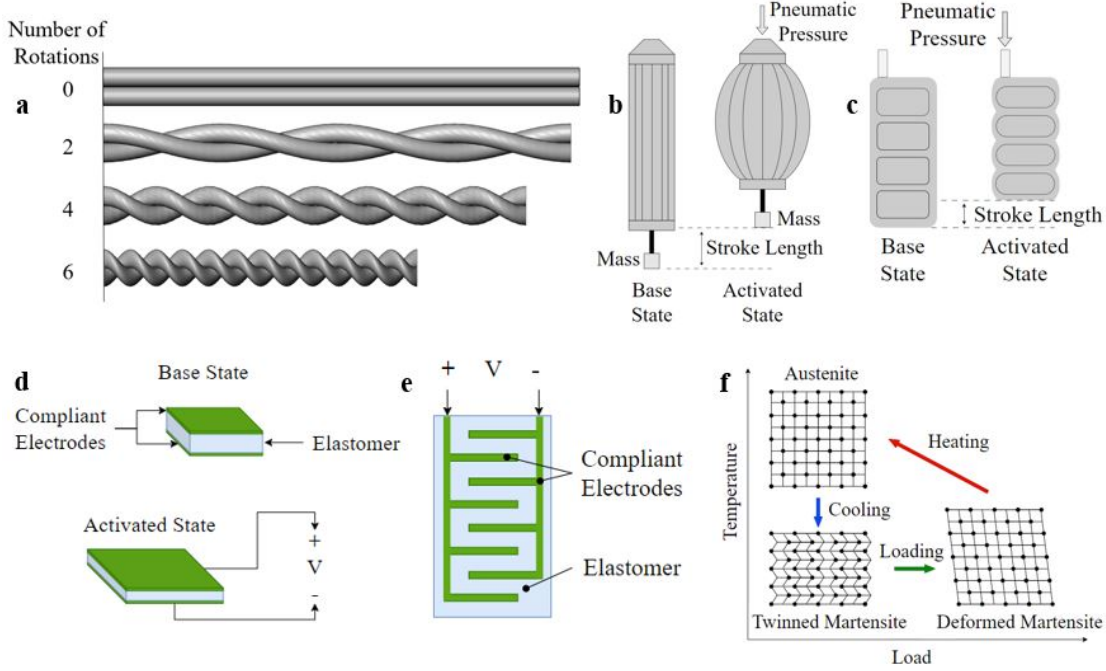


Figure 2.1: Various soft actuator actuation methods. a) Actuation displacement of twisted spring system [28]. Adapted from Palli, G. et al. b) McKibben pneumatic artificial muscle [29]. c) Schematic of linear multi-chamber pneumatic artificial muscles. d) Schematic of dielectric elastomer membrane before and after voltage activation [30]. Adapted from Novelli, G. et al. e) Monolithic stacked dielectric elastomer schematic. Adapted from Shintake, J et al [31]. f) Molecular diagram of Austenite-Martensite phase transformation. Adapted from Jackson, C et al [32].

2.3.1 Cable or Tendon Actuators

Cable or tendon actuators act similarly to biological tendons by transferring load from an actuator to a desired location. Common actuation schemes involve attaching one end of the cable to a motor and running the cable through a sheath to another location on the body. The motor can provide direct linear actuation to the cable, or, in the case of twisted string actuators, can coil the cable and provide linear actuation through the shortening of the cable as it coils [28]. Compliant actuators can also be used in cable designs, instead of motors, for instance by placing a fluidic actuator or shape changing actuator on one end of the cable. For all tendon or cable integration schemes,

the location of the cables must be carefully routed across the body to avoid creating undesirable forces, pressures, and moments on different areas of the body that might detract from the usefulness of the actuation [33].

2.3.2 Fluidic Actuators

Fluidic textile actuators use fluids, both liquids and gasses, to induce actuation through pressurization. This pressurization is commonly achieved through mechanical means using some combination of tanks, pumps, and compressors to inflate a bladder [34], although alternative pressurization schemes have been used as well utilizing thermally induced pressure changes [35]. Common fluidic bladder configurations include braided textile pneumatic artificial muscles (PAMs) (commonly known as the McKibben actuator) [29], linear pouch or bellows designs, and fluidic fabric muscles [36]. Often these designs work by expanding radially and contracting axially when inflated, though inverse PAMs (IPAMs) exist as well that contract radially and expand axially when inflated [37]. PAM systems often have an advantage over traditional hard actuators in being light weight and compliant while enabling a large diversity of motion, but these devices are currently heavily limited by the need for tanks and pumps which reduces the wearability of fluidic designs.

2.3.3 Shape Changing Actuators

While cable and fluidic designs are able to provide soft, wearable actuation through macroscopic physical principles, other classes of actuators exist that actuate through intrinsic material shape changes. Dielectric elastomer actuators (DEA) are one such class that actuates when an electric potential difference is applied across an elastomer, causing the elastomer to compress axially and expand radially [10, 38]. Fiber constrained DEA and monolithic stacked DEA are two DEA schemes that have been proposed for use as artificial muscles [31]. However, current DEA systems require large voltages (into the kilovolt range [38]) to actuate which requires DC-DC converters making such systems potentially dangerous and heavy, as well as reducing their applicability as wearable actuators.

Shape changing actuation has also been achieved through thermally induced material

changes. Shape-memory alloys (SMA), for example, are metals that undergo phase transitions from martensite to austenite when heated [39]. A shape can be "programmed" into the austenite phase such that during the martensite to austenite transition the metal will attempt to return to that preset shape regardless of the material's shape during the martensite phase. This property has been used in SMA wires to create knitted garments [40], and SMA wires have been coiled to create artificial muscle linear actuators [41]. Similar to SMAs, shape-memory polymers (SMPs) can also have "programmed" shapes that can be induced through temperature changes, magnetic fields, light exposure, or chemical immersion. In addition to SMAs, SMP wires have also been coiled to form artificial muscles [42]. So too have carbon nanotube (CNT) yarns, which are thermally or electrochemically actuated [43]. These coiled actuators are collectively known as twisted coiled actuators (TCAs), discussed in more depth in the next section.

2.4 Twisted Coiled Actuators

Multiple twisted coiled actuator (TCA) designs have been developed from a number of different materials. The three primary classes of TCA are twisted coiled polymers (TCPs), shape memory alloys (SMAs), and carbon nanotube yarn (CNT). Each of these classes have distinct properties, but can operate similarly by contracting when heated [11][12]. Figure 2.2 provides a visual representation of how linear actuation is achieved from coiled cables through thermally activated twisting of the cables.

Polymer TCAs often use Nylon polyethylene [42], which can be acquired at relatively little cost in the form of fishing line or sewing thread. Polymers are able to achieve strains of up to 30% at temperatures of 200°C, but have relatively large response times on the order of 10 seconds for both heating and cooling [44], though operating frequencies as high as 5 Hz have been recorded

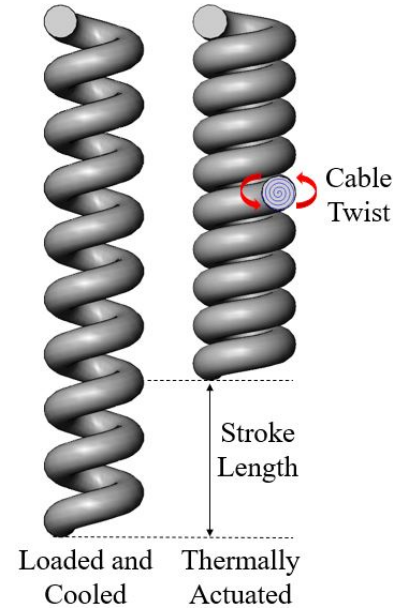


Figure 2.2: Diagram of the actuation mechanics of TCAs.

when the TCA was immersed in water to enable passive cooling [42]. Heat can be applied effectively by running a current through a copper wire wrapped around the polymer coils, resulting in power requirements of 0.2 W/cm [45] and a power-to-weight ratio of 5.3 kW/kg [42].

Shape memory alloys are commonly made from a Nickel-Titanium (NiTi) alloy. The SMAs are able to achieve larger strains than other TCAs, up to 300% at similar temperatures to the coiled polymer. However, their response time is similar to coiled polymers, on the order of 10 seconds for heating and cooling, and they also have similar energy requirements [13].

Another TCA that has been researched is the coiled carbon nanotube (CNT) yarn infiltrated with a thermally responsive material like paraffin wax that allows the nanotube yarn to contract under heating. CNT yarn has a short response time, contracting on the order of 10 ms when heated, and relaxing quickly, on the order of 1 second. However, the strain it produces is relatively small, at around 3% to 7%, occurring at temperatures of between 25 and 200°C [43]. CNTs are also significantly more expensive to produce than SMAs and TCPs, requiring the growing of carbon nanotubes. Despite the technical feasibility of CNT actuators, their high cost has prohibited a broader adoption in contemporary soft robotic systems.

2.5 Latching Devices

Multiple different fields rely on latching systems to achieve variable actuation.

2.5.1 Buckles

Some of the simplest latching devices are buckles that have spring loaded teeth that allow a tab to enter the latching device but not leave, such as the type common on backpacks. Buckle designs have been used with TCA devices successfully [46], but do not allow for variable displacement latching. The latch only engages at a specific location.

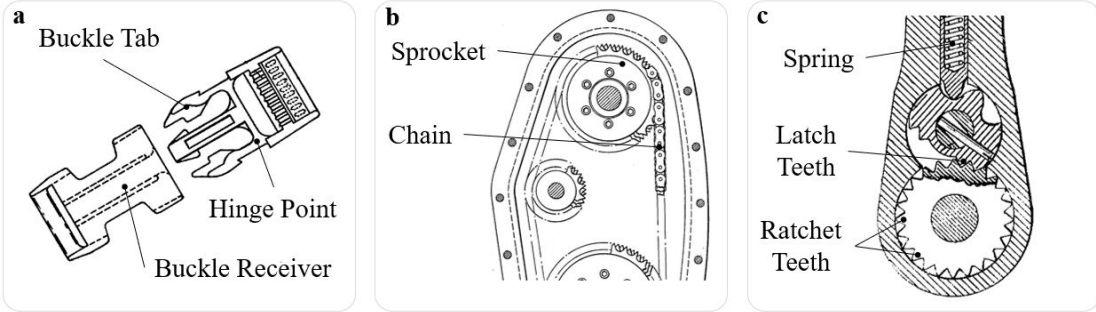


Figure 2.3: A variety of latching methods and mechanisms. a) Schematic of a buckle, commonly seen on backpacks and luggage [47]. b) Chain and sprocket linear system [48]. c) Bidirectional circular ratchet used in a wrench [49].

2.5.2 Motors and Disk Brakes

In contrast, traditional hard robotic systems are heavily reliant on variable position latching. Fixing robotic joints and linkages is commonly accomplished with motors and disk brakes, and motors are also commonly used for linear actuation. For such applications, the rotational motion of the motor is transformed into linear motion, often using rack and pinion drives, linear screws, chain and sprocket drives, or belt and pulley drives. The latter has been used successfully in wearable applications, for example in dynamic shoelace tightening [50], but has not been used in other parts of the body where latch compliance, mass, and size are important factors.

2.5.3 Ratchets and Cable Ties

Another common variable displacement latch is the ratchet. Ratchet devices often have teeth arrayed around a cylinder that only lock in one direction. Ratchet straps wind threaded ribbons around a cylinder as the ratchet is tightened inducing a large tensile force into the ribbon without slipping. Ratchets for tightening bolts are able to twist a bolt to tighten it, then untwist without loosening the bolt. Friction ratchets also exist that don't rely on teeth. For example, eccentric cam ratchets have a cylindrical disk that rotates about an offset hole, that when rotated results in a gradual tightening between the ratchet cam and ratchet disk. Helical spring ratchets are able to grip a shaft with a spring. When the ratchet is tightened the spring tightens around the shaft,

and releases when the ratchet is untightened [51].

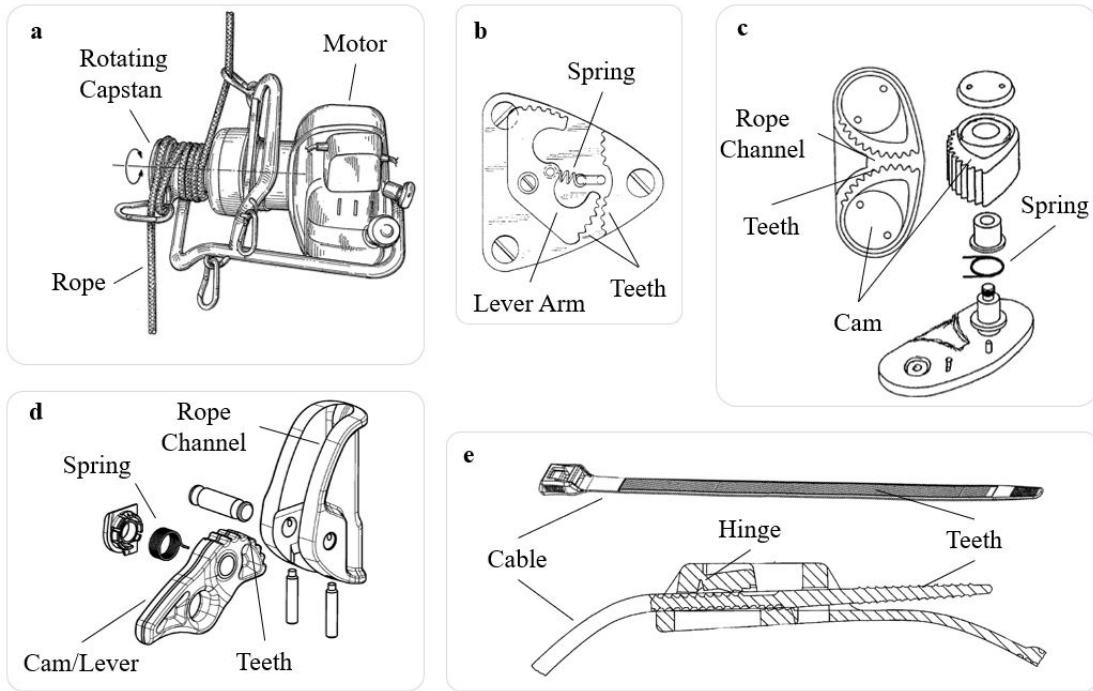


Figure 2.4: A variety of latching methods and mechanisms. a) Motorized rope ascender [52]. b) Cam cleat with dual directional latching [53]. c) Unidirectional cam cleat [54]. d) Manual rope ascender with spring-loaded toothed cam [55]. e) Cable tie with hinged locking arm [56].

A similar technology to ratchets is the cable tie - or zip tie - that allows a flexible cable to move one direction through the latching head but prevents the cable from moving against the teeth. A cable tie inspired device has been used in past TCA latching designs, however existing latching devices have not been flexible and have been energy intensive to release, or even impossible to release without permanently damaging the cable or the latch [57][58].

2.5.4 Rope Traversal

One of the fields most similar to the current research is rope traversal. A common design that robotic rope ascenders have used is a winch or capstan - a rotating drum acting as a force multiplier - with use cases like moving up and down buildings or trees

[52]. Separately, climbers have used multiple designs for rope ascenders that move up with little resistance but are prevented from moving down by a cam or lever arm [55]. Climbers using these designs must carry them in situations where equipment mass is a limiting factor, up a mountain for instance, so these designs have been optimized for mass and space saving. Such a system provides more resistance to movement the greater the applied force, as larger tensile forces are counteracted by the cam or lever. A special rope is not needed for the rope ascenders to work; as long as the cam and lever arm are able to grip the rope they will be able to engage, making these systems versatile. However, large loads have been shown to quickly fatigue rope ascenders [59]. Wearable latching designs based on cams have been successfully prototyped, but no known wearable cam latch has been designed to be remotely releasable or integratable onto wearable garments.

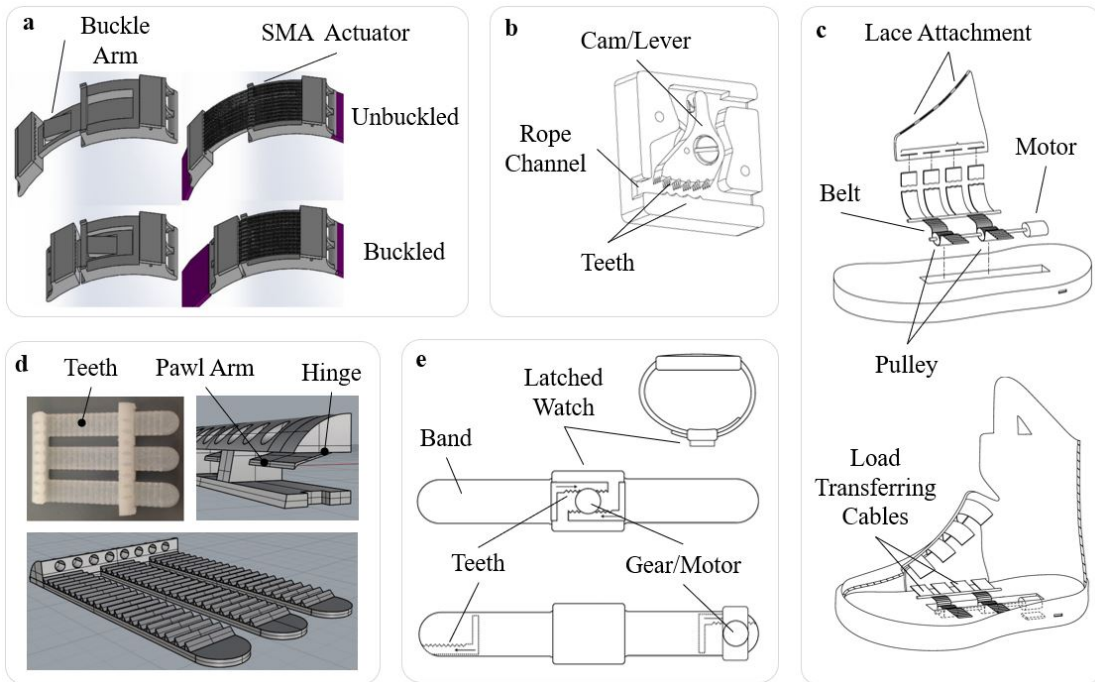


Figure 2.5: Existing wearable latching research and designs. a) Wearable, self-locking SMA actuated latch. Reproduced with permission from Holschuh, B [46]. b) Wearable latching mechanism for use with active compression garments. Reproduced with permission from C. Hansen et al [58]. c) Automatic lacing system for use in athletic footwear [50]. d) Reproduced with permission from M. Clarke et al [57]. e) Watch with dynamic fit adjustable wristband [60].

2.6 State of the Art

The field of soft, wearable robotics has been the focus of an ever growing amount of research. With this growth has come the study of soft, wearable linear actuators, or artificial muscles, with a multitude of designs, actuation methods, and integration schemes. Tensioned coiled actuators in particular have shown great promise as artificial muscles, and have already begun to be produced commercially. However, limitations abound in all contemporary artificial muscle designs, including TCAs. Power consumption is one such limitation, requiring either a permanent electrical tether or a large energy storage device, dramatically limiting the utility of these systems in wearable applications. One potential solution for wearable applications where expected actuation frequency is very low (on the order of minutes to hours) is a soft, wearable latching system. Such a system would preserve the valuable qualities of TCAs, such as their strength, compliance, large stroke length, and automatic control, while enabling the powering off of TCA muscles once a desired force and displacement have been achieved, thereby dramatically reducing the power requirements of such a system. Despite these advantages, existing latching devices have either not been compliant, not been wearable, or not been automatically controllable. This research will attempt to resolve these failures, and provide a path forward for integrating soft, wearable latching devices into future TCA systems.

Chapter 3

Design

A latch is, in the broadest terms, a releasable fastener: a mechanical mechanism that joins two or more objects together while allowing for the objects to be separated in the future. To simplify the design of latches for this research, each latching design was broken into two components: one component doing the latching (the latch) and the other component being latched onto (the cable). Three different designs were chosen to demonstrate a range of latching technologies, with each design representing a separate latch and cable interaction. This section will cover the considerations and specific layout of each design.

3.1 Latch Wearability and Integration

Each latch was designed with wearability in mind. Guidelines for wearability, developed by Gemperle et al.[61], were used as reference. The primary design choice in facilitating wearability was to keep the latches as small as possible given resource and manufacturability constraints. In particular, the height of each latch, measured normal to attachment point, was minimized in an attempt to keep each latch within the wearers intimate proxemic space and perceived as an extension of their clothing/body. Small and rigid latch designs were favored over compliant designs due to the perceived challenge of designing a compliant latch system capable of precise and repeatable latching. Additionally, a compliant design was expected to be heavier and more complex than a rigid design, making rigid systems more attractive with regards to wearability

and manufacturability. For the cable used in each latch, compliance was a much larger concern, with soft, flexible, and lightweight cables being preferred. The potential for the cable to become caught on clothing or other items was also considered.

To facilitate ease of attaching each latch to a garment, all three latches were designed with the same mounting points consisting of two textile friendly metal snaps as seen in figure 3.1. This type of fastener has been common in wearable technology research and provides a strong mounting point while being easily removable and unobtrusive [62, 63, 64]. The small size and ease of integration of snap fasteners allowed the latches to be easily attached to nearly anywhere on the human body.

While integration of the latches with TCA systems was beyond the scope of this research, the *ability* of each latch to be integrated with TCA systems was considered essential for the design of effective latches. As such, four stages of latching were considered during latch design: a passive state where the TCA is unpowered and the latch is un-engaged and applying no force to the cable; a tensioning state where the TCA is actively applying force to the cable and the latch is engaged but applying no force; a latched state where the TCA is unpowered and the latch is applying force to the cable; and a release state where the TCA may be powered on to release tension from the cable and allow the latch to disengage, or where the TCA remains powered off and the latch is disengaged, quickly releasing all tension from the cable. The release state in particular was identified to be potentially challenging, as autonomously releasing a large amount of force in a small latch was expected to be difficult. Additionally, transitioning from tensioning to latched states introduced the potential for the cable to slip through the latch and fail to precisely and reliably engage with the cable at the correct displacement and force requirements. Each latch design attempted to address these concerns, as discussed below.

Two methods for integrating the latches with TCA actuators were considered during latch design: series integration and parallel integration. These can be seen in figures 3.2 and 3.3 respectively. For the series integration scheme, the latch mechanism and TCA would be fastened to one surface, with the cable mated to the TCA, passing through



Figure 3.1: The metal snap fasteners used for attaching each latch.

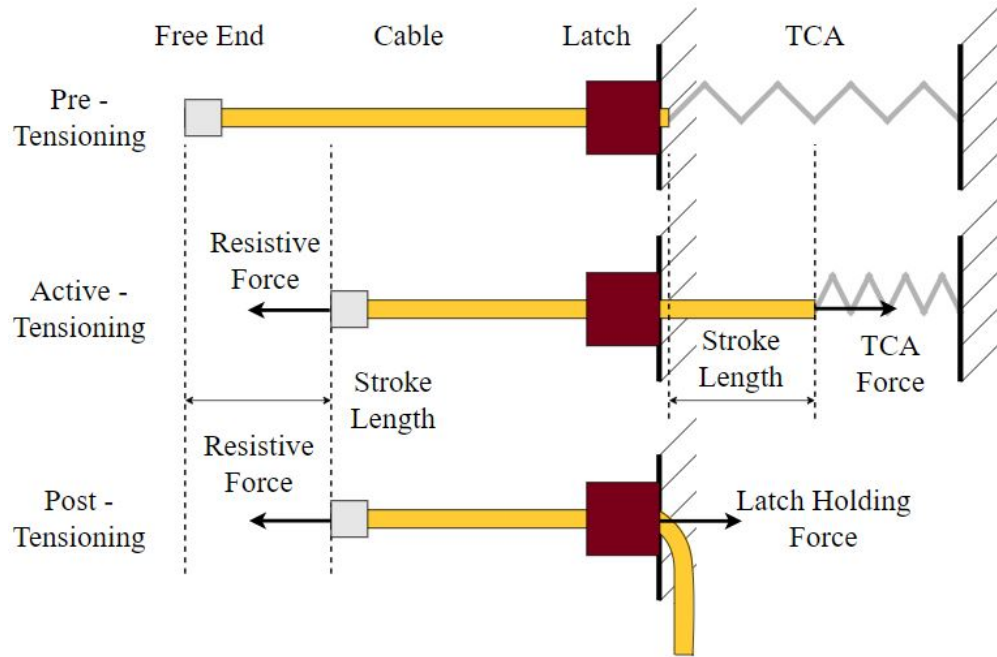


Figure 3.2: Latch and TCA in a serial integration configuration.

the latch, and attaching to a second surface. The actuation of the TCA would then draw the two surfaces together. A concern for this scheme was the cable engaging with the latch during the tensioning stage and drawing the latch and TCA together instead of the two surfaces. Each latch was therefore designed to minimize this risk.

For the parallel integration scheme, one end the TCA would be attached to a surface with the other attached to the cable. The cable would pass through the latch, with the latch mounted on a second surface, with the cable then being attached to surface one in parallel with the TCA. A flexible and inextensible cable with a small minimum bend radius was considered essential for use with this integration scheme, as the cable would need to make a 180 degree bend to travel from the TCA to the latch and back.

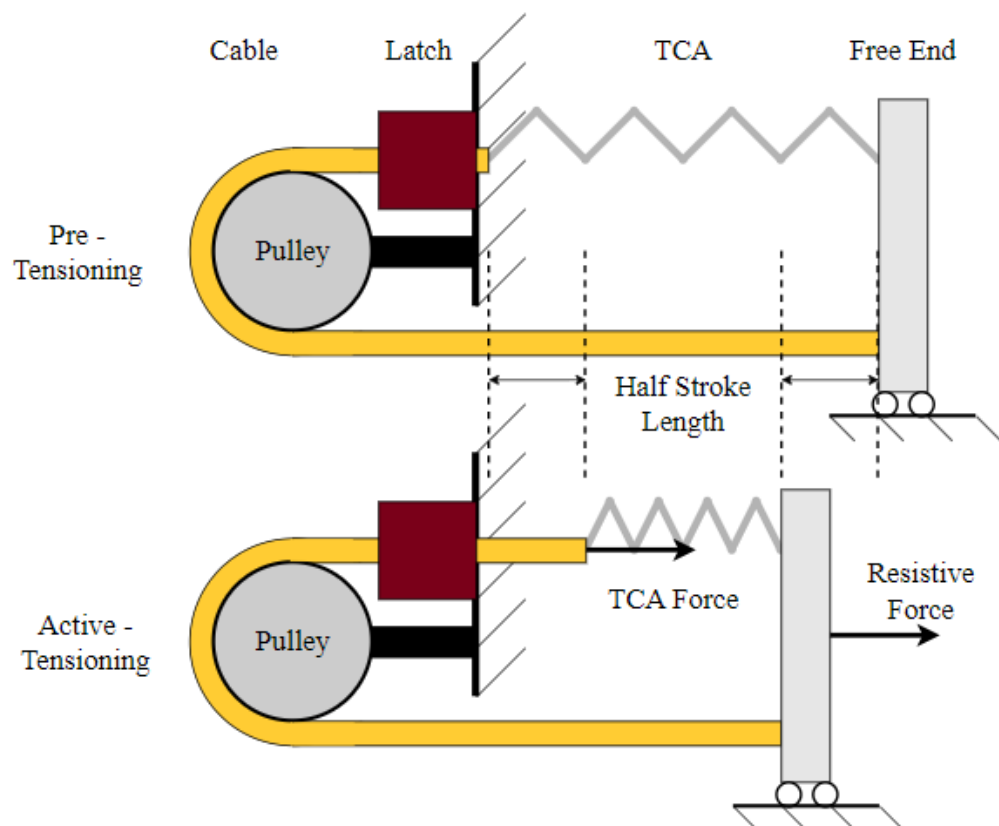


Figure 3.3: Latch and TCA in a parallel integration configuration.

3.2 Latch Designs

3.2.1 Motor Brake Design

For the first design, traditional hard robotic latching mechanisms were considered such as magnetic brakes, spring brakes, and stepper motors. Magnetic brakes and spring brakes were not considered viable for this research due to their relatively high power requirements (on the order of tens of Volts and tens of Watts [65]), large size, and the difficulty in sourcing a holding brake of suitably small size to be considered wearable. The smallest contemporary holding magnetic brakes have heights and diameters on the order of centimeters, and masses on the order of tens of grams [66] which make integration into wearable garments difficult. A stepper motor was then considered, where the torque of the stepper motor could provide a holding force to act as a latch. A 28BY J-48 12V Stepper motor was chosen due to its relatively large gear reduction ratio (1:64), high precision, relatively low power requirements, and reliability [67] (power characterization of the motor is performed in Chapter 4 and motor dimensions are shown in Appendix A).

For the cable mechanism, a belt and pulley combination was required that could reliably maintain position, and therefore needed a low probability of slipping. A toothed belt and pulley system was chosen for this reason, as the teeth are specifically designed to prevent slipping. Even so, the configuration of the latch design made integrating a belt and pulley system challenging. The latch was designed such that the cable would pass through the latch tangential to the pulley, without the cable changing direction, as this design configuration provided the greatest opportunity for integrating the latch into both the series and parallel integration schemes. Many belt and pulley systems are designed so that the belt wraps around the pulley 180 degrees, creating a large amount of engagement area between the belt and the pulley. The tangential cable latch design significantly reduced this engagement area, resulting in slippage for some belt and pulley systems. The FingerTech timing belt in combination with the FingerTech timing pulley 9T was eventually chosen. Designed for use with fighting robots, this system was found to have a tooth design that provided suitable engagement between the belt and pulley, even when the belt only interacted with the pulley tangentially.

The housing for the motor and pulley was 3D printed with fused deposition modeling

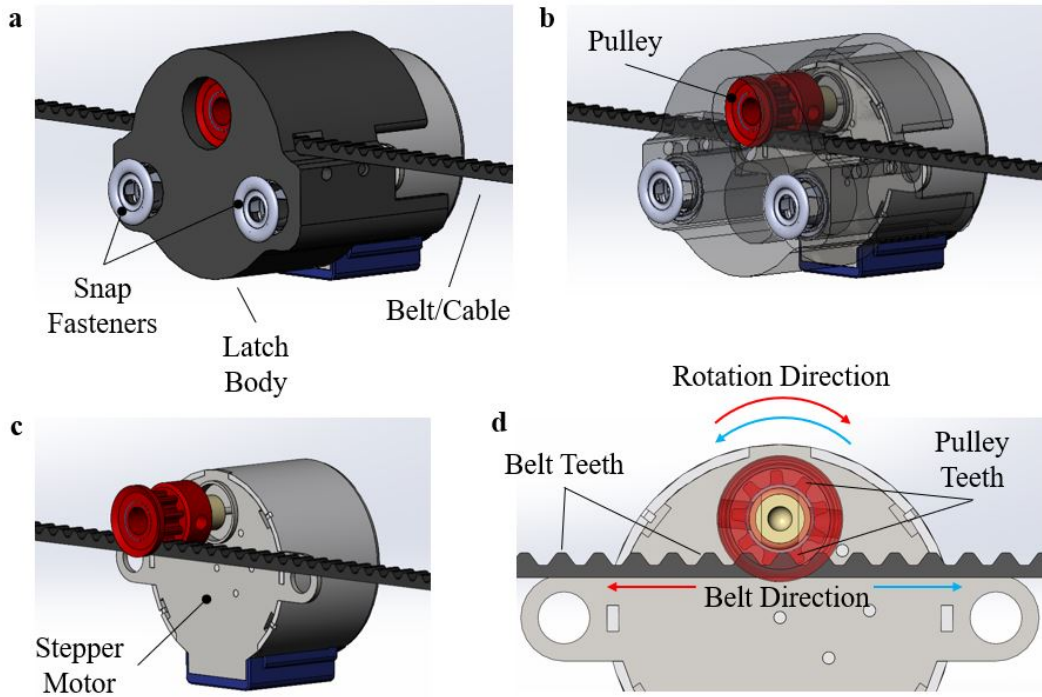


Figure 3.4: Overview of motor design operational concepts. a) Model of full motor latch design with motor cable. b) Model of motor latch design with transparent latch body. Individual components and their interactions can be seen. c) Simplified motor model with only the stepper motor, belt, and pulley visible. d) Diagram of interactions between the stepper motor, belt, and pulley. The rotation of the stepper motor axle causes the pulley to rotate. The teeth of the pulley then engage with the teeth of the belt causing a linear movement of the belt.

using a Prusa i3 MK3S+ 3D printer, printed with PLA filament. A slot was inserted tangential to the pulley and the rotational axis of the motor to allow the cable to pass through the housing and over the pulley. The slot was offset slightly to keep the cable pressed firmly against the pulley while still allowing the pulley and motor to rotate. The motor was driven by a ULN2003A motor driver (STMicroelectronics) and controlled using an Arduino Nano. The motor was operated in four states to control the latch: clockwise, counterclockwise, one coil energized, and all coils off. The clockwise and counterclockwise states passed the cable in one direction or the other, providing latch displacement control. The one coil energized setting worked by constantly powering a single coil, thereby creating a braking torque and holding the cable in place. The fourth

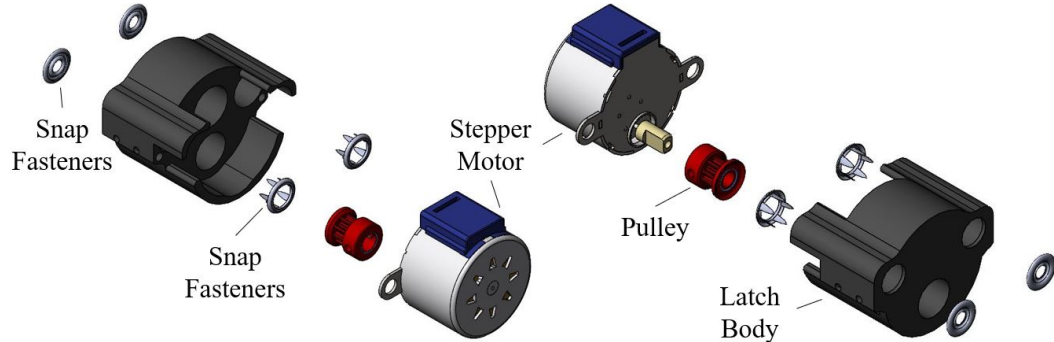


Figure 3.5: Motor design exploded view.

setting de-energized all coils of the stepper motor reducing power consumption. It was found that even de-energized, the stepper motor provided a braking torque that could be used for latching. Both the one coil energized and the motor off settings were tested as potential latching modes.

To manufacture the motor latch design, first the motor housing was 3D printed. Two snap fasteners were affixed to the bottom of the motor housing. The timing pulley was not able to fit over the shaft of the motor, so the pulley was bored to the appropriate size, then was affixed to the motor shaft. The pulley and motor were then inserted into the housing. The motor was bound to the motor housing using two zip-ties looped through the motor's attachment points and holes in the motor housing.

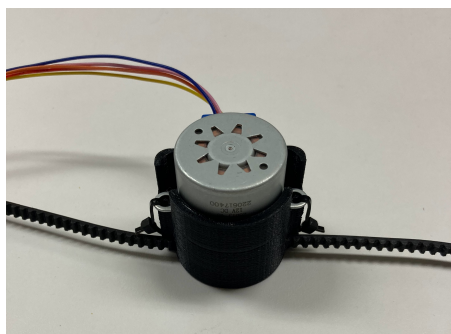


Figure 3.6: Completed motor design assembly.



Figure 3.7: Chloroprene rubber with fiberglass reinforcements toothed belt.

3.2.2 Linear Ratchet Design

The second design was inspired by cable ties, commonly known as zip-ties, and ratchet systems. These systems work by having a belt with grooves and a latch mechanism with a corresponding set of teeth to engage with the grooves of the cable. The teeth are held in place by a spring mechanism that allows the teeth to be disengaged when the cable is moving in one direction but not the other. For this latch system, the teeth were designed with one side of each tooth acting as a ramp to smoothly slide over the grooves of the cable, with the other side of each tooth oriented normal to the movement of the cable, thereby engaging with the grooves and preventing the cable from sliding past. Cutouts were placed in the latch for the cable to slide through, which acted to position the grooves of the cable with the latch teeth. This system allowed the latch to engage with the cable passively, without the need for an external power source.

To disengage the latch, a small linear actuator was used to press against a lever attached to the teeth, pushing them out of the way of the cable. The linear actuator used was a 3.3V 2-phase 4-wire stepper motor with planetary gearbox. The linear actuator was driven with an L293D motor driver (STMicroelectronics) and controlled with an Arduino Uno R3. This linear actuator was chosen because it was the smallest linear actuator found to be commercially available while still providing enough torque to disengage the latch (power characterization of the linear actuator is performed in Chapter 4 and linear actuator dimensions are shown in Appendix B). To allow the teeth of the latch to reengage, the linear actuator was returned to its initial position and the latch spring pushed the teeth back into position. When not actively disengaging and reengaging the latch, the coils of the linear actuator's stepper motor were powered off.

The latch housing was manufactured with fusion deposition 3D printing as with the motor design. The latch, motor housing, and lever were designed to minimize the footprint of the latch while maximizing the torque the motor could provide to disengage the teeth. For the spring system, it was found that a thin strip of 3D printed PLA plastic, incorporated into the latch body, could act as a spring for the teeth of the latch mechanism. This fact, in addition to the additive manufacturing capabilities of the 3D printer, reduced the number of parts needed for assembly of the latch and simplified the design. A back plate and cover were also 3D printed and affixed to the main latch

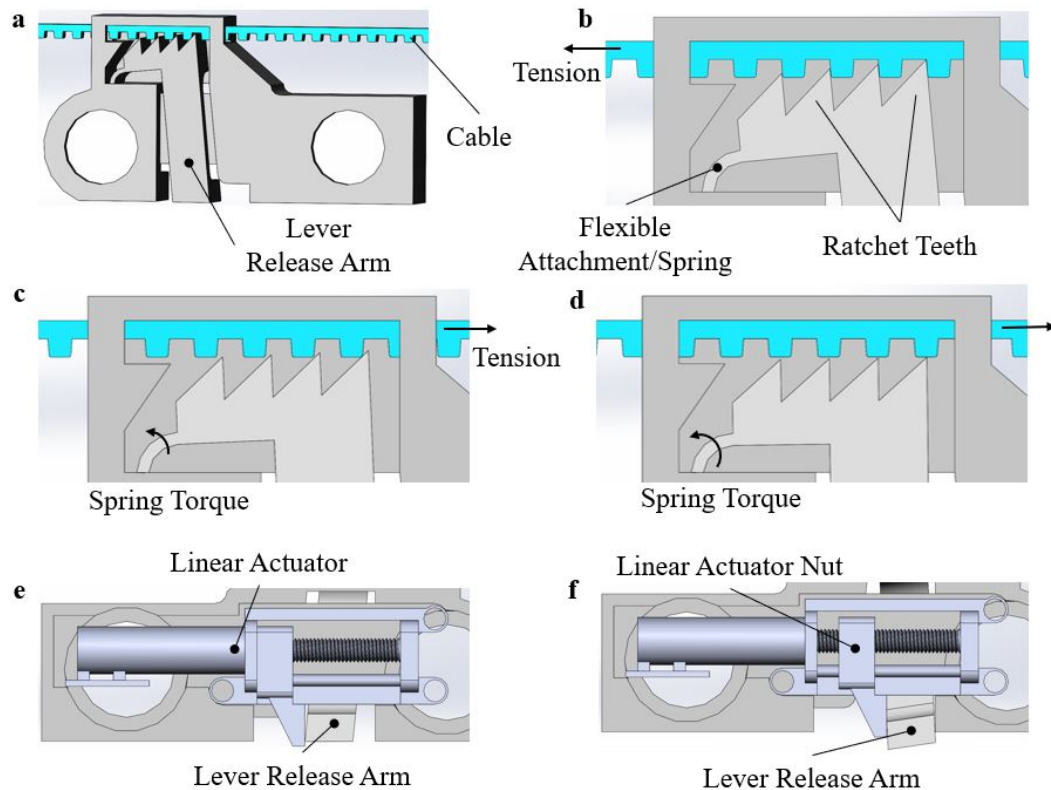


Figure 3.8: Overview of ratchet design operational concepts. a) Model of latch body with cable in the latch. b) Diagram of ratchet teeth while in the latched position. The cable is prevented from moving to the left due to the ratchet teeth engaging with the grooves of the cable. c) Diagram of ratchet teeth in the tightening position. The teeth are partially depressed by the cable as the cable moves to the right. d) Diagram of ratchet teeth when fully depressed by the cable during tightening as the cable moves further to the right. e) Model of linear actuator placed in the latch body. The actuator is in its passive state and not applying pressure to the lever release arm. f) Model of interaction between the linear actuator and the lever release arm during disengagement. The active linear actuator is pressing the lever arm into the disengaged position which moves the teeth down and out of the way of the cable.

housing to prevent foreign objects from interfering with the operation of the latch. The back plate was permanently affixed using snap fasteners. The linear actuator was placed inside the latch housing and the cover was placed on top. The cover was held in place with friction and was easily removable to provide access to the linear actuator.

For the cable of the ratchet design it was desired to use a commercial zip tie cable of at least 500 mm in length. This length was believed to be sufficient for use anywhere on the body. The width of the cable was also deemed important, as a wider cable would necessitate a larger latch. A suitably long and thin cable could not be found, so a cable of suitable length was purchased and modified to reduce its width. The cable chosen was a Nylon-66 cable tie commonly used for securing luggage. The cable tie was cut lengthwise with a band saw, reducing the width of the cable from 9 mm to 1.5 mm. The process of reducing the cable width resulted in variations of up to one millimeter, however a suitable length of cable with width of 1.5 ± 0.2 mm was eventually produced.

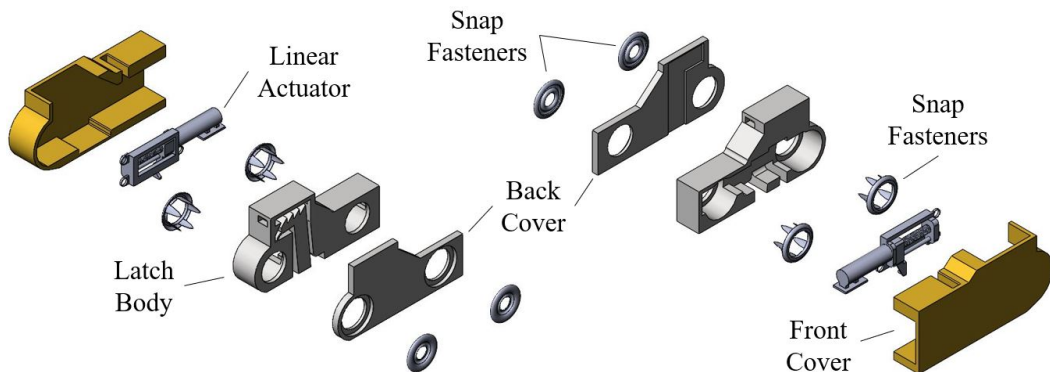


Figure 3.9: Ratchet design exploded view.

3.2.3 Tooothed Cam Design

A cam and rope design was used as the basis for the third latching mechanism. These systems are commonly used in climbing, such as in rope ascenders, and sailing, such as in sailing cleats. These systems use teeth affixed along the edge of the cam, and the curved rotating design of the cam is such that the teeth dig deeper into the rope the more tension is applied to the rope, making the system highly reliable. The cable in this system was a synthetic braided polymer rope with a diameter of 2mm. The latch

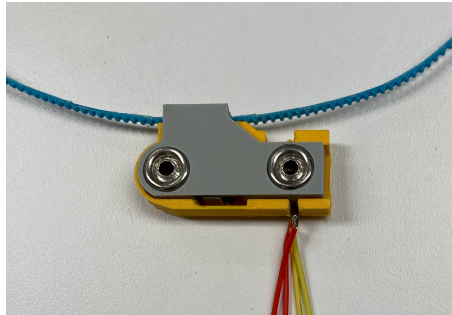


Figure 3.10: Completed ratchet latch assembly.



Figure 3.11: Nylon-66 grooved cable tie cable.

mechanism was composed of the primary latch housing, the toothed cam, a spring to apply constant force to the cam, a pivot pin for the cam to rotate around, and a stepper motor controlled linear actuator to disengage the cam. The linear actuator used was the same as in the previous design and used the same control system.

The radius of a cam is directly proportional to the force it can apply to a rope. The cam and housing were thus designed with the goal of minimizing the footprint of the latch while maximizing space for the cam within the latch, thereby maximizing the cam radius. To release the latch, a lever arm was attached to the cam for the linear actuator to push against. The latch was designed to maximize the length of this lever arm without changing the footprint of the design, similar to the ratchet design.

Slots were placed in the main latch housing for the cable to pass through and position the rope to remain under the cam. Getting the teeth of the cam to reliably engage with the rope was found to be a major challenge during design. The cam and housing were initially manufactured using fused deposition 3D printing as in the previous two designs, however the resulting latch was not able to reliably engage with the rope, as the teeth of the cam were too rounded and did not provide enough surface area for the rope to be caught by the teeth. The teeth were redesigned to be serrated which had been shown in similar designs to be effective at improving the ability of the teeth to catch the rope[58]. Additionally, the method of manufacturing of the cam and cam housing was changed to stereolithography using Formlabs Form 3+ SLA 3D printer, printed with proprietary clear V4 resin produced by Formlabs. This printer was able to produce sharper teeth due to its higher tolerances. The resulting latch was capable of reliably engaging with

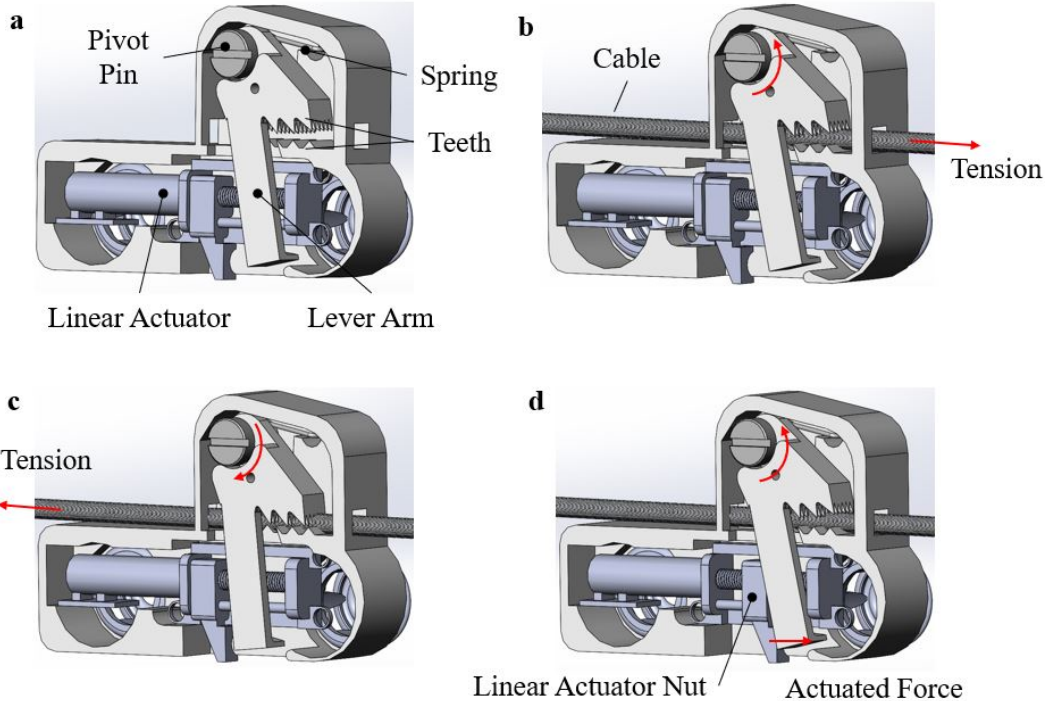


Figure 3.12: Overview of cam design operational concepts. a) Model of latch body with cover removed. b) Model of cam latch with cable in the tightening position. c) Model of cam latch in the latched position. The teeth of the cam are engaged with the rope preventing it from moving. d) Model of cam latch with the linear actuator pressing against the lever arm of the cam to disengage the cam teeth from the cable.

the rope.

The first step of manufacturing the cam latch was to affix the snap fasteners to the latch body. The linear actuator was then placed into the cam housing. The spring and cam-and-lever component were attached to the housing by the pivot pin, which was screwed into the housing until just before fully tightened, fixing the cam and lever in place while still allowing them to rotate about the pin. Finally, a front cover was slid over the housing to prevent foreign interference with the cam design. The cover was removable and held in place with friction to allow for easy access to the linear actuator and cam.

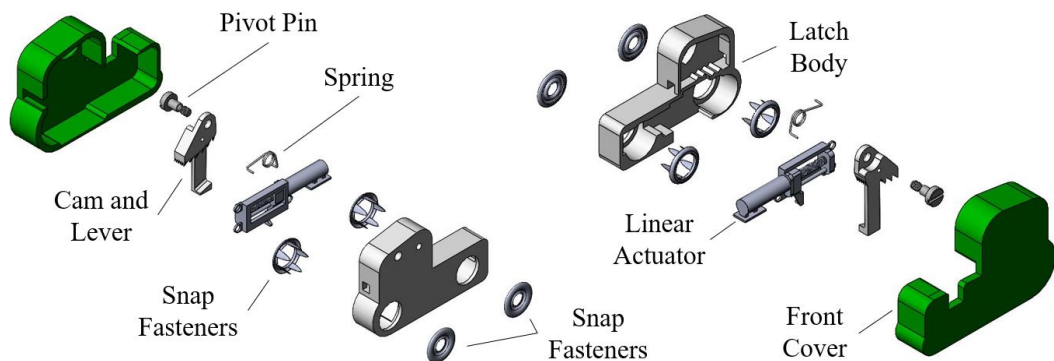


Figure 3.13: Cam design exploded view.

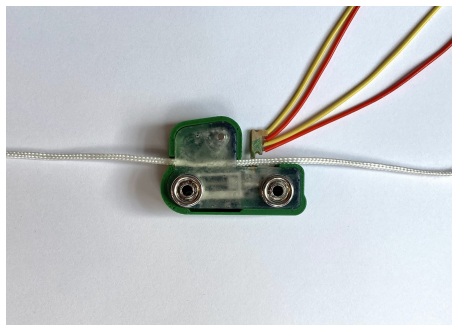


Figure 3.14: Completed cam latch assembly.



Figure 3.15: Polypropylene rope used with cam latch design.

3.3 Latch Dimensions Summary

The mounting area, height, volume, and mass of each latch are shown in table 3.1. Additionally, the cross-sectional area, width, and bend radius of each latch cable is shown in table 3.2.

Table 3.1: Latch dimensions and masses.

Test	Latch Dimensions		
	Motor	Ratchet	Cam
Mounting area (mm ²)	932 ± 10	782 ± 6	899 ± 7
Height (mm)	41 ± 0.5	9.5 ± 0.2	10.5 ± 0.4
Volume x10 ³ (mm ³)	38.2 ± 0.5	6.3 ± 0.1	8.1 ± 0.1
Mass (g)	42.4 ± 0.2	8.9 ± 0.2	9.6 ± 0.2

Table 3.2: Cable cross sectional areas, widths, and minimum bend radii.

Test	Cable Characteristics		
	Motor	Ratchet	Cam
Cross Sectional Area (mm ²)	4.0 ± 0.3	1.5 ± 0.3	3.1 ± 0.3
Width (mm)	4.0 ± 0.2	1.5 ± 0.2	2.0 ± 0.2
Min Bend Radius (mm)	1.5 ± 0.2	3.0 ± 0.2	< 0.5 ± 0.2

Chapter 4

Methods

4.1 Objective

Testing was performed to assess the characteristics of each latch and assist in the evaluation of how well each latch met the stated performance requirements. For latch tensile tests, displacement was set for a range of values to induce forces, stresses, and strains in each latch-cable system, which were recorded using displacement and force measuring equipment. The goal with these tests was to perform a comprehensive characterization of each latching system to enable quantitative and qualitative evaluations of each latching system. These evaluations enabled a comparison of each latch with the state of the art, a comparison between each latching system, and an analysis of how well each latching system lent itself to integration into a TCA powered, soft, wearable robotic system.

4.2 Apparatus

Tensile tests were performed using a standard tensile testing machine (Instron, model #3365) with a 100 Newton (N) load cell (0.5% accuracy to 1/100 of reading, Instron 3300 series), 1 Kilo-newton (KN) load cell (0.5% accuracy to 1/100 of reading, Instron 3300 series), and pneumatic side-action grips (70 pound per square inch (psi), Instron #2732-006). For current and voltage measurements, an AstroAI AM33D digital multimeter was used.



Figure 4.1: Ratchet latch clamped into tensile testing machine.

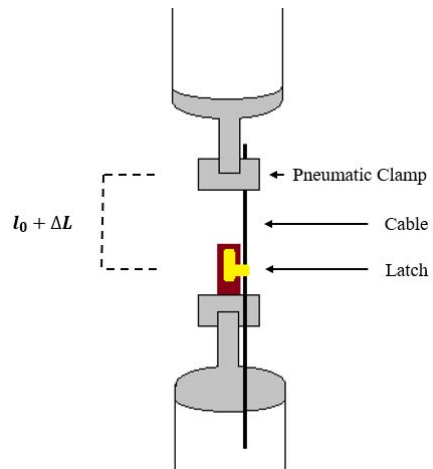


Figure 4.2: Experimental setup diagram of latch and cable configuration within the tensile testing machine.

4.3 Experimental Setup

To evaluate the capabilities of each latch, a number of tensile tests were performed with each latch in a variety of configurations. In each tensile test, the latch was fastened to a plastic plank with corresponding snap fasteners. The plank was clamped between the lower clamp of the tensile testing machine. For each latch, the corresponding cable was then run through the latch mechanism. One end of the cable was clamped between the upper clamp of the tensile testing machine with the other end of the cable unencumbered. This setup was used to approximate the use of each latch in conjunction with a TCA actuator.

An attempt was made to test each latch under the exact same conditions, however, due to the unique characteristics of each latch and each cable, some differences in testing existed from one latching system to the next. For instance, only the motor latch was capable of successfully engaging with the cable under high forces, thus the motor design was the only latch tested at specific target forces for several of the experiments. Additionally, the characteristics of the cam cable meant it slipped out of the clamps

Test	Force (N)											To Release
	0.1	1	2.5	5	10	15	20	30	40	50	60	
Tightening Speed & Force	■	■	■									
Static Hold	■	■	■	■	■	■	■	■	■	■	■	
Release Under Tension												
Ratchet Displacement		■										
Ratchet & Cam Release Forces												■

Latches: ■ Unpowered Motor ■ Powered Motor ■ Ratchet ■ Cam

Figure 4.3: Overview of the different experiments performed on each latch and the range of forces that were used for each experiment. The colored squares indicate whether a latch was tested in an experiment and for what force.

of the tensile testing machine during the cable stress-strain experiment, requiring yarn clamps for that specific test instead of pneumatic clamps. Aside from variations within each test, different tests were also occasionally required to characterize specific qualities of a given latch. For example, while the motor design performed both engagement and release using the same mechanism (the motor latch's stepper motor), the ratchet and cam designs both employed passive engagement designs with separate linear actuator powered release mechanisms. To fully characterize these release mechanisms, tests evaluating ratchet and cam lever release forces were performed only on the ratchet and cam designs. The motor design did not receive this test, as it did not contain a lever, therefore a lever release force could not be quantified for said design. Additionally, the discrete teeth of the ratchet design created a unique displacement profile that did not exist for the motor and cam designs. Therefore, a displacement test was performed on the ratchet design to characterize this property, with the other two designs not receiving this test. A full breakdown of which tests were performed for each latch design can be seen in figure 4.3.

The values of time, force, and displacement were recorded from the tensile testing machine for each experiment. The initial displacement between the clamping points of the machine was also recorded for each test. Values of stress σ and strain ϵ were calculated using:

$$\sigma = \frac{F}{A}, \quad \epsilon = \frac{\Delta L}{l_0}$$

where σ is stress, F is the force measured by the tensile testing machine, A is the cross

sectional area of the cable, ϵ is the strain of the latching system, ΔL is the change in length of the latching system as measured by the tensile testing machine, and l_0 is the initial length of the cable as measured between the clamps of the machine.

Each of the following subsections describes the specifics of latch characterization testing for each tensile testing experiment, as well as variations, where they exist, between the various tensile tests performed. Different tensile tests were needed to evaluate different latch characteristics, among them: the ability of each latch to maintain force and displacement over time, the time to release each latch for a given force, accuracy and precision of latch engagement, and the requisite actuator release forces for each latch. Additionally, various tests used to characterize latch cables and their utility in wearable systems are described below.

4.3.1 Tightening Latch Speed and Drag

The interaction between each latch and cable was evaluated to determine how each latching system would perform in the latch tightening phase of operation. To determine cable velocity when traveling through the latches in the tightening direction, each latch was placed in the bottom clamp of the tensile testing machine and the top end of each cable was placed in the top clamp, as described above. To the bottom end of the cable was affixed a mass of 100 g. The latch was oriented such that the cable would engage with the latch when pulled up. The top clamp that held the top end of the cable was then released, and the time taken for each latch to travel 100 mm was recorded. The maximum velocity reached by each cable was then calculated.

The drag force on each cable was also found using the tensile testing machine. The same setup as before was used, except the orientation of the latch was changed such that the cable would engage when traveling down. The latches were set to engage with the cables such that the cables were prevented from moving downwards. With the top end of each cable held between the top clamp, the tensile testing machine was programmed to move upwards at 2 mm/s for 10 seconds. The average force required to pull each cable through its respective latch was recorded. Three tests were run for each latch configuration for both the velocity and drag force experiments.

4.3.2 Static Hold

To evaluate the ability of each latch to maintain force and position over time, each latch was placed in the tensile testing machine and placed under load for 10 minutes at a time. The latch was oriented such that it would resist upward movement of the cable. The tensile testing machine was programmed to quickly increase the displacement of the latch until a target force was reached, then hold that displacement for 10 minutes. A range of target forces were used from 1 to 60 Newtons (N) to characterize the force holding abilities of each latch for a variety of likely wearable use force requirements. Forces above this range were not expected to be encountered in most soft, wearable applications, and testing forces below this range were thought to be well characterized by the 1 N testing given the characteristics of the specific latch designs evaluated in this research.

The free end of the cable was loaded with 100 grams (g) of mass, and the initial displacement between the latch and top clamp was 130 mm. The motor brake design was tested in two separate configurations for this test, once with one coil of the stepper motor energized, and once with the motor powered off. Three tests were run for each latch configuration and each force value for this experiment. The force and displacement over time were recorded by the tensile testing machine. Additionally, the vertical displacement of the free end of the cable was measured before tensioning, at the moment of target force being reached, and at 10 minutes just before the tension in the cable was released. After each set of three tests the force target was increased incrementally up to 60 N or until a latch failed to reach the target force.

4.3.3 Latch Release Under Tension

For this experiment, the initial setup was the same as for the static hold, with a 100 g mass affixed to the free end of the cable, the latch resisting upward movement of the cable, and displacement of the tensile testing machine set to increase until a target force was reached. Target forces used were between 1 to 50 N, or until a latch failed, with target forces chosen for their utility in fully characterizing each latch and their applicability in wearable designs. Unlike with the previous experiment, instead of holding said displacement for 10 minutes, each latch was set to release the tension in the cable 15

seconds after reaching the target force. The ability of the latch to successfully release was recorded, and if the latch released the tension successfully then the time taken to release the latch was recorded. Release time was measured from the moment the release signal was sent to the latch to the moment the force, as measured by the tensile testing machine, passed below 10% of target force. The motor was tested with only the one coil powered configuration for this experiment. Three tests were again run for each latch configuration and for each target force.

4.3.4 Displacement Characterization of Ratchet

Due to the discrete latching displacement of the ratchet latch, an additional test was performed to characterize its displacement. For this test, a 100 g mass was attached to the free end of the cable, and the latch was oriented to prevent the cable from moving down. The tensile testing machine was set to move up and back down, increasing the amplitude of displacement by 0.2 mm every cycle. A video was taken of the free end of the cable, which moved up every time the top clamp of the tensile machine moved up, and moved down with the tensile testing machine except for when the teeth of the latch engaged the next groove of the cable. The video was used to identify the number of cycles between each new groove, and thereby characterize the precision and accuracy of the latch. The test was repeated for 85 cycles of the tensile testing machine, representing a final displacement of 17 mm. This displacement and number of cycles was chosen to provide enough teeth engagement steps to characterize the displacement characteristics of the ratchet latch.

4.3.5 Characterization of Latch Release Forces For Ratchet and Cam Designs

Latch disengagement was achieved differently in the different latches. For the motor brake design, the coils simply needed to be activated to allow the cable to release its tension, but for the ratchet and cam designs the teeth of each latch needed to be physically disengaged from the cable. This disengagement required a force, which this experiment sought to characterize. Thus, only the ratchet and cam designs were tested in this experiment.

Due to the design of the ratchet and cam latches, the layout of the tensile testing was changed so that the latch attachment plank was clamped between the top latch and one end of the cable was clamped between the bottom clamp with the other end free. The latch was oriented such that the cable was prevented from moving downward. This position was chosen so that the lever arm to release each latch would disengage by traveling downwards. Similar to previous tests, the tensile testing machine was programmed with a force target ranging from 1 to 50 N or until the latch failed. The force as measured by the tensile testing machine was kept constant by varying the displacement to keep a constant tension in the cable. Weights were then hung from the lever release arm of the latch. The weight hung from the arm was incremented by 10 g at a time until the latch successfully disengaged with the cable and the force measured by the tensile testing machine dropped to below 10% of the original target force. This test was repeated three times for each target force for both the ratchet and cam designs.

4.3.6 Cable Characterization

Each latch cable was evaluated for wearability. Testing was performed to quantify wearability metrics, such as the bending radius of each cable, the stress-strain relationship in each cable, the static friction each cable would experience sliding across a garment, and the pressure each cable would generate based on its surface area relative to a given body part where latching was likely to occur. The specific tests performed to quantify cable wearability is presented in this section.

For characterizing the cables used in each latching design, the relationship between stress and strain was evaluated. Each end of the cable was clamped between the top and bottom clamps of the tensile testing machine with the 1 KN load cell. The displacement of the machine was increased at a rate of 2.0 mm/s until either the machine reached 1 KN of force or the cable broke. Stress and strain were then calculated as described above.

The coefficient of static friction of each cable against a garment was evaluated. Such

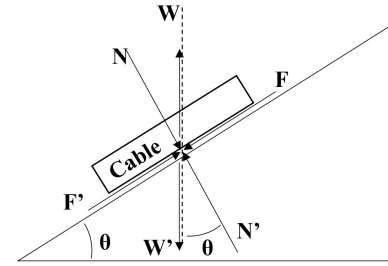


Figure 4.4: The forces on an inclined plane which can be used to derive the coefficient of static friction.

an evaluation is used to explore the specific wearability of each cable. For example, a cable with high static friction used in a wearable setting may pull garments along with the cable during the latching process. Such undesired garment motion can cause discomfort for the wearer and decrease the effectiveness of a given latch by reducing effective displacement. The coefficient of static friction of each cable was therefore considered important to fully characterize the wearability of each latch design. The coefficient of static friction of each cable was evaluated by placing a segment of each cable upon a surface of 100% polyester knitted fabric sheet. Polyester was chosen due to its common usage in wearable fabrics, thus it was used as a reference point for how each cable would interact with any worn garment. A more comprehensive evaluation of cable static friction against a range of fabric types is a matter of future research. For the test, the surface was slowly rotated until the cable segment began to slip, at which point the angle between the surface and the horizontal plane was measured (see figure 4.4). The equations for normal force N' and friction force F' :

$$F' = W' \sin(\theta), \quad N' = W' \cos(\theta)$$

were used to derive an equation for coefficient of static friction μ_s with respect to slope θ :

$$\mu_s = \frac{F'}{N'} = \frac{W' \sin(\theta)}{W' \cos(\theta)} = \tan(\theta)$$

This test was repeated three times for each cable, and an additional three times for the cables with teeth or grooves to evaluate the coefficient of static friction on both the smooth and toothed/grooved sides.

The pressure of the cable on the human body was also evaluated using circumferential pressure. Using figure 4.5 as reference, the circumferential pressure, or hoop pressure, was calculated using the equation for hoop stress in a cylinder wall:

$$\sigma_\theta = \frac{F}{t * l}$$

where F is the tensile force on the cylinder exerted circumferentially, t is the radial thickness of the cylinder, and l is the axial length of the cylinder.

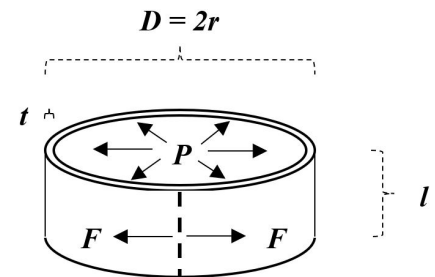


Figure 4.5: Diagram of the relevant parameters for calculating circumferential pressure on a cylinder.

Using the thin-walled assumption for the cable (when $D/t > 20$) the Young-Laplace equation could be used:

$$\sigma_\theta = \frac{P * r}{t}$$

where P is the internal pressure and r is the mean radius of the cylinder. Solving for the internal pressure results in:

$$P = \frac{F}{r * l}$$

Internal pressure, or hoop pressure, represents the force per unit area that is exerted by a cable onto whatever surface the cable is wrapped around. This is useful for determining for what cable tensions a potentially dangerous pressure will be generated, for example on a human extremity where high pressures could result in a decrease of blood flow to said extremity.

4.4 Experimental Parameters

The parameters of the two actuators used in the three design is shown in table 4.1. The value of force of the 28BY J-48 stepper motor was measured using the tensile testing machine. One end of the motor latch cable was placed into the upper clamp of the machine, with the latch placed in the lower clamp. The motor was programmed to turn, and the force of the motor latch was recorded. The force of the linear actuator was found in a similar way, with the linear actuator placed in the lower clamp of the tensile testing machine and one end of a cable clamped in the upper clamp. The other end of the cable was tied around the linear actuator. The linear actuator was turned on and the force it generated was recorded.

Current and voltage draw were measured using a digital multimeter, with the results recorded in table 4.1. The power draw of the two actuators was measured using:

$$P = I * V$$

where P represents power, I represents current, and V represents voltage. The available operating time of each actuator was also calculated using the charge of an Energizer Industrial 9V battery as reference. The milliamp-hours were found from the battery datasheet [68], and the time that the actuators could remain active was calculated using:

$$T = I/C$$

Table 4.1: Power characteristics of the stepper motor and linear actuator. Charge and time were calculated using a 9V Energizer Industrial battery [68].

Motor	Force (N)	Current (A)	Voltage (V)	Power (W)	Charge (mAh)	Time (hr)
Linear Actuator	1.47	0.130	3	0.39	460	3.5
28BY J-48 Stepper	7	0.075	12	0.90	525	7

Table 4.2: Average circumferences of various body parts likely to be used as mounting locations for wearable applications [69, 70].

Measurement	Arm	Waist	Hip	Thigh	Calf
Circumference (mm)	325	850	1025	550	375

where T is time, I is current, and C is charge. The speed of the motor and linear actuator were also recorded. The stepper motor was found to rotate at 0.25 mm/s, resulting in the cable moving at 6 mm/s. The linear actuator was found to move at 1.67 mm/s.

To enable an evaluation of how much pressure a given cable tensile forces might impart on a human body part, hoop pressures were calculated. The average circumferences of various body parts were taken from Heymsfield et al [69] and Polymeris et al [70]. The circumference values used for each body part are shown in table 4.2. These values were used to calculate hoop pressure for each design.

Chapter 5

Experimental Results

The results of the experiments described in chapter 4 are shown and explored in this chapter. Each experiment was performed multiple times, with the average values of each test result being indicated in the various tables and figures of this chapter. Standard deviation values between experiments are given in the text, tables, and figures when such information is valuable and can be shown without detracting from the presentation of the data.

5.1 Latch Tightening and Engagement

The ability of each latch to adjust displacement and engage with cables on command is evaluated in this section. First, the characteristics of latching displacement are evaluated. The speed with which cables were able to move through each latch was tested, as well as the force required to pull each cable through the latches. These results are shown in table 5.1, where velocity and force were measured as positive in the direction of travel of the cable and drag force measured as positive opposite the direction of travel of the cable. The motor design was significantly slower than the ratchet and cam designs when moving the cables through the latch. The passive torque of the motor and the constant engagement of the motor cable with the pulley meant that the cable was only able to pass through the latch as fast as the motor was able to turn. In contrast, the ratchet and cam designs only engaged with their cables in the latching direction, so when pulled in the tightening direction these latches imparted very little resistance,

Table 5.1: Velocity and drag forces for each latch. Drag force is positive in the direction opposite to the direction of cable displacement.

Measurement	Motor	Ratchet	Cam
Velocity (mm/s)	6.0 ± 1.0	> 100	> 100
Drag Force (N)	-6.8 ± 0.2	0.14 ± 0.05	0.93 ± 0.05

allowing the cables to move quickly through the latches. However, some resistance did exist, which was recorded as drag force on the cable. This value was highest in the cam design, which imparted a drag force of 0.93 ± 0.05 N on the cable. The drag force was measured when the cable and latch were aligned vertically, however analysis of drag forces when the cable was aligned at an angle to the latch showed forces could increase significantly in non-optimal orientations. The mechanics of the motor design imparted a force on the cable of 6.8 ± 0.2 N creating a negative drag force.

The ability of each latch to engage with the cable was evaluated for a range of target forces. Using the static hold tensile test described in chapter 4, it was found that for all three latches, each latch would reliably engage with the cable below 15 N of tensile force. However, after 15 N the ratchet and cam latches both failed to latch onto the cable.

One of the primary ways effective latching was measured was through the strain experienced by the latching systems. The values of measured strain are plotted in figure 5.1 showing the strain response of each latch configuration between 1 N and 60 N. The same plot showing strain for target forces up to 15 N can be seen in figure 5.2. The stress found in each cable was plotted in addition to force. This can be seen in figure 5.3.

The majority of strain experienced by each system was observed to occur within the first 20 seconds of the 10 minutes of the static hold test, with relatively small strains seen for the remaining time between 20 seconds and 10 minutes. This strain was measured between the upper and lower clamps of the tensile testing machine. As can be seen from the plots, the two motor configurations consistently exhibited lower strains than the other two designs for the same target forces. Both configurations experienced similar strains to each other up to around 35 N, at which point the unpowered motor

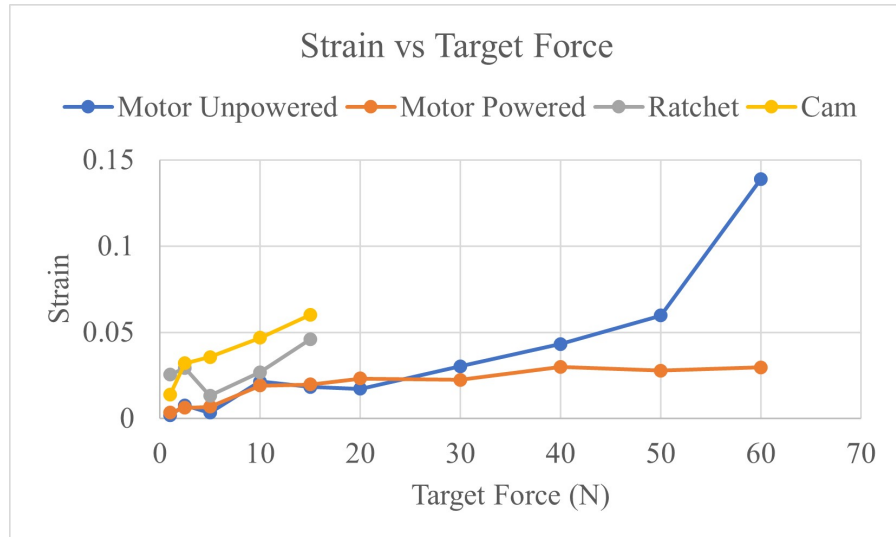


Figure 5.1: Relationship between strain and force for each latch configuration.

configuration experienced significantly higher strains than the powered motor configuration.

The ratchet and cam designs experienced similar strains for target forces of 1 N and 2.5 N, however at higher forces the ratchet design consistently experienced less strain than the cam design. The reasons for these differences in strain are explored throughout this section.

5.1.1 Causes of Strain

The strain represented in these figures was the result of several displacement modes, primarily: slack in the latch system and snap fasteners, stretch in the cables, and the cables slipping in the latches after partial engagement.

Slack

To characterize the slack, the strain under low force loads was analyzed as the cables exhibited much less strain under low loads and were never seen to slip under low loads. Slack was seen in both the attachment mechanism of the snap fasteners and in the

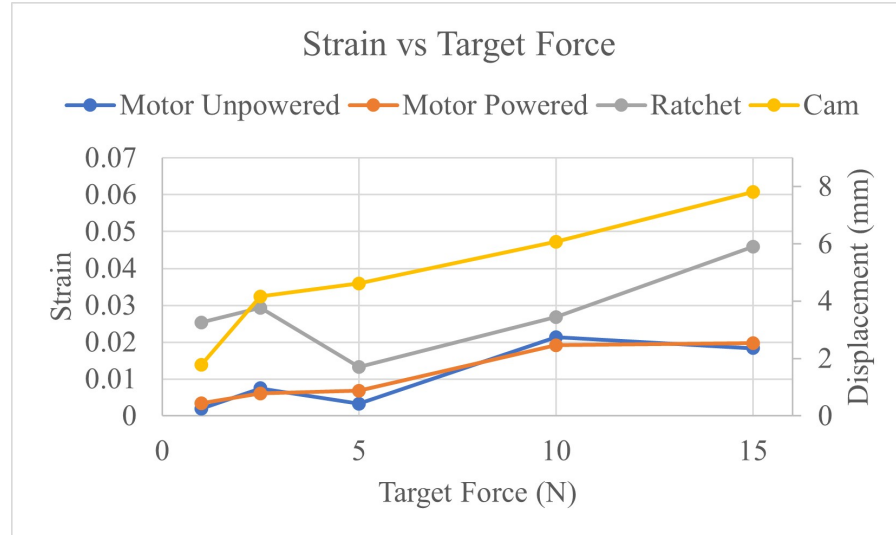


Figure 5.2: Relationship between strain and force for each latch configuration for 1 to 15 N.

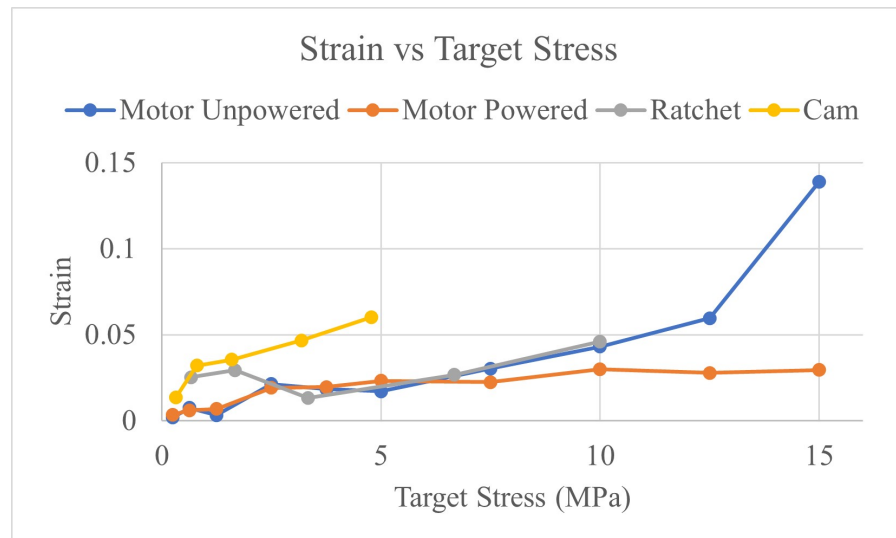


Figure 5.3: Relationship between strain and stress for each latch configuration.

latching devices themselves. Measurements of the latch position relative to the attachment points showed all three latches moving 1.0 ± 0.5 mm when under tension versus when they were unlatched and untensioned. These measurements were taken using snap fasteners mounted to a rigid plank held in place by the clamps of the tensile testing machine. However, a real world application of these latches would likely have them attached to fasteners mounted to fabric, which could increase the slack of the latching system.

In addition to the slack present in the snap fasteners was slack in the latching mechanisms themselves. For the motor design, each step of the stepper motor represented 0.01 mm of travel for the cable through the latch. More significantly, the cable was found to have a 0.5 ± 0.2 mm of slack relative to the teeth of the pulley.

For the ratchet mechanism, slack existed due to the way the teeth of the latch engaged with the latch cable. To quantify the precision of the teeth engagement, the data from the displacement characterization of the ratchet latch was analyzed and plotted in figure 5.4. In this test, the tensile testing machine was programmed to raise and lower once per cycle. The displacement of the free end of the cable on the other end of the latch was simultaneously measured. A theoretically perfect latch would be measured to perfectly match the displacement of the tensile testing machine, while a non-perfect latch would have a measurable displacement difference, measured as slack. The tensile testing machine returned back to a displacement of zero between each cycle, meaning that engagement of the latch was the only force on the cable between each cycle. It was found that, over several cycles, the ratchet design was able to engage a new groove only after the groove had fully passed the teeth. The groove had to have passed the teeth an average of 0.98 ± 0.23 mm before the groove was successfully able to engage with the tooth. This is because of the geometry of the grooves and teeth, with the flat side of the ratchet teeth not perfectly normal to the cable, but instead slightly angled to prevent the grooves from sliding past the teeth while engaged. This meant that once a groove successfully slid past a tooth, the cable had to travel backwards a distance before being engaged by the ratchet teeth, with this distance being the 0.98 ± 0.23 mm mentioned. The average displacement between each latching engagement was found to be 1.99 ± 0.02 mm. This displacement, in addition to the slack from the snap fasteners, explains the strain experienced by the ratchet latch for forces below 10 N.

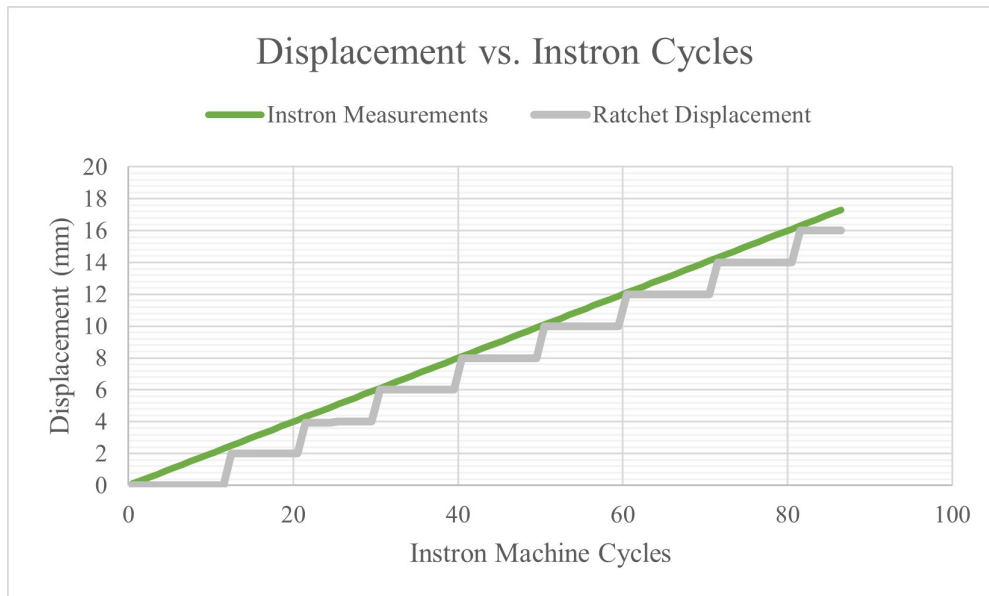


Figure 5.4: Characterization of teeth engagement for the ratchet design. The green Instron machine measurements represent the theoretical perfect displacement response, while the gray line represents the ratchet designs actual engagement response

For the cam latch design, the slack of the latching mechanism existed due to the cam needing to rotate before engaging with the cable. This can be seen in figure 5.5, with the un-tensioned and tensioned orientations of the latch. In the process of engaging with the cable, the cam latch allowed the cable to travel 1.0 ± 0.5 mm, contributing to the strain seen. However, for the cam latch, the snap fastener slack and cam rotation do not fully explain the strain seen for low target forces. Additional strain contributions are needed to fully explain the operation of the cam latch design.

Cable Stretch

The second major cause of strain was the stretch in the cables, which was characterized by measuring the difference in displacement measured above the latch and below the latch. The difference between the two values can be seen in figures 5.6 (force) and 5.7 (stress). These results show to what degree the movement of the top clamp corresponded to the movement of the free end of the cable below the latch. If the cables experienced no strain it would be assumed that these two values would be equal. This was seen to

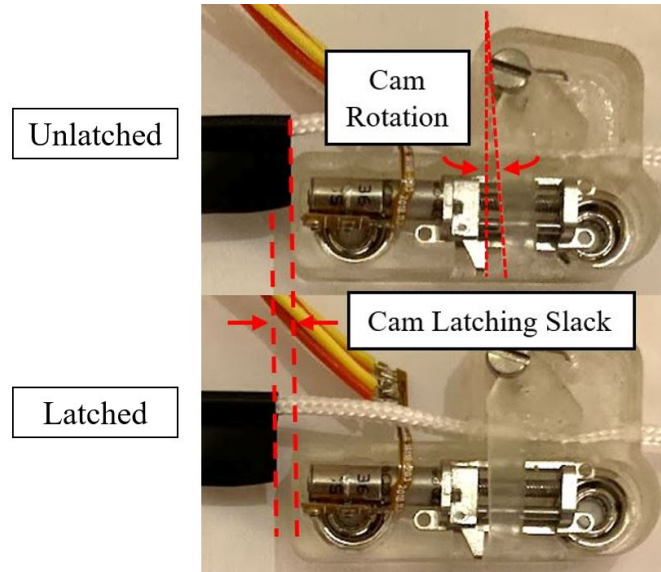


Figure 5.5: Comparison of cam rotations before and after cable engagement for the cam latch design.

be the case for the motor configurations, and for the ratchet design below 5 N. However, this did not hold true for the ratchet design above 5 N or the cam design for any target force. This suggests that the cable in these designs was stretching: experiencing high strain at low stresses. Stress-strain analysis was thus performed on each of the cables used, with results shown in figure 5.8. The yield stress of each cable is shown in table 5.2.

The yield stress measured for the motor cable was found to occur when the teeth of the cable began to shear, resulting in the cable slipping through the clamps of the tensile testing machine at 20.14 ± 1.20 MPa. This represented a critical failure of the cable, as without the cable teeth the latch would be unable to engage with the cable. The yield stress of the ratchet cable was found to be the lowest of the three cables tested at 7.85 ± 0.13 MPa. Unlike the motor cable, the grooves of the ratchet cable did not significantly contribute to yield stress. Instead, the entire cable plastically deformed. Notably, this yield stress was below the stress values experienced by the latch in several tests, indicating that the ratchet cable was consistently operating above its yield point during latch evaluation.

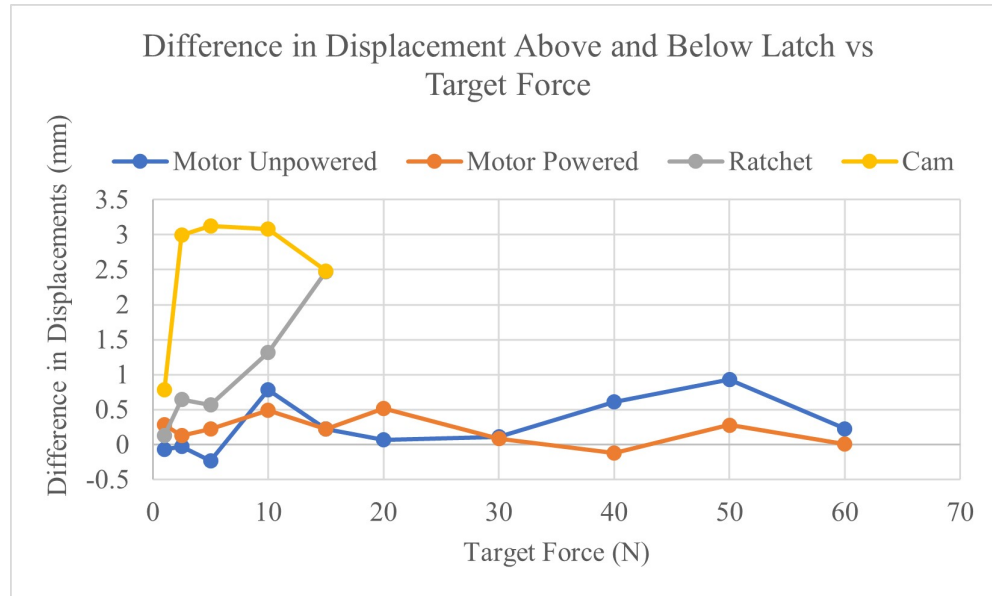


Figure 5.6: The difference in displacement measurements taken above and below each latch for a range of target forces.

The yield stress of the cam cable could not be determined, as the cam cable did not break even up to the 1 kN tensile testing machine limit, however it was found to be greater than 315 MPa. Despite this high yield point, the cable experienced very low stress values even at high strains. The stress in the cam cable did not equal that of the ratchet cable until a strain of 0.08 and a stress of over 15 MPa. Additionally, the cam cable was found to break under lower stresses under certain conditions. When the cam cable was held in the tensile testing machine using yarn clamps at a 90 degree angle, the cable was found to break at 183.03 ± 11.26 MPa, indicating that the orientation of the cable had a significant impact on yield stress.

The stress-strain relationships found helps explain the difference in displacements above and below the latches, with the differences in strains measured for the ratchet and cam cables closely matching the stress-strain curves of those cables. However, the difference in displacement experienced by the cam at higher forces is not well explained by cable properties. Instead, the decrease in strain in the cam design may be the result of the cable slipping through the latch at higher forces, resulting in the difference between the clamped and free ends of the cable becoming smaller. This is explored more below.

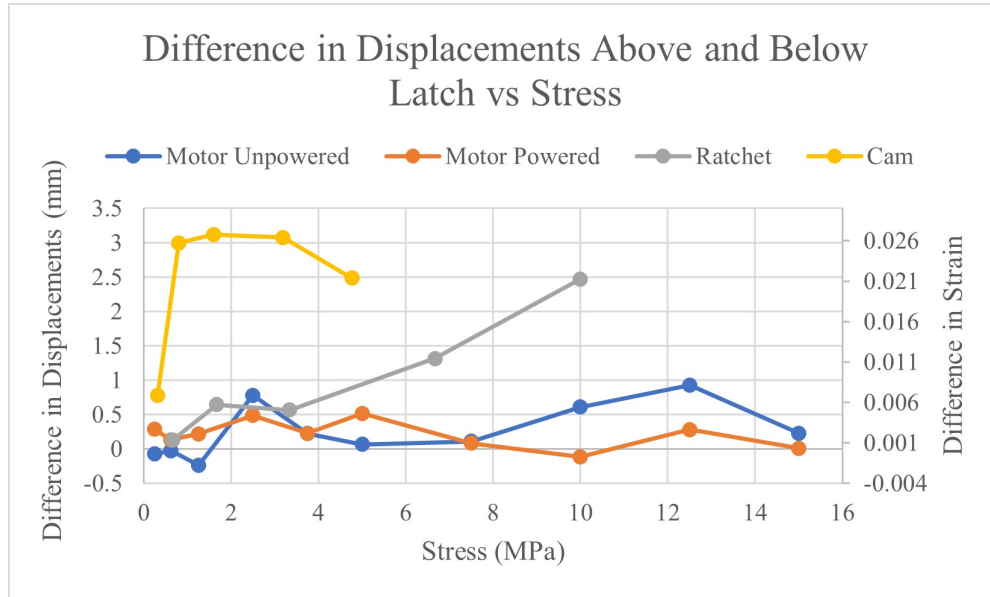


Figure 5.7: The difference in displacement measurements taken above and below each latch for a range of cable stresses.

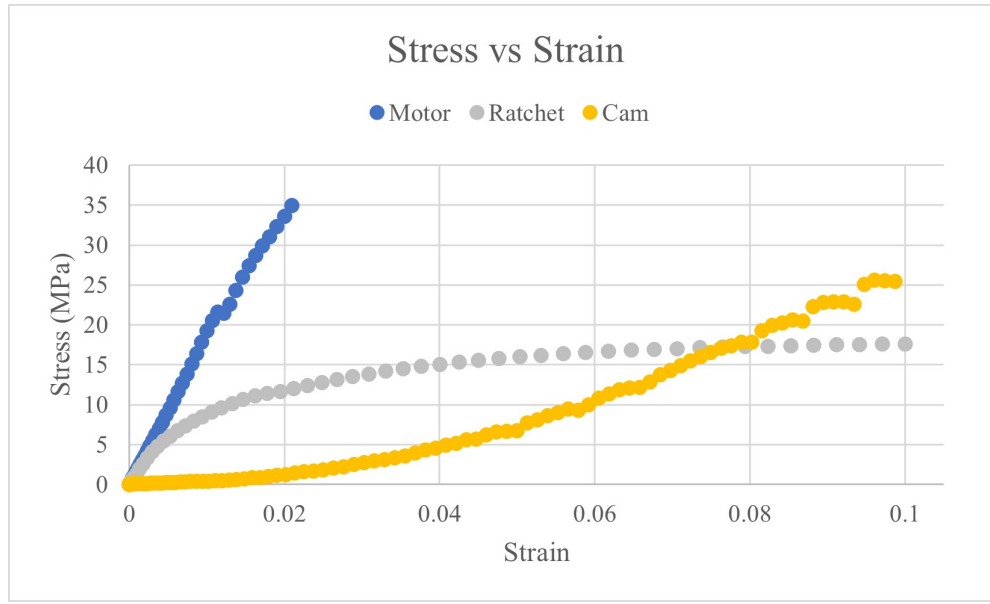


Figure 5.8: Stress versus strain for each latch cable. The motor cable was a chloroprene rubber toothed timing belt with fiberglass reinforcements; the ratchet cable was a Nylon-66 grooved cable tie cable; the cam cable was a polypropylene braided yarn.

Table 5.2: Cable yield stress in megapascals.

Yield Stress (MPa)		
Motor	Ratchet	Cam
20.14 ± 1.20	7.85 ± 0.13	>315

Cable Slipping

The third contributing factor to strain was the cables slipping through latches after having been partially engaged. This occurred for different reasons and under different stresses for each latch. Some example failures modes are shown in figures 5.9, 5.10, and 5.11. The unpowered configuration of the motor latch failed when the tension in the cable produced a torque that overcame the static torque of the unpowered motor. It was found that, at around 50 N of tension in the cable, the motor would rotate slightly, releasing tension in the cable, before remaining static again. The magnetic coils of the stepper motor appeared to apply a braking force, even when unpowered, so that even when the motor slipped it quickly returned to rest. In the example shown in figure 5.9 the motor slipped several times before finally being able to hold the cable in place. The powered motor configuration never exhibited this failure mechanism, and the cable in this configuration was never seen to slip during testing up to 60 N. The yield point of the motor cable was not believed to have contributed to the slipping of the cable as the stress in the cable only approached 15 MPa, still well below the yield stress of the cable.

The failure of the ratchet latch to engage with the cable appeared to be the result of grooves in the cable pushing the teeth of the latch out of the way, consequently releasing all of the tension in the cable. As seen in figure 5.10, the ratchet design consistently failed to latch at around 16.5 N. Additionally, 16.5 N of tension in the ratchet cable represented 11 MPa of stress, which was above the yield stress of the cable. It is possible that local stresses in the cable were even greater, increasing the strain of the cable and allowing the cable to slip through the latch.

The failure of the cam design to engage with the cable was also due to the cable slipping through the latch. Unlike the ratchet, the cam design did not release all of its

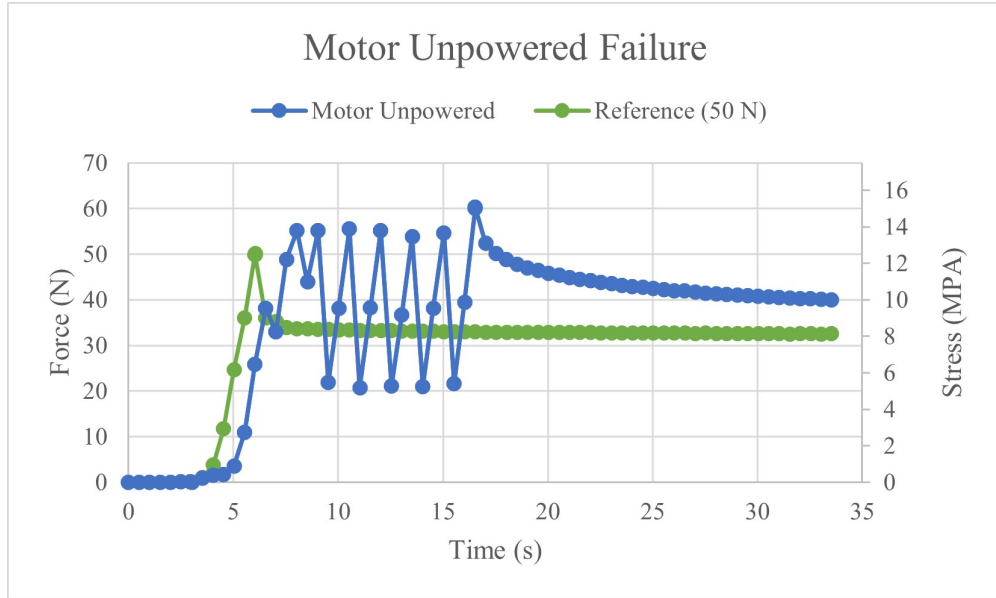


Figure 5.9: Failure characteristics of the unpowered configuration of the motor design represented by the blue data points. The green data points represent a similar test conducted with a target force of 50 N where the design did not exhibit any failure modes.

force at once, instead only releasing a small amount of tension, allowing the cable to slip while not releasing the cable entirely. This was in part due to the material and design of the teeth of the cam design. The soft plastic teeth quickly wore down during testing, reducing their ability to hold high forces. As the cable began to slide, the teeth wore out faster, further reducing the ability of the latch to engage with the cable. The beginning of the cable slipping through the cam latch can be seen in figure 5.11 between 7 and 10 seconds, where the force measured by the tensile testing machine repeatedly increased and decreased.

5.2 Latch Holding

Each latch was evaluated for its ability to maintain force and displacement over ten minutes to determine the long term ability of each latch to maintain force and displacement. For this test, the strain of the latch cable was increased until the target tension

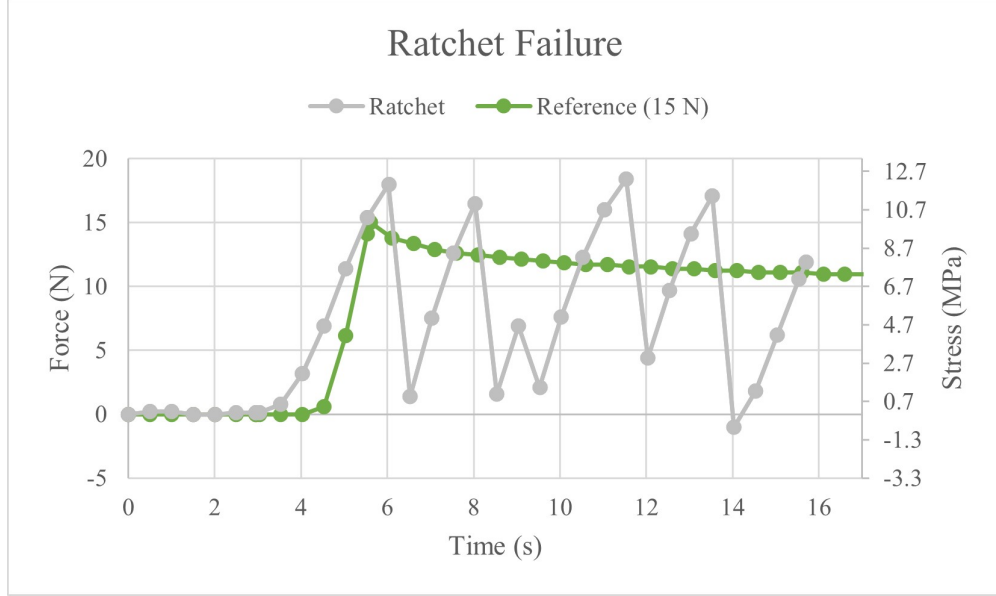


Figure 5.10: Failure characteristics of the ratchet design represented by the gray data points. The green data points represent a similar test conducted with a target force of 15 N where the design did not exhibit any failure modes.

in the cable was reached, at which point the cable displacement was held constant for 10 minutes. The tension in the cable was measured for those 10 minutes. An example test of each latch for each target force is shown in figures 5.12 and 5.13 for the unpowered motor configuration, figures 5.14 and 5.15 for the powered motor configuration, figure 5.16 for the ratchet design, and figure 5.17 for the cam design. Data on the force and stress held by each latch for each target force is also shown in tables 5.3 and 5.4 for the unpowered motor configuration, tables 5.5 and 5.6 for the powered motor configuration, tables 5.7 and 5.8 for the ratchet design, and tables 5.9 and 5.10 for the cam design. These tables show the peak force value reached for each latch and target force, as well as forces measured at 6, 60, and 600 seconds after the peak force was measured. The percent decrease in force from the peak force to the forces at 6, 60, and 600 seconds is also shown. Each test for each latch was performed three times, with deviations between tests indicated by standard deviation in the tables.

The unpowered motor configuration after 10 minutes held up to 36 N or 9 MPa. The powered configuration performing slightly better, reaching a maximum held force of 44 N

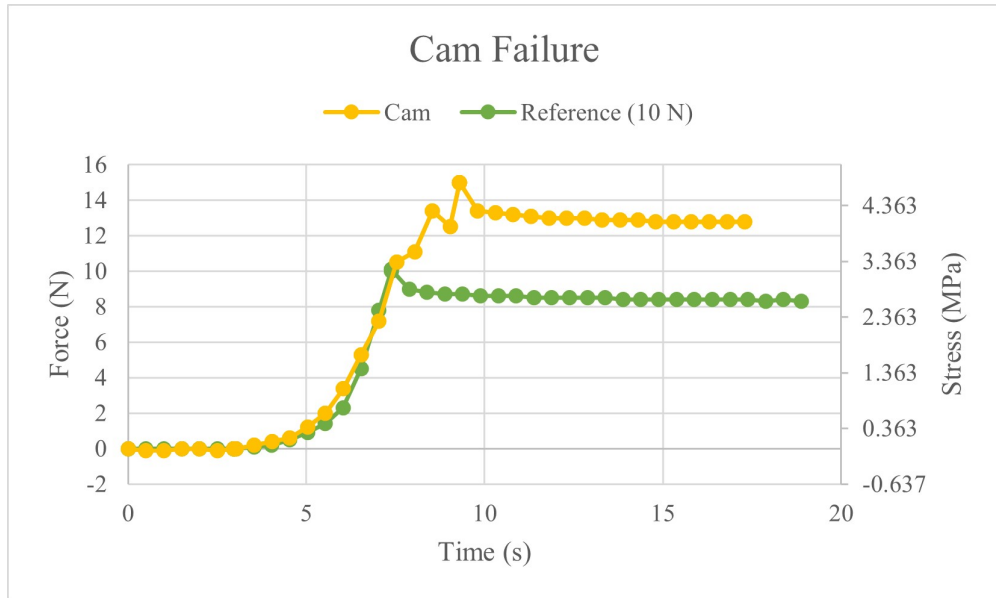


Figure 5.11: Failure characteristics of the cam design represented by the yellow data points. The green data points represent a similar test conducted with a target force of 10 N where the design did not exhibit any failure modes.

or 11 MPa. Below these limits both motor configurations demonstrated relatively little drop in force during the 10 minute test, generally losing between 10 and 20 percent of the peak force with most of this loss occurring within the first six seconds. The ratchet design performed worse, consistently losing 40 % of peak force after 10 minutes, with losses continuing well past the initial six seconds. Interestingly, the largest percent force drop occurred for the 1 N target force tests, though the majority of force lost at this target force occurred in the first six seconds, suggesting the latch was the most stable at this low force value. The cam design performed similarly to the motor design, holding almost as much force over 10 minutes. Like the motor design, the majority of the force decrease occurred in the first six seconds, and like the ratchet design the cam latch lost the largest percentage of force at a target force of 1 N, though the amount of force lost was relatively small.

The final force and stress held for the four latch designs and configurations is shown in figures 5.18, 5.19, and 5.20. These results show that the ratchet design consistently held the least amount of force and stress at the end of the 10 minutes, with the two

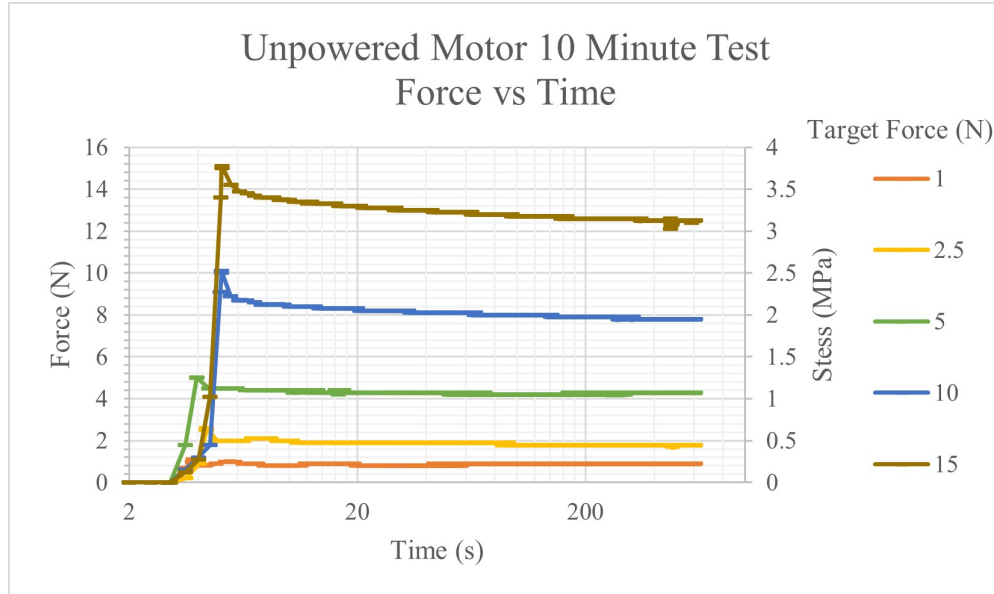


Figure 5.12: Measurements of tensile force taken over 10 minutes for the unpowered motor latch (target forces between 1 and 15 Newtons).

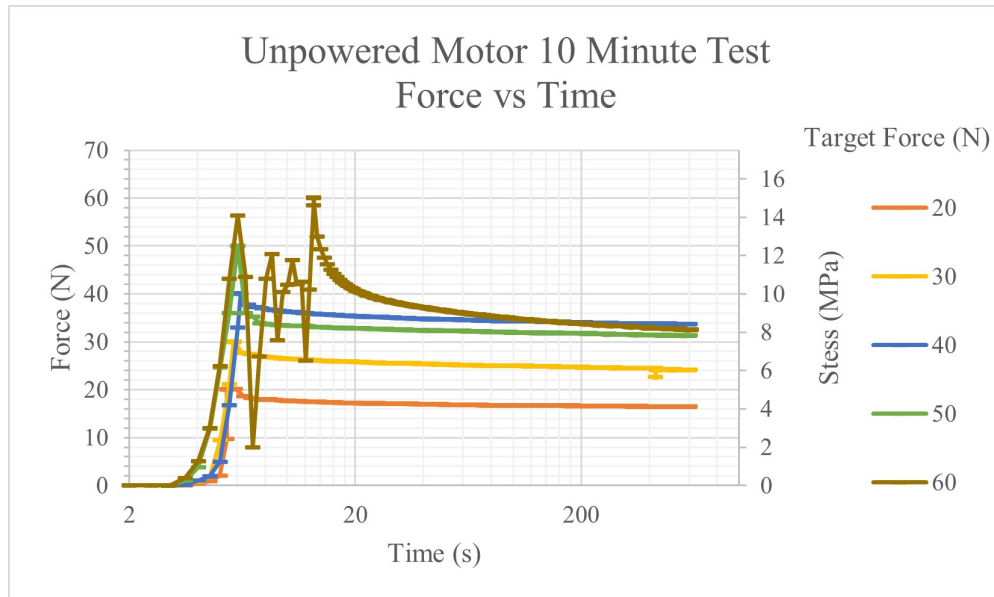


Figure 5.13: Measurements of tensile force taken over 10 minutes for the unpowered motor latch (target forces between 20 and 60 Newtons).

Table 5.3: Results of 10 minute tensioned hold experiment for the unpowered motor configuration. Measured values of tensile force as measured by the tensile testing machine are shown for values of peak force, force measured six (6) seconds after peak force, 60 seconds after peak force, and the final force measured at ten minutes (600 seconds) after peak force. The percent of force lost relative to the peak force measured is also shown.

Target Force (N)	Peak Force (N)	6 Seconds		60 Seconds		600 Seconds	
		Force (N)	% Decrease	Force (N)	% Decrease	Force (N)	% Decrease
1.0	1.3 ± 0.10	1.0 ± 0.10	23.1 ± 2.31%	1.0 ± 0.15	20.5 ± 3.03%	1.0 ± 0.15	20.5 ± 3.03%
2.5	2.7 ± 0.12	2.1 ± 0.23	20.0 ± 2.17%	2.1 ± 0.29	22.5 ± 3.14%	2.0 ± 0.26	25.0 ± 3.31%
5.0	8.2 ± 0.85	7.3 ± 0.78	11.3 ± 1.21%	7.1 ± 0.75	13.4 ± 1.41%	7.1 ± 0.69	13.8 ± 1.34%
10	10.6 ± 0.25	9.1 ± 0.10	13.9 ± 0.15%	8.8 ± 0.06	17.0 ± 0.11%	8.6 ± 0.06	18.9 ± 0.13%
15	16.0 ± 0.46	14.2 ± 0.61	11.5 ± 0.49%	13.6 ± 0.72	14.8 ± 0.78%	13.4 ± 0.67	16.5 ± 0.82%
20	21.1 ± 1.00	18.3 ± 0.53	13.4 ± 0.39%	17.5 ± 0.62	17.2 ± 0.61%	17.0 ± 0.81	19.4 ± 0.93%
30	30.9 ± 0.61	26.9 ± 2.15	13.1 ± 1.04%	25.9 ± 2.18	16.3 ± 1.37%	25.2 ± 2.38	18.6 ± 1.75%
40	40.3 ± 0.12	36.2 ± 1.15	10.2 ± 0.32%	34.7 ± 1.60	13.7 ± 0.63%	33.8 ± 2.00	16.1 ± 0.96%
50	51.7 ± 1.48	38.5 ± 5.27	25.5 ± 3.48%	37.1 ± 4.67	28.2 ± 3.54%	36.0 ± 4.14	30.3 ± 3.48%
60	63.7 ± 1.45	34.2 ± 20.09	46.3 ± 27.19%	29.7 ± 16.31	53.4 ± 29.30%	27.7 ± 14.53	56.4 ± 29.56%

Table 5.4: Unpowered motor configuration cable stress measurements for six (6) seconds after peak stress, 60 seconds after peak stress, and the final stress measured at ten minutes (600 seconds) after peak stress.

Target Stress (MPa)	Peak Stress (MPa)	6 Second Stress (MPa)	60 Second Stress (MPa)	600 Second Stress (MPa)
0.25	0.3 ± 0.03	0.2 ± 0.03	0.3 ± 0.04	0.3 ± 0.04
0.625	0.7 ± 0.03	0.5 ± 0.06	0.5 ± 0.07	0.5 ± 0.07
1.25	2.1 ± 0.21	1.8 ± 0.20	1.8 ± 0.19	1.8 ± 0.17
2.5	2.6 ± 0.06	2.3 ± 0.03	2.2 ± 0.01	2.1 ± 0.01
3.75	4.0 ± 0.11	3.5 ± 0.15	3.4 ± 0.18	3.3 ± 0.17
5.0	5.3 ± 0.25	4.6 ± 0.13	4.4 ± 0.16	4.3 ± 0.20
7.5	7.7 ± 0.15	6.7 ± 0.54	6.5 ± 0.55	6.3 ± 0.59
10.0	10.1 ± 0.03	9.0 ± 0.29	8.7 ± 0.40	8.4 ± 0.50
12.5	12.9 ± 0.37	9.6 ± 1.32	9.3 ± 1.17	9.0 ± 1.04
15.0	15.9 ± 0.36	8.6 ± 5.02	7.4 ± 4.08	6.9 ± 3.63

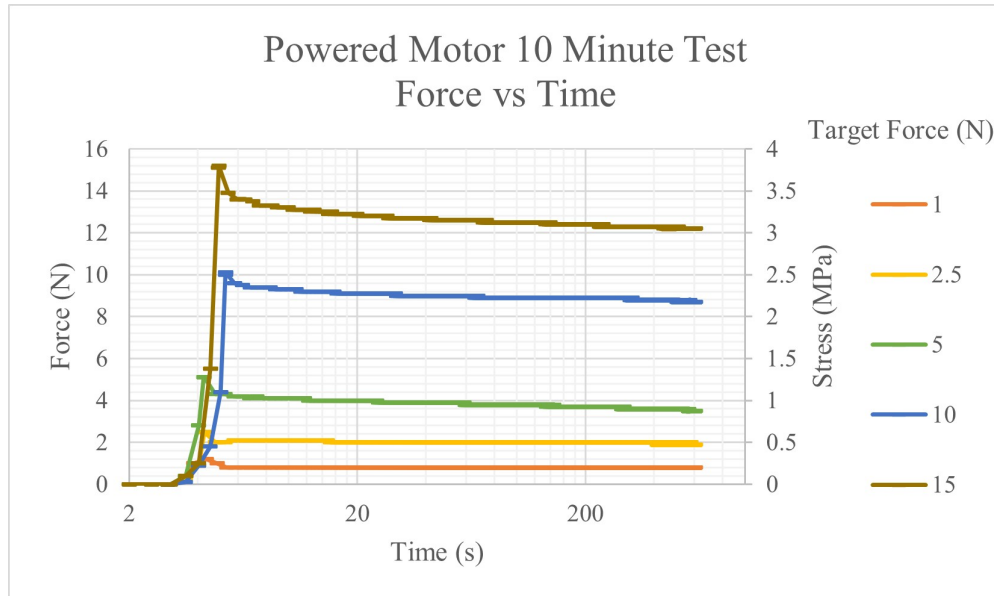


Figure 5.14: Measurements of tensile force taken over 10 minutes for the powered motor latch (target forces between 1 and 15 Newtons).

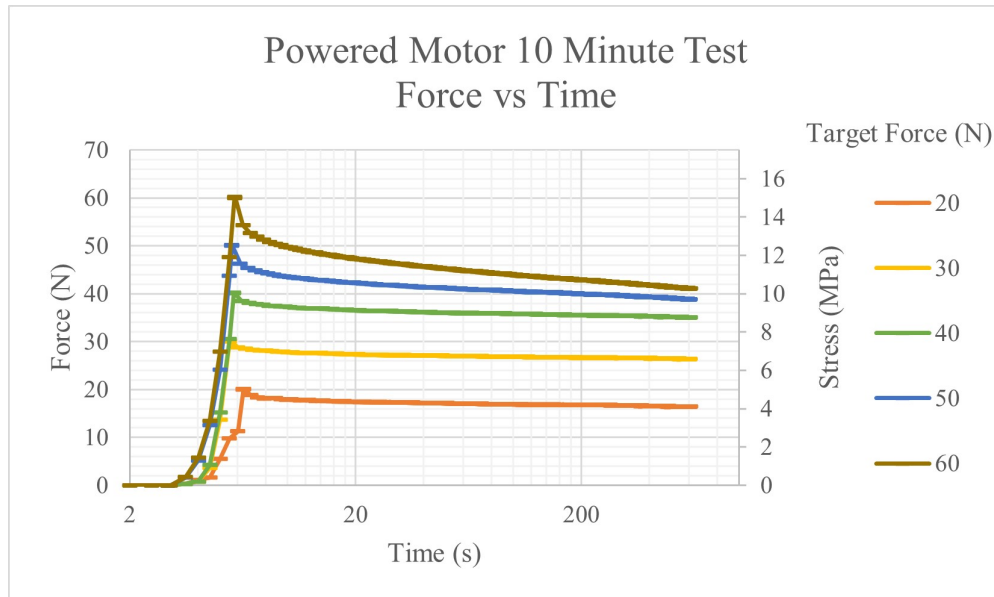


Figure 5.15: Measurements of tensile force taken over 10 minutes for the powered motor latch (target forces between 20 and 60 Newtons).

Table 5.5: Results of 10 minute tensioned hold experiment for the powered motor configuration. Measured values of tensile force as measured by the tensile testing machine are shown for values of peak force, force measured six (6) seconds after peak force, 60 seconds after peak force, and the final force measured at ten minutes (600 seconds) after peak force. The percent of force lost relative to the peak force measured is also shown.

Target Force (N)	Peak Force (N)	6 Seconds Force (N)	60 Seconds Force (N)	600 Seconds Force (N)	% Decrease	% Decrease
1.0	1.2 ± 0.06	0.8 ± 0.10	35.1 ± 4.39%	0.8 ± 0.10	35.1 ± 4.39%	0.8 ± 0.10
2.5	2.6 ± 0.06	2.3 ± 0.12	13.9 ± 0.71%	2.2 ± 0.12	17.7 ± 0.94%	2.1 ± 0.10
5.0	7.6 ± 2.14	6.7 ± 2.22	11.0 ± 3.63%	6.5 ± 2.14	14.1 ± 4.64%	6.2 ± 2.00
10.0	10.4 ± 0.17	9.3 ± 0.59	10.9 ± 0.69%	9.0 ± 0.59	13.8 ± 0.90%	8.7 ± 0.57
15.0	15.7 ± 0.71	13.8 ± 0.57	12.5 ± 0.52%	13.3 ± 0.49	15.3 ± 0.56%	13.1 ± 0.38
20.0	20.8 ± 0.71	18.9 ± 0.81	9.4 ± 0.40%	18.2 ± 0.87	12.6 ± 0.60%	17.6 ± 0.95
30.0	31.1 ± 0.70	28.6 ± 0.72	7.9 ± 0.20%	27.8 ± 0.90	10.5 ± 0.34%	27.2 ± 1.10
40.0	41.0 ± 0.76	36.8 ± 2.80	10.2 ± 0.78%	35.3 ± 3.67	13.9 ± 1.44%	34.1 ± 4.36
50.0	53.0 ± 0.38	44.8 ± 0.97	15.6 ± 0.34%	41.4 ± 2.63	21.9 ± 1.39%	38.9 ± 3.39
60.0	63.3 ± 1.25	50.9 ± 2.52	19.6 ± 0.97%	47.0 ± 2.50	25.8 ± 1.38%	44.0 ± 2.59

Table 5.6: Powered motor configuration cable stress measurements for six (6) seconds after peak stress, 60 seconds after peak stress, and the final stress measured at ten minutes (600 seconds) after peak stress.

Target Stress (MPa)	Peak Stress (MPa)	6 Second Stress (MPa)	60 Second Stress (MPa)	600 Second Stress (MPa)
0.25	0.3 ± 0.01	0.2 ± 0.03	0.2 ± 0.03	0.2 ± 0.03
0.63	0.7 ± 0.01	0.6 ± 0.03	0.5 ± 0.03	0.5 ± 0.03
1.25	1.9 ± 0.53	1.7 ± 0.55	1.6 ± 0.53	1.6 ± 0.50
2.50	2.6 ± 0.04	2.3 ± 0.15	2.2 ± 0.15	2.2 ± 0.14
3.75	3.9 ± 0.18	3.4 ± 0.14	3.3 ± 0.12	3.3 ± 0.09
5.00	5.2 ± 0.18	4.7 ± 0.20	4.5 ± 0.22	4.4 ± 0.24
7.50	7.8 ± 0.17	7.2 ± 0.18	7.0 ± 0.22	6.8 ± 0.27
10.0	10.3 ± 0.19	9.2 ± 0.70	8.8 ± 0.92	8.5 ± 1.09
12.5	13.3 ± 0.09	11.2 ± 0.24	10.3 ± 0.66	9.7 ± 0.85
15.0	15.8 ± 0.31	12.7 ± 0.63	11.7 ± 0.63	11.0 ± 0.65

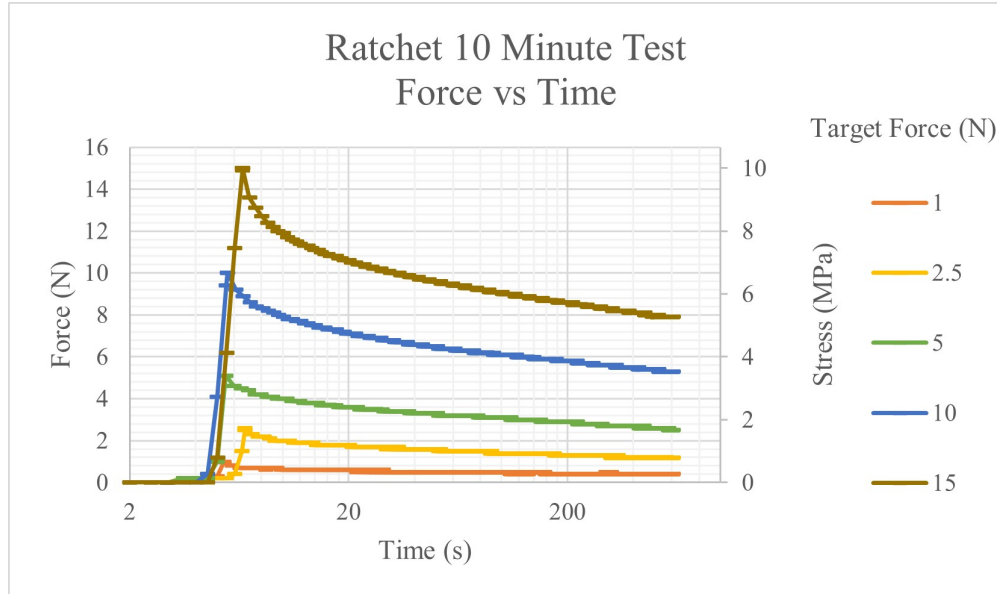


Figure 5.16: Measurements of tensile force taken over 10 minutes for the ratchet latch (target forces between 1 and 15 Newtons).

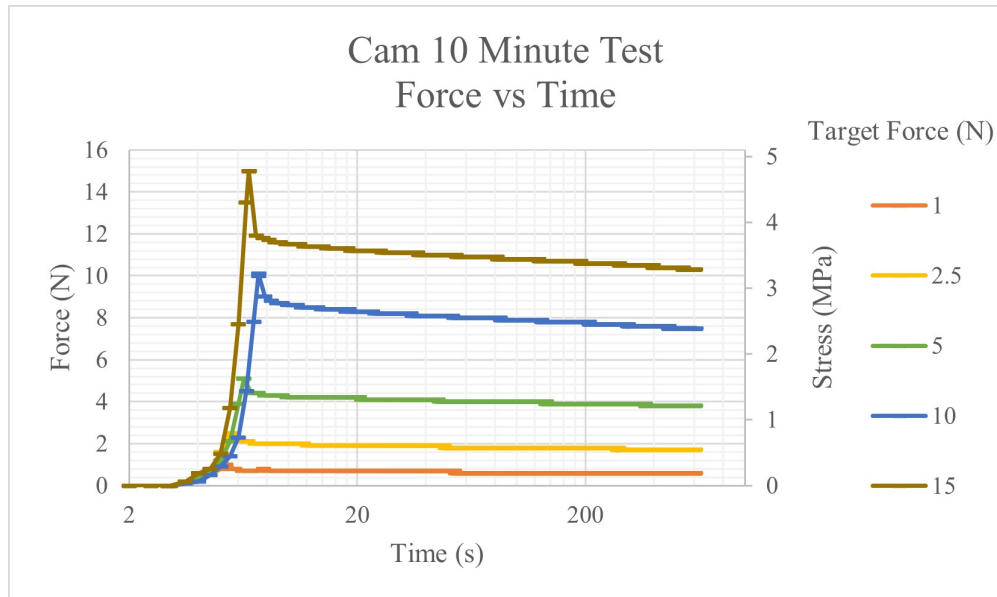


Figure 5.17: Measurements of tensile force taken over 10 minutes for the cam latch (target forces between 1 and 15 Newtons).

Table 5.7: Results of 10 minute tensioned hold experiment for the ratchet design. Measured values of tensile force as measured by the tensile testing machine are shown for values of peak force, force measured six (6) seconds after peak force, 60 seconds after peak force, and the final force measured at ten minutes (600 seconds) after peak force. The percent of force lost relative to the peak force measured is also shown.

Target Force (N)	Peak Force (N)	6 Seconds Force (N)	60 Seconds Force (N)	% Decrease	600 Seconds Force (N)	% Decrease
1.0	1.0 ± 0.00	0.6 ± 0.00	40.0 ± 0.00%	0.5 ± 0.00	50.0 ± 0.00%	0.4 ± 0.06
2.5	2.4 ± 0.15	1.8 ± 0.12	24.7 ± 1.55%	1.5 ± 0.10	38.4 ± 2.56%	1.2 ± 0.10
5.0	6.2 ± 0.21	5.2 ± 0.26	16.6 ± 0.84%	4.5 ± 0.36	27.8 ± 2.23%	3.9 ± 0.47
10.0	11.1 ± 0.00	9.0 ± 0.12	18.6 ± 0.24%	7.7 ± 0.31	30.3 ± 1.20%	6.8 ± 0.40
15.0	16.1 ± 0.10	12.8 ± 0.20	20.5 ± 0.32%	10.8 ± 0.35	32.7 ± 1.06%	9.5 ± 0.50

Table 5.8: Ratchet design cable stress measurements for six (6) seconds after peak stress, 60 seconds after peak stress, and the final stress measured at ten minutes (600 seconds) after peak stress.

Target Stress (MPa)	Peak Stress (MPa)	6 Second Stress (MPa)	60 Second Stress (MPa)	600 Second Stress (MPa)
0.67	0.7 ± 0.00	0.4 ± 0.00	0.3 ± 0.00	0.3 ± 0.04
1.67	1.6 ± 0.10	1.2 ± 0.08	1.0 ± 0.07	0.8 ± 0.07
3.33	4.2 ± 0.14	3.5 ± 0.18	3.0 ± 0.24	2.6 ± 0.32
6.67	7.4 ± 0.00	6.0 ± 0.08	5.2 ± 0.20	4.5 ± 0.27
10.0	10.7 ± 0.07	8.5 ± 0.13	7.2 ± 0.23	6.3 ± 0.33

Table 5.9: Results of 10 minute tensioned hold experiment for the cam design. Measured values of tensile force as measured by the tensile testing machine are shown for values of peak force, force measured six (6) seconds after peak force, 60 seconds after peak force, and the final force measured at ten minutes (600 seconds) after peak force. The percent of force lost relative to the peak force measured is also shown.

Target Force (N)	Peak Force (N)	6 Seconds		60 Seconds		600 Seconds	
		Force (N)	% Decrease	Force (N)	% Decrease	Force (N)	% Decrease
1.0	0.9 \pm 0.12	0.7 \pm 0.06	21.4 \pm 1.69%	0.6 \pm 0.06	32.1 \pm 2.93%	0.6 \pm 0.06	32.1 \pm 2.93%
2.5	2.5 \pm 0.06	2.1 \pm 0.00	17.1 \pm 0.00%	2.0 \pm 0.06	22.4 \pm 0.66%	1.9 \pm 0.12	23.7 \pm 1.41%
5.0	5.1 \pm 0.00	4.3 \pm 0.10	15.7 \pm 0.36%	4.1 \pm 0.12	19.0 \pm 0.53%	4.0 \pm 0.15	22.2 \pm 0.86%
10.0	10.5 \pm 0.36	9.0 \pm 0.46	14.3 \pm 0.73%	8.5 \pm 0.46	19.0 \pm 1.03%	8.1 \pm 0.51	23.2 \pm 1.47%
15.0	15.6 \pm 0.40	13.0 \pm 1.19	16.9 \pm 1.55%	12.4 \pm 1.14	20.5 \pm 1.88%	11.8 \pm 1.13	24.4 \pm 2.33%

Table 5.10: Cam design cable stress measurements for six (6) seconds after peak stress, 60 seconds after peak stress, and the final stress measured at ten minutes (600 seconds) after peak stress.

Target Stress (MPa)	Peak Stress (MPa)	6 Second Stress (MPa)	60 Second Stress (MPa)	600 Second Stress (MPa)
0.32	0.3 \pm 0.04	0.2 \pm 0.02	0.2 \pm 0.02	0.2 \pm 0.02
0.80	0.8 \pm 0.02	0.7 \pm 0.00	0.6 \pm 0.02	0.6 \pm 0.04
1.59	1.6 \pm 0.00	1.4 \pm 0.03	1.3 \pm 0.04	1.3 \pm 0.05
3.18	3.3 \pm 0.11	2.9 \pm 0.15	2.7 \pm 0.15	2.6 \pm 0.16
4.78	5.0 \pm 0.13	4.1 \pm 0.38	3.9 \pm 0.36	3.8 \pm 0.36

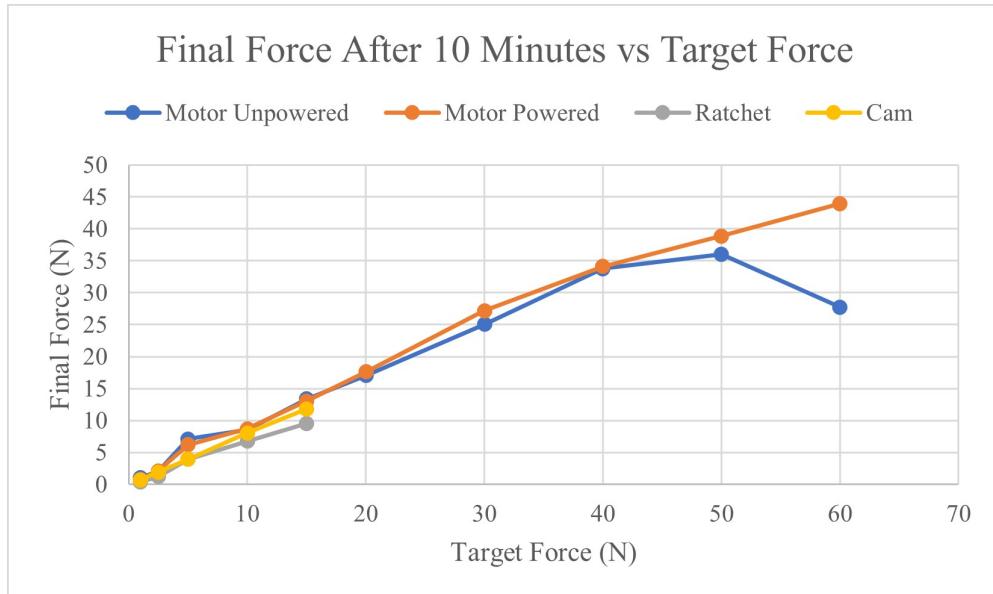


Figure 5.18: The final tensile force measured after 10 minutes for each latch for target forces between 1 and 60 Newtons.

motor configurations holding the most force and stress. The cam design was consistently in between the ratchet and motor designs for both force and stress. The two motor configurations performed nearly identically up to 40 N, but diverged at higher forces. The unpowered configuration held less force when targeting 60 N than when targeting 40 N.

The difference between the peak force measured and final force after 10 minutes is plotted in figure 5.21. The same data is shown for target forces between 1 and 15 N in figure 5.22. The ratchet latch can be seen to consistently hold less force than the other design, with the cam design only marginally worse than the motor configurations. The percent differences between peak force and the force held after ten minutes is shown in figures 5.23 and 5.24. The same trends can still be seen of the ratchet design being less able to hold force than the other designs. Additionally, all latches performed worse for target forces below 5 N than at or above 5 N.

The stress of each system was also measured for the latch holding tests. Figure 5.25 shows the difference between the peak stress reached by each latch and the resulting stress after ten minutes. Observe that all latches lost more stress at higher loads, with

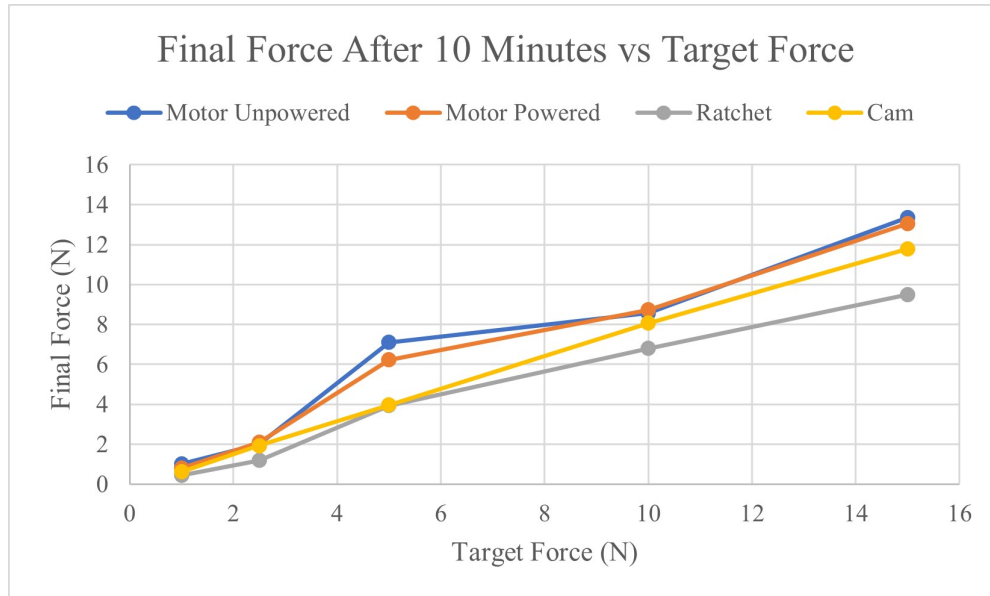


Figure 5.19: The final tensile force measured after 10 minutes for each latch for target forces between 1 and 15 Newtons.

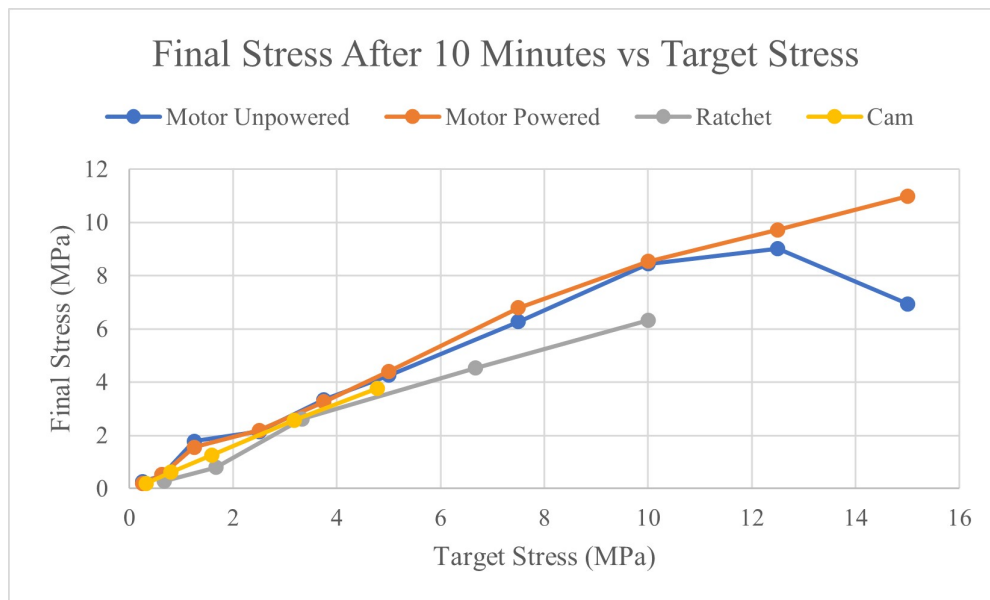


Figure 5.20: The final tensile stress measured after 10 minutes for each latch for a range of stresses.

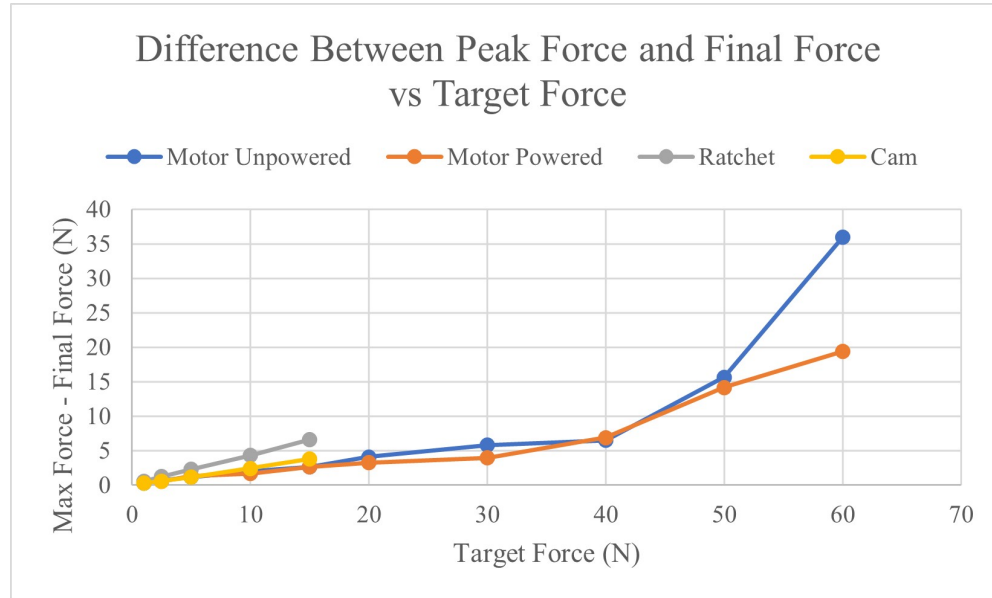


Figure 5.21: Measured difference between peak force and final tensile force measured after 10 minutes for each latch for target forces between 1 and 60 Newtons.

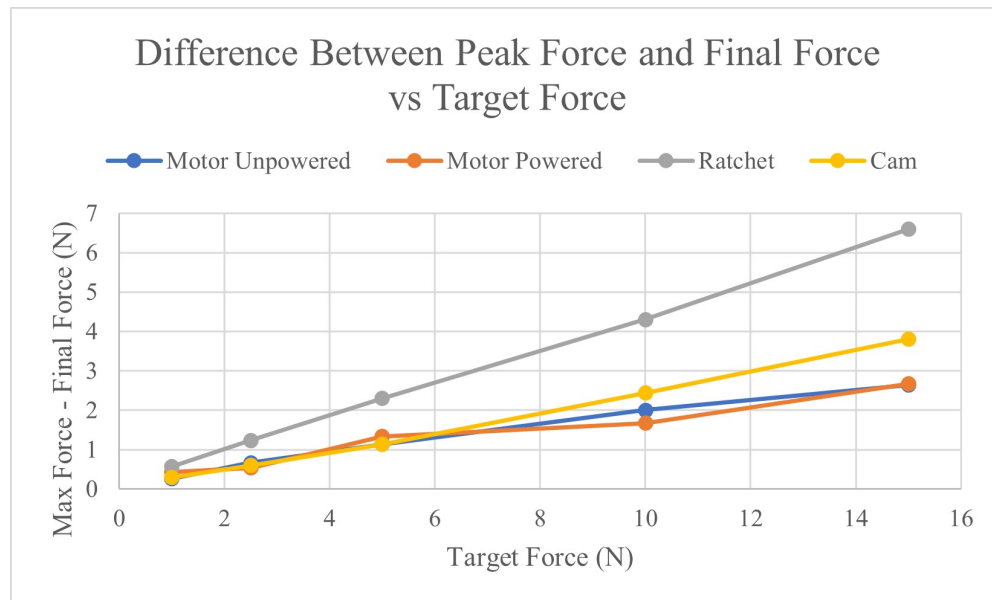


Figure 5.22: Measured difference between peak force and final tensile force measured after 10 minutes for each latch for target forces between 1 and 15 Newtons.

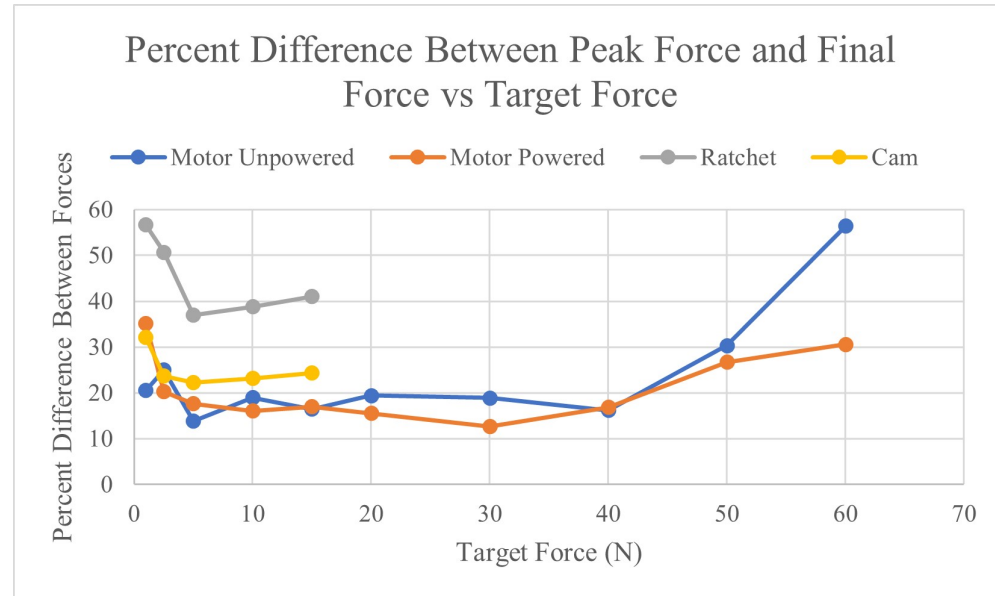


Figure 5.23: Percent difference between peak force and final tensile force measured after 10 minutes for each latch for target forces between 1 and 60 Newtons.

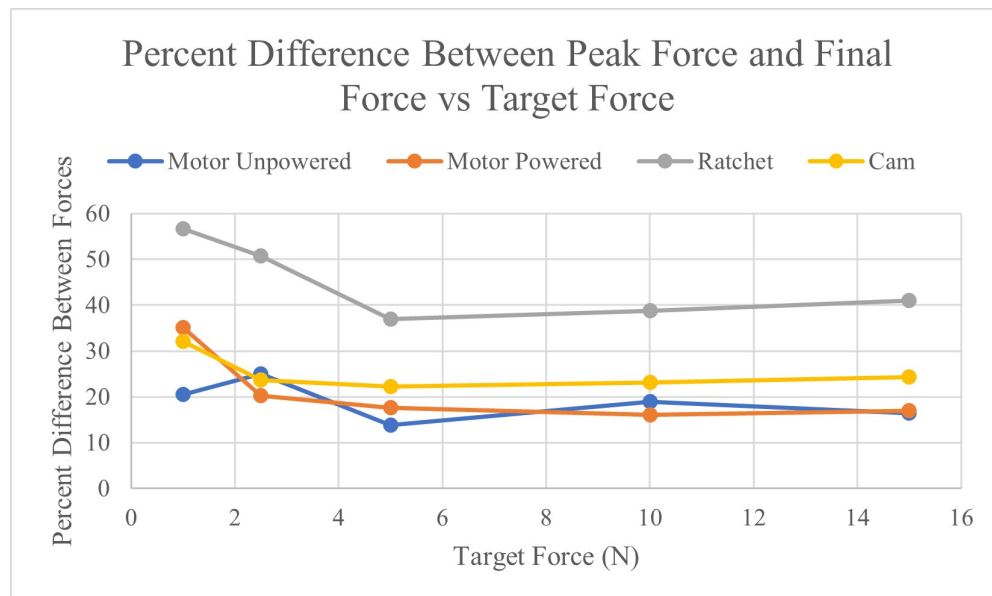


Figure 5.24: Percent difference between peak force and final tensile force measured after 10 minutes for each latch for target forces between 1 and 15 Newtons.

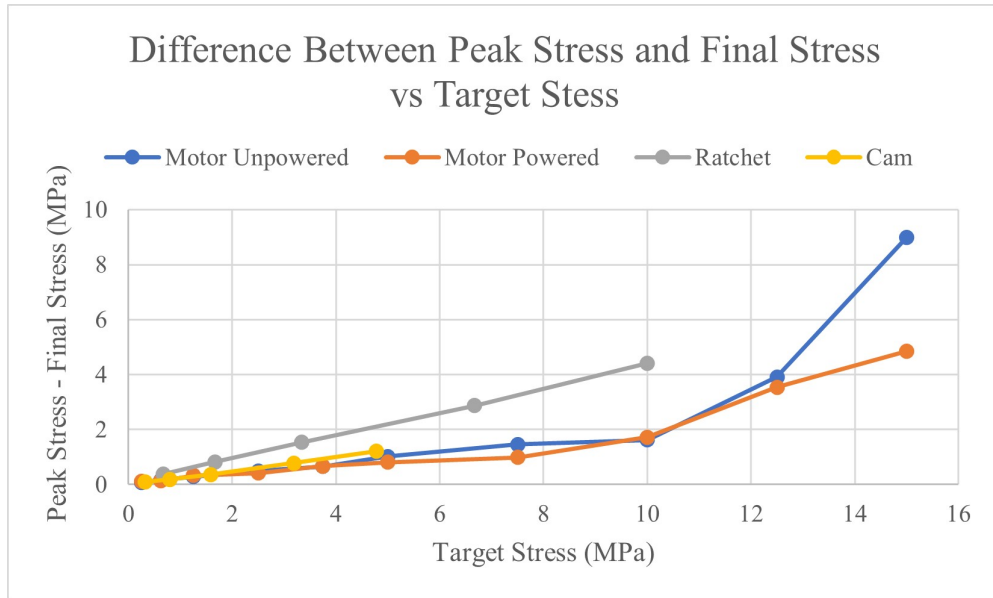


Figure 5.25: Measured difference between peak cable stress and final cable stress measured after 10 minutes for each latch.

the ratchet latch performing particularly poorly. This can be seen more clearly in figure 5.26 showing the percent difference between peak and final stress, with the ratchet design consistently holding 10% less stress than the other designs. The cam latch and both motor configurations were able to maintain a similar amount of stress, with the cam latch holding approximately 5% less stress than the motor configurations. The motor configurations performed similarly to each other except for stresses above 14 MPa where the powered motor design performed significantly better.

The hoop pressure was calculated as described above using the holding force of each latch. Figures 5.27, 5.28, 5.29, and 5.30 show the hoop pressure generated by each latch on different parts of the body. Hoop pressures were calculated using average body circumferences from Heymsfield et al [69] and Polymeris et al [70]. The hoop pressure generated by all latches for just the thigh is shown in figures 5.31 and 5.32. It can be seen that the pressure of the cam latch was the highest due to the small thickness of the cam latch cable. The pressure of both motor configurations and the ratchet design were nearly identical up to 15 N of target force. This is despite the lower holding force of the ratchet design, as the thickness of the ratchet cable is less than half that of the

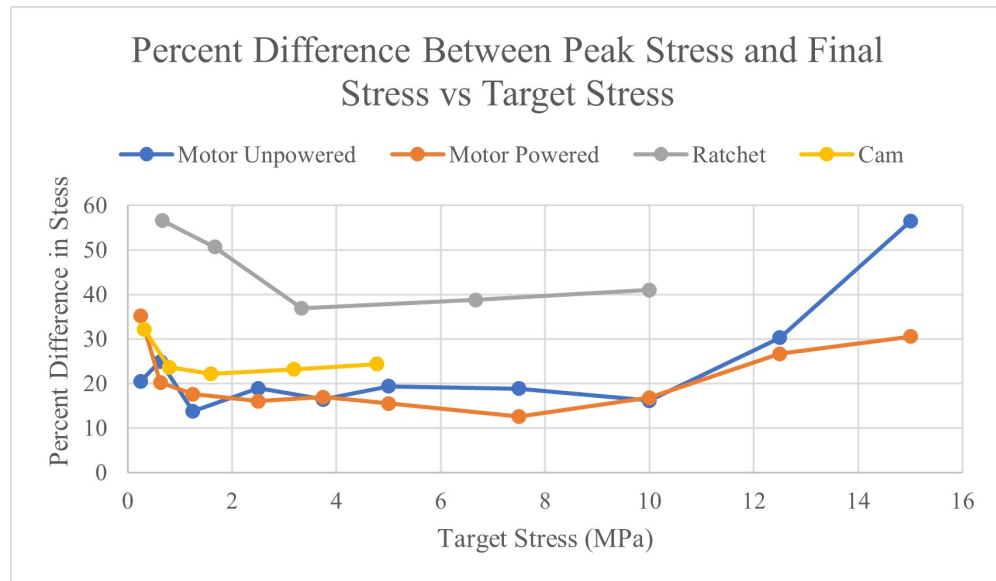


Figure 5.26: Percent difference between peak cable stress and final cable stress measured after 10 minutes for each latch.

motor design, resulting in the hoop pressure of the designs being very similar. All four designs and configurations have the potential to cause bodily harm if used incorrectly. Using a blood pressure value of 120/80 mmHg [71] as reference, all designs were capable of greater hoop pressure than human diastolic and systolic pressure on all parts of the body.

5.3 Latching Release

The ability of each latch to release and the time taken to release each latch was measured for a range of target forces. The results of the release testing are shown in table 5.11 and figure 5.33. The time to release the cam design exhibited the greatest increase as the force on the latch increased, likely because the cam needed to rotate more the greater the force. The motor and cam designs both took longer to release as the force on the latch increased. For the motor design, to release the force on the latch the motor needed to turn enough to release the tension in the cable. With higher tension the motor needed to turn a greater distance, thus taking longer. To release the ratchet latch the teeth of

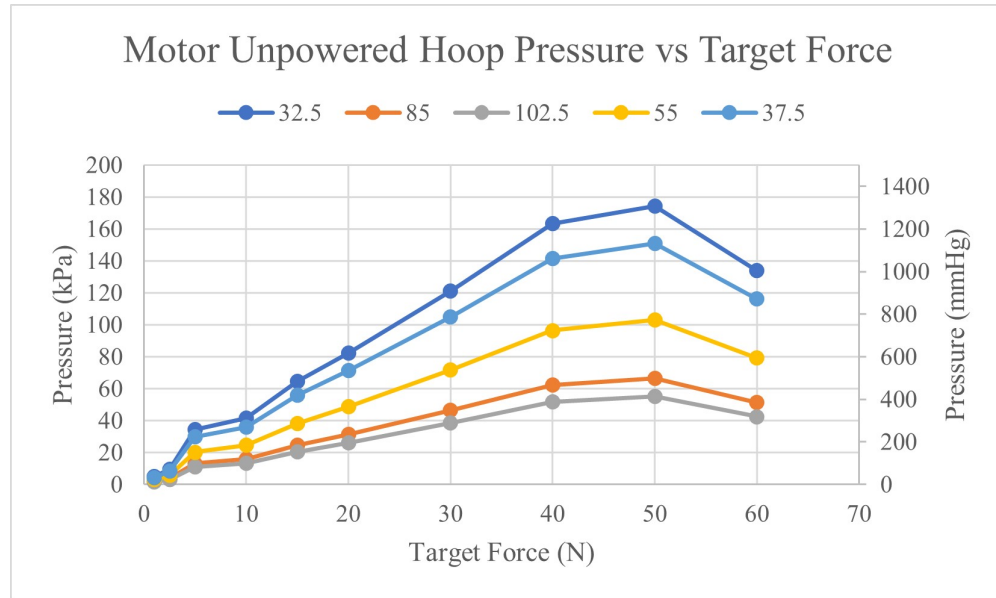


Figure 5.27: Hoop pressure applied by the the unpowered motor latch, calculated for a variety of latch locations on the body.

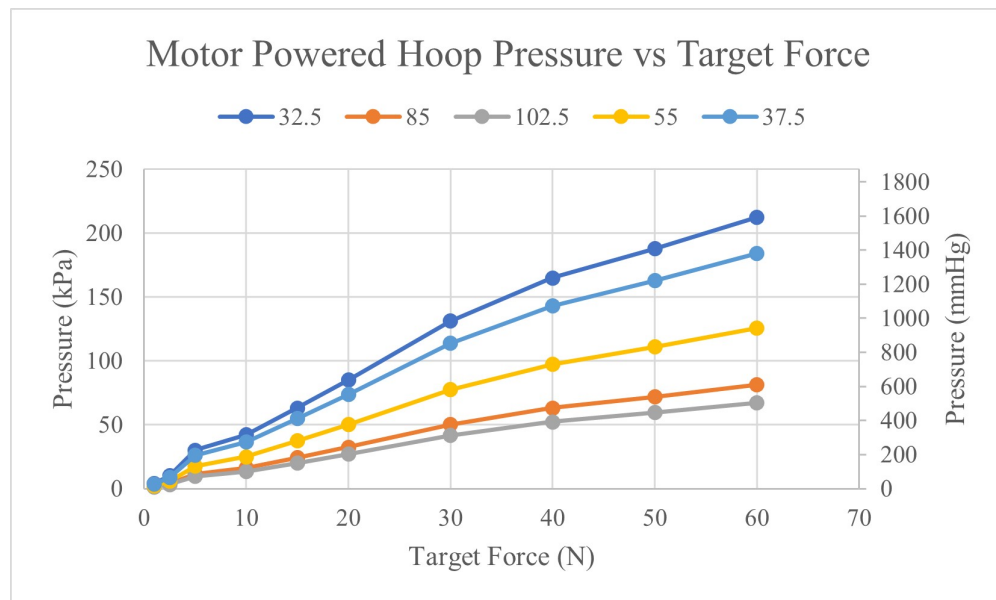


Figure 5.28: Hoop pressure applied by the the powered motor latch, calculated for a variety of latch locations on the body.

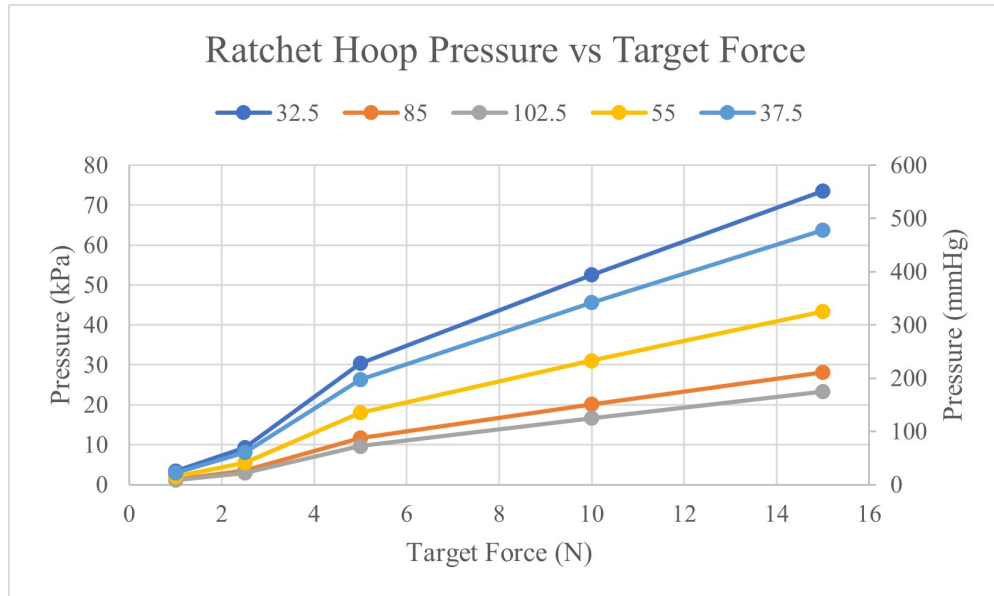


Figure 5.29: Hoop pressure applied by the the ratchet latch, calculated for a variety of latch locations on the body.

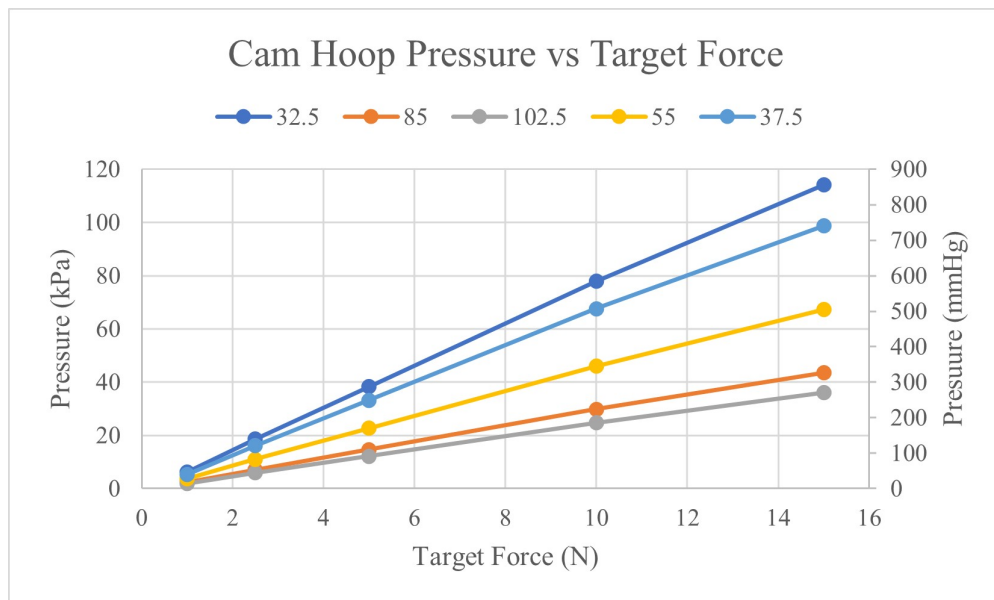


Figure 5.30: Hoop pressure applied by the the cam latch, calculated for a variety of latch locations on the body.

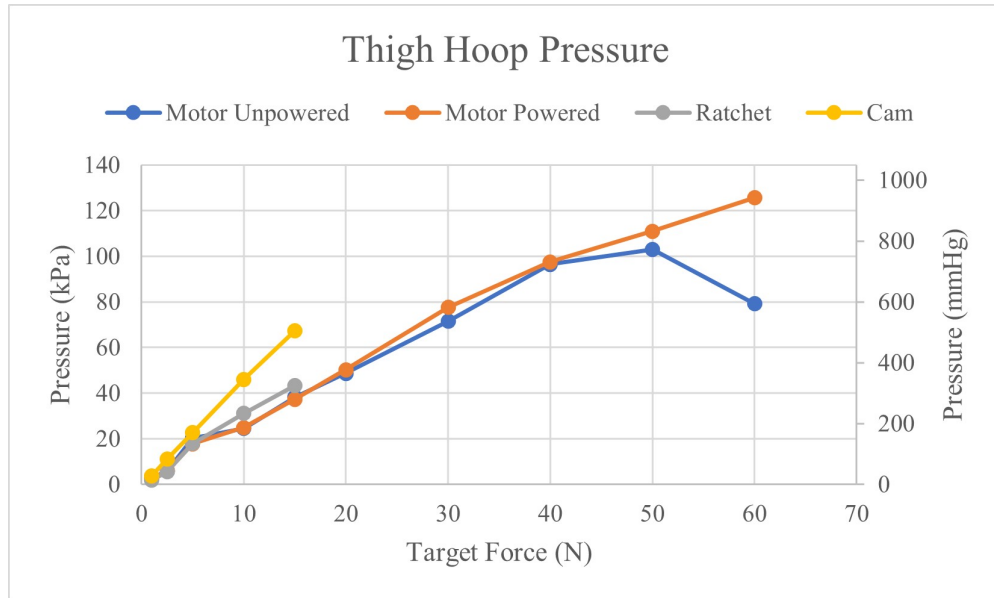


Figure 5.31: Calculated value of hoop pressure on an average human thigh for each latch for target forces between 1 and 60 Newtons.

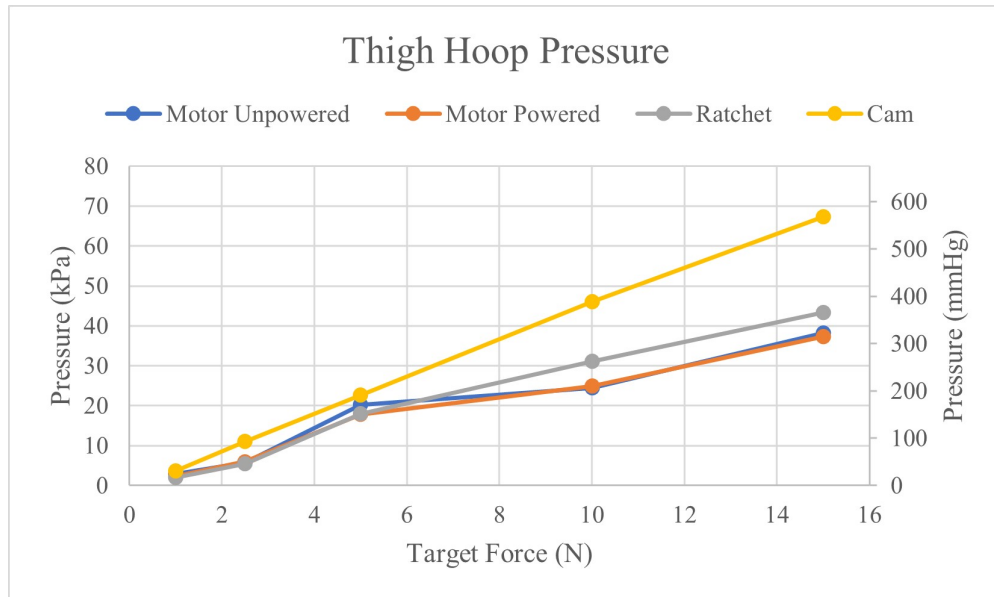


Figure 5.32: Calculated value of hoop pressure on an average human thigh for each latch for target forces between 1 and 15 Newtons.

Table 5.11: Time taken for each latch to reduce cable tension to below 10% of initial tension.

Target Force (N)	Release Time (s)		
	Motor	Ratchet	Cam
1	0.67 ± 0.59	1.00 ± 0.50	1.00 ± 0.50
2.5	0.83 ± 0.59	1.00 ± 0.50	1.33 ± 0.59
5	0.83 ± 0.59	1.17 ± 0.59	2.00 ± 0.50
10	1.00 ± 0.50	Fail	Fail
15	1.33 ± 0.59	1.00 ± 0.50	Fail
20	1.67 ± 0.77		
30	1.33 ± 0.77		
40	1.67 ± 0.59		
50	1.50 ± 0.71		

the latch were disengaged with the grooves of the cables. This happened very quickly, and the distance the teeth needed to travel to disengage the cable did not change with force, so release time was theoretically independent of the forces on the latch. This was observed in testing, with the time taken to release the ratchet design remaining relatively constant for all forces.

The ratchet and cam designs both failed to release the cable under certain loads. For the ratchet design, the ratchet failed to release the cable during all three tests conducted at 10 N. For the cam design, two out of the three tests at 10 N failed and all three tests at 15 N failed. To understand these failures, the force needed to release each latch was measured as a function of cable tension, with the results shown in figure 5.34. The results are shown with the strength of the linear actuator plotted for reference. From this plot, it can be seen that the force required to release the ratchet design increases with increasing tension until around 10 N, after which the force needed to release the latch becomes constant. The standard deviation of the release force was measured to significantly increase with increased tension, suggesting that the latch becomes less stable under higher tensions. It is hypothesized that under tensions above 15 N the grooves of the cables begin to put so much force on the teeth of the latch that the teeth

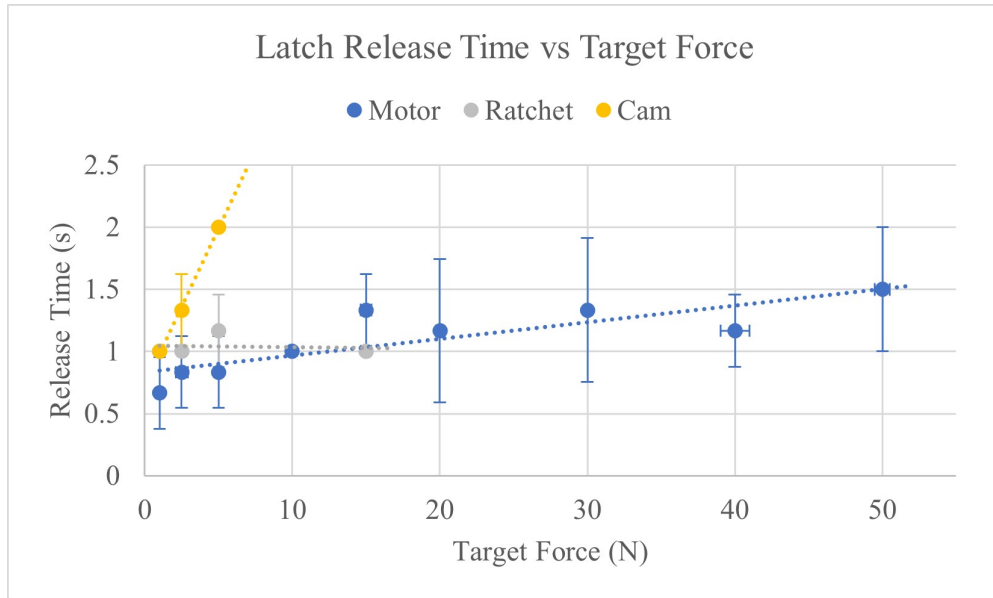


Figure 5.33: Time taken for each latch to release cable tension, with linear trend lines indicating the relationship between release time and cable tension.

begin to slide out of the way, potentially making the ratchet latch easier to release. This could explain why the ratchet latch was able to consistently release the cable at 15 N but not 10 N, however further testing and manufacturing changes are needed to fully explain this phenomenon.

The force required to release the cam design increased at approximately the same rate as the ratchet design, but consistently required a higher release force for the same cable tension. Figure 5.34 shows that the ability of the cam design to release reaches the limit of the force the linear actuator can apply at around 6 N of cable tension, and exceeds that limit after 10 N. This closely matches what was seen with the release testing of the cam latch, where the cam latch failed consistently at 10 N and 15 N.

5.4 Cable Friction

The friction of each cable was measured as described in chapter 4, with the results of friction testing shown in table 5.12. The flat side tests were performed with the flat part of the cables against the polyester fabric, and the ridged side tests performed with

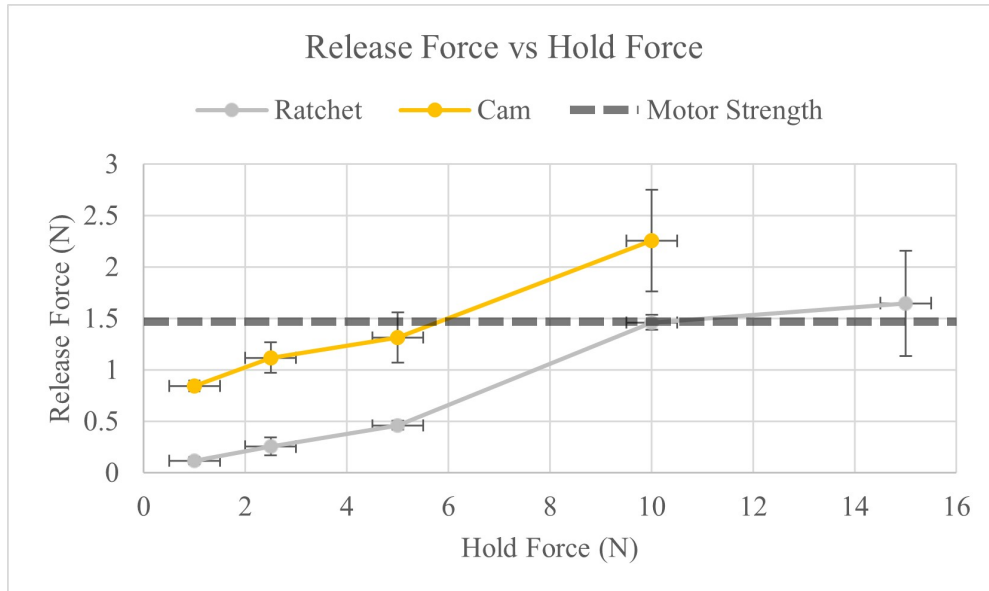


Figure 5.34: Measured force applied to ratchet and cam release levers required to disengage each latch. The measured force output of the linear actuator is shown for reference.

the teeth or grooves of the cables against the fabric. The cam cable did not have a side with teeth or grooves, thus no friction was measured for that cable in that test. These measurements were taken in ideal conditions with flat surfaces, however in a real use case scenario it is possible that the teeth and grooves of the motor and ratchet cables could interact with clothing to create localized increases in effective friction.

Table 5.12: Static friction of each cable against a polyester fabric sheet.

Test	Static Friction		
	Motor	Ratchet	Cam
Flat Side	3.0 ± 0.10	1.4 ± 0.06	1.1 ± 0.03
Ridged Side	1.8 ± 0.06	1.2 ± 0.12	

Chapter 6

Discussion

These data show that a wearable length fastening latch has the potential to complement the functions of linear actuators, such as SMA springs. The latch designs and configurations evaluated have been demonstrated to effectively and reliably hold force over long durations for a nearly continuous range of displacements, and do so repeatedly for a range of tensile loads. The latches have also demonstrated the ability to quickly and autonomously disengage, while remaining small, wearable, and energy-efficient. The three designs that were constructed each met the design goals of this research. The benefits and drawbacks of each design will be evaluated in this section.

6.1 Latch Tightening and Engagement

One of the major drawbacks of the motor design is its slow speed when moving the cable to the correct displacement. The measured speed of 6 mm/s may not be an issue if only small adjustments to displacement are being made, but the design is still significantly slower than the other two designs which may cause a problem for large displacements. The other disadvantage of the motor for latch tightening is the need for active control of displacement. For integrating the latch into a TCA, design the control of the latch and TCA would need to be synchronized to avoid unnecessarily stressing the latch or TCA. The passive design of the ratchet and cam designs would be much more straightforward, with the TCA simply needing to contract the desired amount without having to worry about latch control. However, the benefit of having the motor being constantly engaged

and restricting cable movement in both directions is the ability for relatively precise control of displacement.

Additionally, with the nearly 7 N of force that the motor design imparts on the cable, it is possible to make adjustments to displacement even after the TCA is powered off. This is not possible with the passive designs. Making fine level adjustments using either the ratchet or cam designs would be quite challenging. For instance, if the TCA over-tightened a latch and needed to be loosened the TCA would need to be partially relaxed, the latch would then need to release and allow the cable to loosen, then the latch would need to reengage, allowing the TCA to re-tension the cable and pull it to the correct displacement. This is an inherent problem with the unidirectional control of the ratchet and cam designs.

The ratchet and cam designs also require higher forces from the TCA due to the drag force they impart on the cable. For the ratchet design this force is quite small, only 0.14 ± 0.05 N which should not have a significant impact on the TCA, however for the cam design the drag force is 0.93 ± 0.05 N. For a wearable device this could have a significant impact on TCA force requirements. To mitigate these drag forces, the latching mechanisms of the ratchet and cam latches could be disengaged during most of the stroke length of the TCA, and only be put into a position to engage once the TCA has neared its desired displacement. This operation mode would not be difficult to implement, but would mean that the latches are not fully passive and would require additional considerations for controller design.

Once the desired displacement was achieved, the ability of each design to reliably and precisely engage with the cable was found to be very effective. Up to 10 N all designs latched without any slipping of the cable and with a displacement of only a few millimeters. Below 10 N the cam design consistently had the highest displacement, but even at 10 N this displacement was limited to only 6 mm, a relatively small amount of travel. The motor and ratchet designs allowed for even less displacement, between 0.5 mm and 3.5 mm up to 10 N. Below that force, the greatest contributors to displacement were mechanical slack and cable strain, with the motor design performing the best of the three designs in slack and strain. The constant engagement of the motor design and the specific design of the belt and pulley teeth meant that there was very little slack in the design, and the reinforced rubber of the timing belt experienced very little strain at

low forces.

The ratchet design had slightly worse characteristics, with the spacing of the latch teeth and cable grooves contributing the most to displacement. A design with grooves closer together could reduce this slack, but would also require higher manufacturing precision and potentially reduce reliability. The nylon cable used by the ratchet also performed worse than the rubber of the motor cable, but below 10 N the two materials had similar characteristics. Only above 10 N did the nylon begin to significantly differ from the motor strain. This is understandable, as the yield point of the nylon was found to be 7.85 ± 0.13 MPa, which corresponded to 11.78 N, indicating that the nylon had begun to plastically deform after the 10 N test. A cable made from different material may perform better than the nylon, or a larger cable may be needed if the forces on the cable are expected to exceed the yield point. However, the height to width relationship of the cable would need to be maintained if changing the cross-sectional area, with the cable width being wide enough to prevent rotation within the latch. Potential cable rotation was one of the major limitations found with using a flat cable, as the latch is only effective if the grooves of the cable are well aligned with the teeth of the latch. A cylindrical cable with grooves wrapping around the cable could mitigate this drawback of the ratchet design.

As discussed above and in previous chapters, the cam design experienced mechanical slack due to the cam needing to rotate past the cable before fully engaging. This slack was smaller on average than the ratchet slack, but the overall displacement of the cam design was higher due to the rope used in the design. The rope had very high strains at low stresses, partially due to the ability of the rope to compress. The movement of the fibers within the rope meant that the rope was not able to reach its elastic deformation region until after it was pulled taught, which did not happen until the rope was tensioned under 10 MPa of stress. This stress was higher than the latch itself could support, which was somewhere around 5 MPa, so some of the useful tensile properties of the rope were never truly utilized with this design. A stiffer rope could have experienced less strain and resulted in a better design, however changing the rope material could also have an impact on how effectively the teeth of the cam are able to engage with the rope. For higher forces this was already a major issue with the cam latch, with the rope able to slide under the teeth of the cam. Stronger and harder teeth may be better able to

engage with the rope and prevent slipping.

The failure modes of all three designs are worth discussing. All three designs underwent sudden failures when latching, abruptly losing tension before reengaging with the cable. However, only the ratchet design lost all tension during failure. Both the motor and cam designs still maintained some engagement force on the cable even after a failure, but the ratchet latch did not. The design of the ratchet latch with teeth engaging with the cable every two millimeters meant that if the cable slipped past one tooth it would not experience any engagement until the next groove hit the next tooth. If the force on the cable remained the same, then it is likely that the cable would slide past the next tooth as well. This could result in a runaway effect, with only one slip of the cable resulting in a complete loss of tension in the cable. While a high constant force on the motor or cam cables would also likely result in complete loss of tension, the constant engagement of those two designs would likely decrease the speed of any such failure and provide a more constant force opposing the failure. It is assumed that such a gradual failure of the latch would be preferable to a sudden failure, particularly when the cable is in close contact with the body, though some latching applications may favor abrupt failure conditions.

6.2 Latch Holding

Each latch was evaluated for its ability to maintain force and displacement over time. All latch designs and configurations experienced a noticeable decrease in force during the 10 minute tensile test, however none of the designs showed any noticeable displacement over that time. The decrease in force is likely due in part to the setup of the tensile test. For each test, the tensile testing machine was displaced until it measured a tensile force greater than or equal to the target force, at which point the displacement was stopped. This meant that each latch was only tensioned under the target force for a fraction of a second. For most target forces tested, the majority of tension lost occurred in the first six seconds after displacement was paused, then held relatively stable for the remaining time. It is believed that various components within each latch experience small strains that took up to several seconds to stabilize, such as springs and teeth. It is theorized that the latches need to be initialized to the desired force for potentially

several seconds before the latching force is released to achieve the most stable long term force results. This is supported by the testing results, where once the force held by each latch stabilized the force remained relatively constant for the remainder of the test.

6.2.1 Motor Latch

Both motor configurations held force and stress better than the ratchet and cam designs. They experienced the smallest initial force and stress drop-off as well. This is likely related to the small slack and strain experienced by the motor design: the component parts within the motor design need to move less distance to fully support the tensile force, and thus are able to hold the force better when that force is only applied for a fraction of a second. This seems to hold true for the different configurations of the motor design as well. The powered motor configuration was able to hold more force with less drop-off than the unpowered configuration, especially for higher target forces. While the high static torque of the unpowered motor made it able to quickly support a tensile load at low forces, at high forces the motor likely turned several steps as the force was applied. The coils within the motor applied a dynamic braking torque, which then allowed the motor to support the tensile load, but the time needed for that braking force to be applied was enough for some of the tensile load to be lost by the latch. At high forces, it is also possible that the motor was slowly turning over time, decreasing the load held. In contrast, the powered motor design applied a higher static torque, which allowed it to more quickly take on a high tensile load and decreased the amount of force lost over time.

6.2.2 Ratchet Latch

Compared to the other two designs, the ratchet latch performed the worst in ability to maintain tension in the cable. It consistently held the smallest amount of force after 10 minutes and exhibited the largest change in force and stress over those 10 minutes. This was true for all forces and stresses tested. The reason for this is thought to be two-fold. Firstly, the 3D printed spring component of the latch is thought to plastically deform over time. While this structure dramatically simplifies the manufacture of the latch, more analysis is needed to determine how this spring would compare to a more

traditional metal spring, such as the one found in the cam design. Secondly, the low yield stress of the ratchet cable meant that the latch was operating much closer to its plastic deformation limit than the other latch designs. It is also possible that nature of the ratchet latch does not lend itself well to holding sudden forces. The teeth of the latch may be able to quickly tension the cable before the spring has had time to deform, meaning the tensile testing machine would stop tensioning the cable before the latch had fully taken the load of the cable. This is especially possible for low target forces. For instance, at the target force of one Newton the ratchet latch lost $56.7 \pm 7.55\%$ of the tension in the cable. At such a small force, it is possible that even small displacements of the cable and the spring could have relaxed the cable enough to cause such a significant loss of tension. This could also explain why the other latches also lost a significant percentage of cable tension at low target forces. Notably, for these low target forces, these losses occurred almost entirely in the first six seconds for all three latches. It is possible that, if the tensioning machine had held the tension of the cables for a longer period of time, the losses in force would have been lower.

6.2.3 Cam Latch

The cam design performed similarly to the motor design, losing only a slightly larger percentage of cable tension than the motor. The superior performance of the cam design over the ratchet design makes sense, as the spring of the cam design does not directly hold the tension of the cable, as is the case in the ratchet design. Instead, the cable tensile load in the cam design is transferred to the cam axle, which is unlikely to experience as large of deformations as the thin strip of 3D printed plastic that carries the load in the ratchet design. Additionally, the cam cable was operating far from its yield point, suggesting constant forces over time would not significantly change the mechanical properties of the cam cable. This lack of strain over time would explain why the cam design was able to hold so much more force than the ratchet design over the 10 minute test.

6.2.4 Hoop Pressure

To evaluate how each latch may perform when placed on the human body, the hoop pressure was calculated for each latch on different parts of the body. The results showed that all latches could be potentially harmful if used under high tension on any part of the body. The motor design, with the highest holding force, was capable of applying the highest potential pressure, but the narrow cross section of the cam cable meant that the cam design could apply the greatest hoop pressure for a given target force. However, this assumes that the rectangular cross sections of the motor and ratchet cables would always lie flat against the body. In reality, a cable worn on the body is likely to twist, which could create higher localized pressures from the motor and ratchet designs than what the theory suggests. If these latches were to be used in a real world setting a guide of some sort may be necessary to keep the cables from twisting, or the tensile force in each cable may need to be decreased to account for the maximum possible localized hoop pressure that a twisted cable may impart. The pressures applied by each cable may also need to be reduced, potentially by distributing the cable pressure through the use of protective materials placed between the cable and the wearer.

6.3 Latching Release

The ability of each latch to release and the time taken to release was measured for a range of target forces. For low target forces below 2.5 N all three latch designs released successfully and quickly, at around one second. The time to release the motor design was generally the fastest, and increased gradually as force increased. This was due to the greater displacement at higher forces, thus the more the motor needed to rotate.

The time to release the ratchet design also increased gradually as force increased. This is because, for the ratchet latch, the displacement of the teeth did not change as force changed. This meant that the linear actuator always needed to move the same amount to release the latch regardless of force. The linear actuator successfully released the latch for forces of 5 N and below, however the latch failed to release when under the target force of 10 N. For this target force, the lever release force was approximately equal to the maximum force that the linear actuator could apply. The latch did successfully release when at a target force of 15 N, which was unexpected. It is believed that under

this high load, with the latch cable above its yield point, the latch became unstable and occasionally became susceptible to release when perturbed. The lever release force was much more variable under a 15 N load, measured to be 1.65 ± 0.51 N, and the high standard deviation reinforces this theory.

Unlike the motor and ratchet designs, the time needed to release the cam latch increased significantly as the force on the latch increased. This is due to the displacement of the cam teeth of the latch. Under higher loads, the teeth displacement increased, meaning the linear actuator would need to travel a greater distance to release the latch. The cam latch successfully released the cable up to 5 N but was unable to release for higher forces. Even at 5 N, however, the force needed to release the latch approached the force limits of the linear actuator, suggesting that latch release under this target force may fail on occasion.

To mitigate these failures in a wearable application, the TCA could be retensioned during latch release to reduce the load on the latches. This would be particularly useful for the ratchet and cam designs when operating above their release limits. This could also reduce the potential danger from these two designs of releasing the tension in the cables too quickly. For some applications, having the TCA reduce the load gradually may be desired. This would be less necessary for the motor design, which is already capable of gradually releasing cable tension, however the speed of the motor design may be a drawback. For the ratchet and cam designs, once the latches are released the cables can pass through the latch at nearly any velocity, but the motor design is limited to approximately 6 mm/s, which is likely too slow for some wearable applications.

6.4 Wearability

The primary measure of wearability for this analysis was the size and mass of each latch. Metrics of cable bend radius, cross-sectional area, and coefficient of static friction were also used to evaluate potential difficulties with integrating each latch into a wearable system.

Motor Latch

For metrics of size and mass the motor design performed the poorest. The mounting area that the motor design covered was only slightly larger than that of the other two designs, but it was over four times taller and four times more massive than the other designs. The height of the latch makes it much less wearable than the other designs, as it extends so far from the body that it would be noticeable to the wearer no matter where it was placed on the body. The large mass also limits the locations it could be worn, as a 40 g mass could be quite noticeable when worn on e.g. a forearm or foot, particularly in a wearable application requiring multiple latches. The slow speed of the motor also decreases the wearability of the design, as a garment that takes a long time to don and doff is likely less attractive in most situations than one that can be donned and doffed quickly.

The motor cable is also quite poor for wearability. The minimum bend radius of the cable was small enough that the cable could be comfortably wrapped around all body parts, but only if oriented in the correct way. The rectangular cross-section of the motor cable means that its bend radius along certain axes is too high to wrap around certain parts of the body without twisting, which could result in localized increases in pressure as discussed above. The friction of the motor cable was also the highest of the three cables, and the teeth of the cable mean that it could potentially get caught on pieces of clothing, jewelry, or the surrounding environment more easily than a smooth cable.

6.4.1 Ratchet Latch

The ratchet design was found to be more wearable than the motor design, with a similar mounting area, a shorter height, and a smaller mass, all of which met the performance requirements laid out in chapter 1. The height of around one centimeter means that the ratchet design could be placed nearly anywhere on the body without hindering movement. The short and wide design of the ratchet is also more aesthetically pleasing for a wearable device than the abrupt verticality of the motor design, and the small mass of the design makes it nearly imperceptible for most wearable applications. The quick release of the ratchet design also makes it more attractive than the motor design, allowing for much greater latching displacement in a short amount of time enabling

faster donning and doffing.

The ratchet cable was less wearable than the other cables tested, with the highest minimum bend radius of the three. It also has a rectangular cross-section, meaning it has variable off-axis bend radii and the potential for localized increases in pressure like the motor cable. The large minimum bend radius is of particular concern for a wearable application as it could become folded or bent during normal use, which could cause the cable to break or deform. The ratchet cable was also significantly weaker than the other cables, with a much lower yield point making it more susceptible to deformation and less capable of holding high forces over a long period of time. The ratchet cable experienced less static friction against polyester fabric than the motor cable, but the grooves of the ratchet cable mean that it is susceptible to the same type of environmental interference as the motor cable.

6.4.2 Cam Latch

The cam latch is very similar to the ratchet latch in size and mass, making it similarly attractive for latching on many areas of the body. The design is slightly larger and more massive than the ratchet design but the differences are not significant. Additionally, the cam design is capable of quickly releasing the cam cable like the ratchet design, allowing for large cable displacement quickly and enabling fast donning and doffing of latched garments.

The cam cable had the best wearability characteristics of the three cables, with a small bend radius, low static friction, and it was compliant. This was expected, as synthetic rope is the most similar to traditional garments, and thus should lend itself to wearable applications. This also has the benefit of potential wearers of the latch already being comfortable with having a rope cable against their body, which may not be the case for the toothed rubber and solid nylon cables of the other designs. The design of the cam latch also allows for different off-the-shelf cables to be used, so long as the cam teeth are still able to engage with the cable. This would allow a higher degree of aesthetic customization than the other designs, and increase the chance that an individual would want to wear the latch. The cam cable was also superior to the other cables with its circular cross-section allowing the cable to twist without changing the pressure of the cable on the body. However, the theoretical hoop pressure exerted by

the cam cable exceeded that of the other cables and could apply a potentially dangerous amount of pressure under high tensile loads. This potentially limits the latch to smaller tensile loads, or requires some amount of padding between the cable and the body to decrease the pressure.

6.4.3 Dynamic Systems

While each design was well characterized for relatively static and controlled latching scenarios, real-world wearable systems are subjected to dynamic forces and perturbations resulting from human movement and activity. Further testing is needed to fully evaluate how each latch would perform in such a dynamic setting, but existing results allow for some limited analysis. One major concern for a wearable latching system is the potential for over-tightening. For example, use of handcuffs and zip ties by law enforcement for the purposes of restraint have been well documented to cause injuries [72], as the unidirectional control of these restraints allows for constant tightening while preventing loosening. Such restraints operate similarly to the ratchet and cam designs, making these latches potentially dangerous. To mitigate this risk, bidirectional latches can be used like in the motor design. The ability of the motor design to control latching in both directions, as well as to loosen without releasing the cable, makes the motor design relatively safe from the danger of over tightening. These benefits could be applied to the other latches as well, as bidirectional control is not limited to active latches. The ratchet and cam designs could be made to be bidirectional by placing two latches in series and placing the latches in opposing directions. While tightening, one latch would be disengaged, but once a desired displacement was reached both latches could be engaged, preventing cable movement in either direction. Future latching designs could also incorporate bidirectional engagement into a single latch mechanism, simplifying latch-garment integration. Despite this improvement, passive bidirectional latches would still be unable to loosen a cable and remain latched at the same time.

In addition to over tightening, dynamic latch perturbations also cause a problem with potential loosening of the latches. One potential cause of loosening is sudden large forces on the latch cable that briefly exceed the expected design load. Analysis of forces on cables traversing the body will need to be well characterized to ensure a latch is capable of meeting design requirements and not at risk of failure. Cable twist is another

potential problem for latch engagement. A twisted cable may reduce the available latching surface area or cause wear at a latch-cable interface. Further experiments are needed to determine how these dynamic environments impact latch operation.

6.5 Manufacturability and Cost

Each latch had certain challenges associated with its design, parts sourcing, and assembly. The specific manufacturing difficulties and costs should be considered when evaluating the viability of each design.

6.5.1 Motor Latch

The motor design was overall relatively simple to design and construct. The motor housing was able to be 3D printed using commercial extrusion printers as the design did not have particularly high tolerances. This was made possible by the belt and pulley system used, which allowed the latch to engage with the cable without needing sub-millimeter precision in the cable guide of the latch body. The motor and belt-and-pulley system used were all commercially available, making the construction of future motor latch designs relatively simple. However, the bore hole of the pulley was too small for the shaft of the motor, requiring a widening of the pulley bore hole. This presents a major limitation of motor designs in general: the design relies on multiple precision manufactured components, and is only effective if those components can be integrated with each other. Custom manufacturing of any of these precision components would drive up cost significantly, both in terms of design time and sourcing difficulties.

6.5.2 Ratchet Latch

In contrast, the ratchet design only relied on a single precision component: the linear actuator used to release the latch. The rest of the latching mechanism was built around this one component, instead of having to integrate multiple precision components. The rest of the design was able to be 3D printed using commercial extrusion printers, just as with the motor design. This made the design easy to construct, as the linear actuator simply needed to be placed into the latch without the need for any additional tools or manufacturing processes. Injection molding would also be viable for this design, just as

is done with commercially available zip ties. However, the cable was difficult to source commercially for this design. Most commercially available cable tie cables are either too short to be useful for high stroke latching, or too wide to be comfortably wearable. For this design, a long cable tie cable was sourced then reduced in width using a band saw. The cutting of the cable was relatively easy but introduced width variability and potential structural defects. A custom molded cable would eliminate these problems, but would drive up initial costs substantially.

6.5.3 Cam Latch

The cam design also only relied on a single precision sourced part in the linear actuator used to release the cam, however the rest of the design also relied on high tolerances and precision components. Extrusion 3D printing was found to be inadequate for this design, with stereolithography used instead. The SLA 3D printer was capable of printing with high enough precision to produce a working latch, however the soft proprietary plastic wore out quickly. Stronger cam teeth, such as hard plastic or metal, would be required to produce a design capable of long term use. This would likely increase manufacturing costs. Additionally, unlike the ratchet design, multiple parts were needed to make the latching mechanism work, such as the cam, spring, axle, and latch housing. The small size of this design made the assembly of these parts challenging, taking significantly longer than the other designs.

6.6 Summary

A comprehensive evaluation of the three latches indicates that no one latch is superior to the others. Rather, each latch excelled in some metrics and performed poorly in others. To compare each latch, a number of important latching characteristics were identified and each latch was evaluated based on the latch testing results presented in this paper. The relative strengths and weaknesses of each latch can be seen in figures 6.1, 6.2, 6.3, and 6.4. The latches were evaluated against each other and against the performance requirements laid out in chapter 1. Each latch received a rating of three, six, or nine for each latch variable, with scores of nine, six, and three representing latches that outperformed, met, or underperformed the performance requirements respectively.

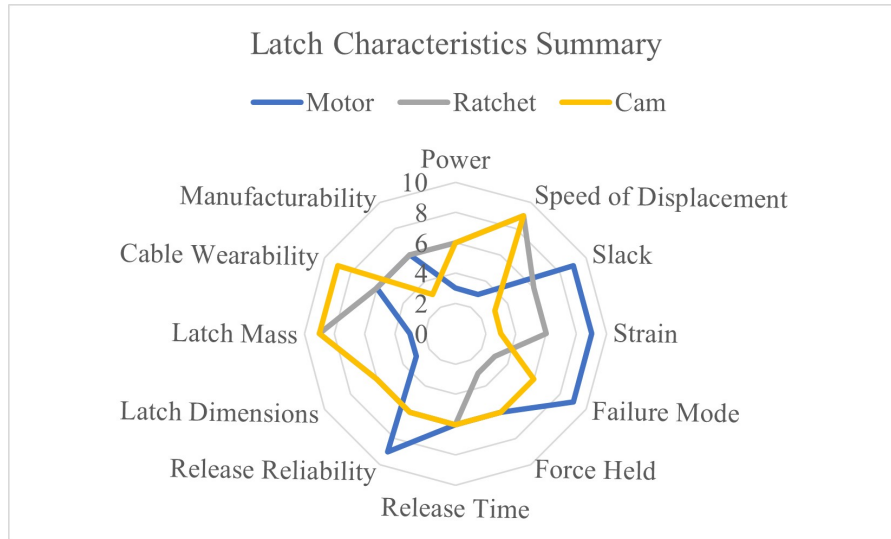


Figure 6.1: Radar plot showing the characteristics of the three latch designs.

For latch variables not covered by performance requirements, the latches were evaluated against each other, with nine, six, and three awarded to the latches with the best, second best, and worst testing results respectively.

The motor design was the strongest and most reliable of the three designs. It was able to latch over the largest range of forces and did so with the smallest displacement and smallest loss in holding force over time. It also failed relatively safely, still maintaining a percentage of force during failure. Despite these positive characteristics the motor design is not considered viable for most wearable applications. It was the heaviest of the designs which limits its wearability to areas of the body that can comfortably carry weights, for example the waist and hips. The tall design of the motor latch further limits its wearability. It extends far enough from the body that it would likely obstruct movement and be at risk of colliding with objects in the environment. The motor cable was also not ideal for wearability as it had high friction, teeth that could get caught on the environment, and low compliance and flexibility. The motor design was also slow to displace, and more power intensive than the other designs, further reducing wearability. For these reasons the motor design is generally not recommended for wearable applications unless high forces are necessary and integration into wearable garments is of low priority.

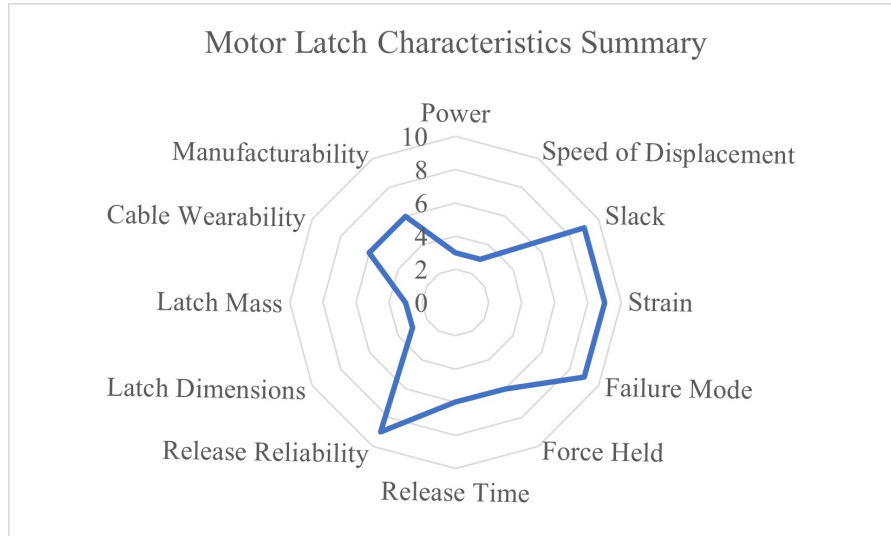


Figure 6.2: Motor design characterization summary.

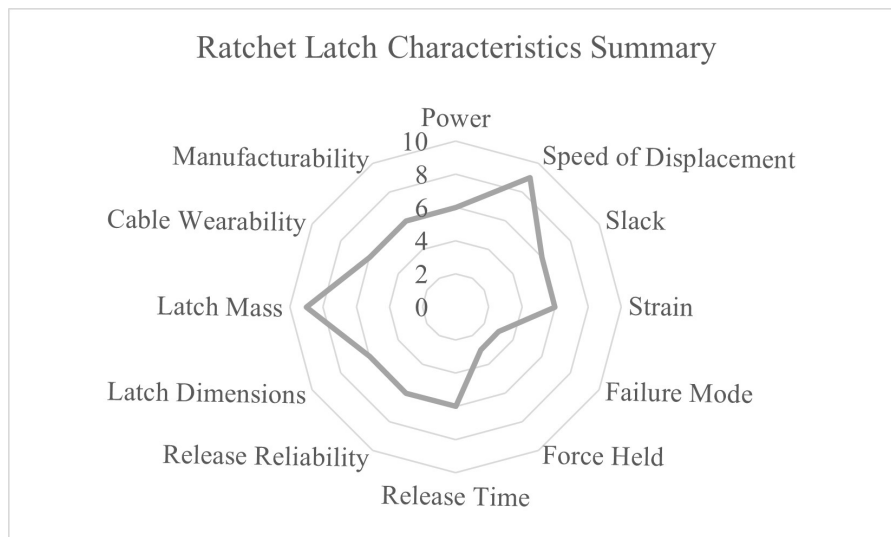


Figure 6.3: Ratchet design characterization summary.

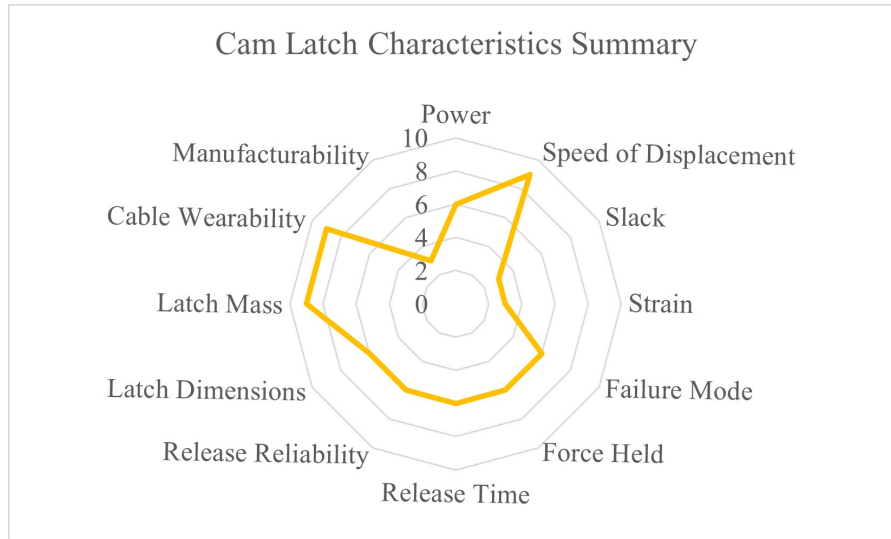


Figure 6.4: Cam design characterization summary.

The ratchet design was much more wearable with a low height and small mass that would allow its use nearly anywhere on the body. It performed the most consistently across all tests, performing poorly in the fewest tests but also excelling in the fewest. For forces below 5 N the ratchet design was nearly as effective as the motor design in minimizing displacement and strain, and it surpassed the motor in displacement speed and power requirements. However, the ratchet design lost a large percentage of force even at low forces due to the low yield points of the ratchet cable and latch spring. It also failed the most catastrophically of the three designs, releasing the totality of cable tension in an instant without the ability to reapply a latching force until the force on the cable was reduced. This is potentially dangerous for a wearable application where safety is of high importance. The ratchet cable was also not ideal for wearability with its low compliance, poor bend radius, and grooves in the cable that could get caught on clothing or the surrounding environment. Despite these problems the ratchet design is recommended for wearable applications as long as small forces are expected and the ability to quickly and easily manufacture a latch is more important than producing a strong and reliable latch with higher cost and manufacturing requirements.

The cam design had the most wearable cable of the three designs, as the rope used with the latch was compliant, flexible, and had a low coefficient of static friction. The

latch itself was also wearable, with similar mass and dimensions to the ratchet design. It also had a high displacement speed like the ratchet design while having a safer failure mode and losing less force over time than the ratchet design. However, the cam design experienced high displacement even at low forces due to the high strain of the rope. The cam design was also the most challenging to manufacture, needing specialized 3D printers and more precision and small parts than the other designs. Wear on the cam teeth was also a major problem, reducing the ability of the latch to hold high forces over just a few uses, requiring either the frequent replacement of the cam or a more durable material used for its construction. Therefore, the cam design is only recommended for applications where wearability is of high enough importance that the drawbacks of increased manufacturing time and costs are offset.

6.7 Potential Improvements and Limitations

The primary constraint for all three designs was the motor/linear actuator used. For smaller and more wearable designs to be viable, smaller actuators would be necessary. This poses a challenge, as traditional motors produce less torque as they get smaller in diameter. This can be mitigated by increasing the length of the motor, but this is only feasible up to a point. The torque of a small motor can be increased through gear ratios, but this comes at the cost of speed. The motor design already suffers from a relatively slow displacement, and decreasing this speed any further would likely render the design unusable for wearable applications. Motor speed is less of a problem for the ratchet and cam designs, as the linear actuator only needs to travel a small distance to disengage each latch. Additionally, mechanisms could be designed that would allow for force to be built up over time, then released quickly to disengage the ratchet and cam latches, similar to how a pistol shrimp is able to slowly flex its claw muscles before quickly applying a large force by releasing the muscle tension. While more complicated, such a system suggests that the ratchet and cam designs can still be shrunk significantly using existing technology, while the motor design is already approaching the limits of its viability at these spatial scales. Future actuator improvements may make the motor design viable at small scales, for instance by using piezoelectric rotary motors, but such improvements are largely conjecture at this time.

In addition to future latch improvement, further work is needed to fully characterize these latching designs in dynamic and wearable applications. While the tests that were performed demonstrate the viability of using latches in wearable systems, many variables concerning latch performance and integration remain unknown. For instance, latch integration with TCAs was never evaluated. Control of forces and displacements of TCAs continues to be a challenge, and it is unclear how a latching system may impact TCA control schemes. Latch integration with wearable systems was similarly not tested. While the snap fasteners integrated into each latch theoretically allows for the latches to be affixed to garments, this was never tested, with the latch snap fasteners only ever being attached to rigid bodies. The forces and dynamics of soft, compliant fabric may change the performance of the latches, and more testing is needed to fully evaluate latch-garment integration. In addition to latches only being affixed to rigid bodies, latches were only tested with optimal orientations. Each latch was tested with the cable and latch being aligned, with no major bends or twists in the cable. In a real-world wearable system it is unlikely that cable-latch interactions would remain ideal. It is unknown how each latch would perform when latching onto twisted cables with poorly aligned forces, and more research is required to evaluate these cases. More testing is also needed to evaluate the long term capabilities of each latch. The force that each latch was able to hold was found to decrease over time for large forces, but it is unclear how force holding might change over hours or days of constant latching, or what lifespan the latches might have after hundreds or thousands of latching cycles. Future work on wearable latching systems should focus on better quantifying these unknowns, and identify which wearable applications might benefit most from wearable latches.

Chapter 7

Conclusion and Future Work

Soft and compliant actuation is a requirement in wearable robotics. Tensioned coiled actuators, particularly shape memory alloy springs, are one method of delivering compliant actuation. However, SMA TCAs are power intensive which limits their use in wearable systems. Three wearable, length-fastening latching system were designed and evaluated, with the goal of maintaining the forces and displacements that could be set by a TCA. The latches were found to hold force and displacement for any arbitrary displacement value within the TCA envelope, and do so for long periods of time. Additionally, in keeping with the electronically controllable nature of TCAs, the latching systems were designed to latch and release on command without the need for direct human interactions.

The three latching designs were based on three separate latching technologies: a stepper motor with a belt and pulley; cable ties and linear ratchets; and rope ascenders and cam cleats. The capabilities of each design were characterized through force and displacement tests. All three latch designs were capable of holding force and displacement values under cable tensions up to 15 Newtons. Additionally, all three designs were capable of automatically disengaging for cable tensions up to 5 Newtons.

The motor design was found to have the most accurate force and displacement values, and was able to reliably latch and disengage for cable tensions up to 60 Newtons, surpassing the other designs. However, the motor design was the least wearable, being large and heavy, as well as more power intensive than the other designs.

The ratchet design was more wearable than the motor design, and performed similarly to the motor design at low forces below 5 Newtons of cable tension. However, the ratchet design was less capable of holding force over time and the ratchet cable easily deformed, and was only moderately wearable. Despite these failings, the ratchet design was easy to manufacture with an extrusion 3D printer, making the design a good option for a simple wearable application requiring only small tensile forces.

The cam latch design was found to be similarly wearable to the ratchet design, but the rope used as the latch cable was compliant and flexible, making it the most wearable cable of the three designs. The cam design was also similar to the motor design for most metrics at small forces, however it suffered from high displacement due to the way the cam mechanism engaged with the cable and the high strain of the cam cable under small forces. The cam design required more precision manufacturing to function, and wear on the cam teeth quickly decreased the forces that the cam was able to hold. These drawbacks mean that the cam design was found to be most viable for applications prioritizing wearability above all else, and where higher manufacturing costs are acceptable.

Future work should focus on integrating the latches and latch cables with TCAs and into garments. The attachment points between TCAs and cables should be considered, as should latch cable management across the body. To improve TCA controls, potentiometers or other displacement measurement devices can be integrated into the latching mechanisms. Bidirectional latching can also be explored, with two latches in series oriented in opposite directions allowing for displacement control in both directions. This should be viable with only relatively minor changes to the existing latching designs. Additional improvements to the existing latches could include shrinking the motors and linear actuators, using plastic or metal molding instead of 3D printing, and refining the teeth and engagement mechanisms of each design to optimize forces and reliability. Finally, new and innovative latching mechanisms can be explored using technologies like MEMS manufacturing, piezoelectric actuators, microfluidics, and draping adhesion surfaces.

The research presented in this paper demonstrates the viability of using latching devices in artificial muscle driven wearable robotic systems. Existing artificial muscles research has often focused on material science breakthroughs and novel innovations,

while ignoring the well-worn technologies that have proved effective in wearable applications for centuries or millennia. This paper makes the case that next generation artificial muscles (high strength, low power, long lifespan, high frequency) are not needed for many contemporary soft, wearable robotic applications. Rather, latching systems make many low frequency wearable systems viable in the present day using existing artificial muscle technology. It is therefore hoped that this research inspires future work in the development of latches that enable low frequency, fully autonomous, soft, wearable robotic systems.

References

- [1] George M. Whitesides. Soft robotics. *Angewandte Chemie (International ed.)*, 57(16):4258–4273, 2018.
- [2] R. K JOSEPHSON. Mechanical power output from striated muscle during cyclic contraction. *Journal of experimental biology*, 114(1):493–512, 1985.
- [3] Diego R Higuera-Ruiz, Kiisa Nishikawa, Heidi Feigenbaum, and Michael Shafer. What is an artificial muscle? a comparison of soft actuators to biological muscles. *Bioinspiration & biomimetics*, 17(1):11001, 2022.
- [4] Ajay Seth, Jennifer L Hicks, Thomas K Uchida, Ayman Habib, Christopher L Dembia, James J Dunne, Carmichael F Ong, Matthew S DeMers, Apoorva Rajagopal, Matthew Millard, Samuel R Hamner, Edith M Arnold, Jennifer R Yong, Shrinidhi K Lakshmikanth, Michael A Sherman, Joy P Ku, and Scott L Delp. OpenSim: Simulating musculoskeletal dynamics and neuromuscular control to study human and animal movement. *PLoS computational biology*, 14(7):e1006223–e1006223, 2018.
- [5] P A Willems, G A Cavagna, and N C Heglund. External, internal and total work in human locomotion. *Journal of experimental biology*, 198(Pt 2):379–393, 1995.
- [6] N. Hogan. Adaptive control of mechanical impedance by coactivation of antagonist muscles. *IEEE transactions on automatic control*, 29(8):681–690, 1984.
- [7] N HOGAN. The mechanics of multi-joint posture and movement control. *Biological cybernetics*, 52(5):315–331, 1985.

- [8] Vanessa Sanchez, Conor J. Walsh, and Robert J. Wood. Soft robotics: Textile technology for soft robotic and autonomous garments (adv. funct. mater. 6/2021). *Advanced functional materials*, 31(6):2170041–n/a, 2021.
- [9] George M Whitesides. Soft robotics. *Angewandte Chemie (International ed.)*, 57(16):4258–4273, 2018.
- [10] Xunuo Cao, Mingqi Zhang, Zhen Zhang, Yi Xu, Youhua Xiao, and Tiefeng Li. Review of soft linear actuator and the design of a dielectric elastomer linear actuator. *Acta mechanica solida Sinica*, 32(5):566–579, 2019.
- [11] Min Zou, Sitong Li, Xiaoyu Hu, Xueqi Leng, Run Wang, Xiang Zhou, and Zunfeng Liu. Progresses in tensile, torsional, and multifunctional soft actuators. *Advanced Functional Materials*, 31, 2021.
- [12] Jun Zhang, Jun Sheng, Ciarán T. O'Neill, Conor J. Walsh, Robert J. Wood, Jee-Hwan Ryu, Jaydev P. Desai, and Michael C. Yip. Robotic artificial muscles: Current progress and future perspectives. *IEEE Transactions on Robotics*, 35(3):761–781, 2019.
- [13] Brad Holschuh and Dava Newman. Low spring index, large displacement Shape Memory Alloy (SMA) coil actuators for use in macro- and micro-systems. In Herbert R. Shea and Rajeshuni Ramesham, editors, *Reliability, Packaging, Testing, and Characterization of MOEMS/MEMS, Nanodevices, and Nanomaterials XIII*, volume 8975, pages 23 – 33. International Society for Optics and Photonics, SPIE, 2014.
- [14] Knut Løklingholm. *Walking robot with artificial muscles made of fishing line*. PhD thesis, University of Oslo, 2018.
- [15] Alireza Golgouneh, Brad Holschuh, and Lucy Dunne. A controllable biomimetic sma-actuated robotic arm. In *2020 8th IEEE RAS/EMBS International Conference for Biomedical Robotics and Biomechatronics (BioRob)*, volume 2020-, pages 152–157. IEEE, 2020.
- [16] Julia C. Duvall, Lucy E. Dunne, Nicholas Schleif, and Brad Holschuh. Active “hugging” vest for deep touch pressure therapy. In *Proceedings of the 2016 ACM*

International Joint Conference on Pervasive and Ubiquitous Computing: Adjunct, UbiComp '16, page 458–463, New York, NY, USA, 2016. Association for Computing Machinery.

- [17] Sharon Ben Davar. How much do watches weigh- does it affect the comfort level?, Sep 2022.
- [18] Jeremy A. Marvel, Joe Falco, and Ilari Marstio. Characterizing task-based human-robot collaboration safety in manufacturing. *IEEE transactions on systems, man, and cybernetics. Systems*, 45(2):260–275, 2015.
- [19] Shuai Wang, Ruifeng Guo, Hongliang Wang, and Birgit Vogel-Heuser. Safe three-dimensional assembly line design for robots based on combined multiobjective approach. *Applied sciences*, 10(24):8844, 2020.
- [20] Afroz Moatari-Kazerouni, Yuvin Chinniah, and Bruno Agard. Integrating occupational health and safety in facility layout planning, part i: methodology. *International journal of production research*, 53(11):3243–3259, 2015.
- [21] Robots and robotic devices—safety requirements for industrial robots—part 1: robot. Standard, International Organization for Standardization, Geneva, CH, 2011.
- [22] Robots and robotic devices—safety requirements for industrial robots—part 2: robot systems and integration. Standard, International Organization for Standardization, Geneva, CH, 2011.
- [23] Robots and robotic devices—collaborative robots. Standard, International Organization for Standardization, Geneva, CH, 2016.
- [24] Varun Gopinath and Kerstin Johansen. Understanding situational and mode awareness for safe human-robot collaboration: case studies on assembly applications. *Production engineering (Berlin, Germany)*, 13(1):1–9, 2019.
- [25] Stephen Fox, Olli Aranko, Juhani Heilala, and Päivi Vahala. Exoskeletons. *Journal of manufacturing technology management*, 31(6):1261–1280, 2020.

- [26] Li Liu, Yangguang Liu, Xiao-Zhi Gao, and Xiaomin Zhang. An immersive human-robot interactive game framework based on deep learning for children's concentration training. *Healthcare (Basel)*, 10(9):1779, 2022.
- [27] Jie Zhou, Huanfeng Peng, Steven Su, and Rong Song. Spatiotemporal compliance control for a wearable lower limb rehabilitation robot. *IEEE transactions on biomedical engineering*, pages 1–11, 2022.
- [28] G. Palli, C. Natale, C. May, C. Melchiorri, and T. Wurtz. Modeling and control of the twisted string actuation system. *IEEE/ASME transactions on mechatronics*, 18(2):664–673, 2013.
- [29] H. Schulte, D. Adamski, and J. Pearson. Characteristics of the braided fluid actuator. Technical report, The University of Michigan Medical School, 1961.
- [30] Guilherme L Novelli, Gabriel G Vargas, and Rafael M Andrade. Dielectric elastomer actuators as artificial muscles for wearable robots. *Journal of Intelligent Material Systems and Structures*, page 1045389, 2022.
- [31] Jun Shintake, Daiki Ichige, Ryo Kanno, Toshiaki Nagai, and Keita Shimizu. Monolithic stacked dielectric elastomer actuators. *Frontiers in Robotics and AI*, 8, 2021.
- [32] Caitlin Jackson, Liam Johnson, Dominic Williams, Hans-Ulrich Laasch, Derek Edwards, and Alison Harvey. A viewpoint on material and design considerations for oesophageal stents with extended lifetime. *Journal of Materials Science: Materials in Medicine*, 57, 01 2022.
- [33] Alan T. Asbeck, Stefano M.M. De Rossi, Ignacio Galiana, Ye Ding, and Conor J. Walsh. Stronger, smarter, softer: Next-generation wearable robots. *IEEE robotics & automation magazine*, 21(4):22–33, 2014.
- [34] Benjamin Gorissen, Dominiek Reynaerts, Satoshi Konishi, Kazuhiro Yoshida, Joon-Wan Kim, and Michael De Volder. Elastic inflatable actuators for soft robotic applications. *Advanced materials (Weinheim)*, 29(43):1604977–n/a, 2017.

- [35] Fabian Meder, Giovanna Adele Naselli, Ali Sadeghi, and Barbara Mazzolai. Remotely light-powered soft fluidic actuators based on plasmonic-driven phase transitions in elastic constraint. *Advanced materials (Weinheim)*, 31(51):e1905671–n/a, 2019.
- [36] Yuki Funabora. Flexible fabric actuator realizing 3d movements like human body surface for wearable devices. In *2018 IEEE/RSJ International Conference on Intelligent Robots and Systems (IROS)*, pages 6992–6997. IEEE, 2018.
- [37] W. Liu and C. R. Rahn. Fiber-Reinforced Membrane Models of McKibben Actuators . *Journal of Applied Mechanics*, 70(6):853–859, 01 2004, https://asmedigitalcollection.asme.org/appliedmechanics/article-pdf/70/6/853/5470497/853_1.pdf.
- [38] Zhijian Ren, Suhan Kim, Xiang Ji, Weikun Zhu, Farnaz Niroui, Jing Kong, and Yufeng Chen. A high-lift micro-aerial-robot powered by low-voltage and long-endurance dielectric elastomer actuators. *Advanced materials (Weinheim)*, 34(7):e2106757–n/a, 2022.
- [39] Petr Šittner, Ludek Heller, Jan Pilch, Caroline Curfs, Thiery Alonso, and Denis Favier. Young’s modulus of austenite and martensite phases in superelastic niti wires. *Journal of materials engineering and performance*, 23(7):2303–2314, 2014.
- [40] Kevin Eschen, Rachael Granberry, Bradley Holschuh, and Julianna Abel. Amplifying and leveraging generated force upon heating and cooling in sma knitted actuators. *ACS applied materials & interfaces*, 12(48):54155–54167, 2020.
- [41] Seong Jun Park and Cheol Hoon Park. Suit-type wearable robot powered by shape-memory-alloy-based fabric muscle. *Scientific reports*, 9(1):9157–8, 2019.
- [42] Carter S Haines, Márcio D Lima, Na Li, Geoffrey M Spinks, Javad Foroughi, John D. W Madden, Shi Hyeong Kim, Shaoli Fang, Monica Jung De Andrade, Fatma Goktepe, Ozer Goktepe, Seyed M Mirvakili, Sina Naficy, Xavier Lepro, Jiyoung Oh, Mikhail E Kozlov, Seon Jeong Kim, Xiuru Xu, Benjamin J Swedlove, Gordon G Wallace, and Ray H Baughman. Artificial muscles from fishing line and

- sewing thread. *Science (American Association for the Advancement of Science)*, 343(6173):868–872, 2014.
- [43] Márcio D. Lima, Na Li, Mônica Jung de Andrade, Shaoli Fang, Jiyoung Oh, Geoffrey M. Spinks, Mikhail E. Kozlov, Carter S. Haines, Dongseok Suh, Javad Foroughi, Seon Jeong Kim, Yongsheng Chen, Taylor Ware, Min Kyoon Shin, Leonardo D. Machado, Alexandre F. Fonseca, John D. W. Madden, Walter E. Voit, Douglas S. Galvão, and Ray H. Baughman. Electrically, chemically, and photonically powered torsional and tensile actuation of hybrid carbon nanotube yarn muscles. *Science*, 338(6109):928–932, 2012, <https://www.science.org/doi/pdf/10.1126/science.1226762>.
- [44] Kihyeon Kim, Sang Yul Yang, Jaehyeong Park, Ho Jung, Jung Ko, Seong Hwang, Ja Koo, Hyungpil Moon, Hugo Rodrigue, and Hyouk Choi. Torque-compensated bundle of artificial muscle to generate large forces. *Materials Research Express*, 8, 11 2021.
- [45] Carter S. Haines and Günter Niemeyer. Closed-loop temperature control of nylon artificial muscles. In *2018 IEEE/RSJ International Conference on Intelligent Robots and Systems (IROS)*, pages 6980–6985, 2018.
- [46] Bradley T. Holschuh, Dava J. Newman, Giacomo Gatto, and Luca Levri. Wearable, self-locking shape memory alloy (sma) actuator cartridge, November 5 2015. US Patent 10828221.
- [47] John A. Bakker and David C. Boyer. Buckle, May 01 1978. US Patent 4171555.
- [48] Hill Claude. Chain-and-sprocket drives, September 14 1960. US Patent 3029654.
- [49] Willard C Kress. Ratchet wrench, January 25 1933. US Patent 1957462.
- [50] Tiffany A. Beers, Michael R. Friton, and Tinker L. Hatfield. Automatic lacing system, September 16 2022. US Patent 20230014734.
- [51] Neil Sclater. *Mechanisms and mechanical devices sourcebook*. McGraw-Hill, New York, 5th ed.. edition, 2011.

- [52] Michele Cazzaro and Andrea Merello. Rope ascender device and method for use thereof, June 1 2010. US Patent 9415244.
- [53] John A. Lowry III. Dual directional cam cleat, August 09 1985. US Patent 4660493A.
- [54] Fred Volkwein. Cam cleat, August 11 2014. US Patent 20150040814.
- [55] Julien Moine, Alain Maurice, and Benoît Vuillermoz. Rope ascender provided with a cam having an improved spring, February 24 2016. European Patent 3064253.
- [56] Robert J. Krisel. In-line cable tie with fixed and hinged locking mechanism, February 06 2007. US Patent 7730592.
- [57] Megan Clarke, Lucy Dunne, and Brad Holschuh. Self-adjusting wearables: variable control through a shape-memory latching mechanism. In *Proceedings of the 2016 ACM International Joint Conference on pervasive and ubiquitous computing*, UbiComp '16, pages 452–457. ACM, 2016.
- [58] Clay Hansen, Colin Erickson, Natas Seekaew, and Justin Barry. Latching mechanism for active compression garments, 2019.
- [59] Brian Kane. Compatibility of toothed ascenders with arborist climbing ropes. *Arboriculture and Urban Forestry*, 37:180–185, 07 2011.
- [60] Andrzej T. Baranski, Serhan O. Isikman, Tyler S. Bushnell, Steven J. MARTI-SAUSKAS, and David I. Nazzaro. Dynamic fit adjustment for wearable electronic devices, November 20 2018. US Patent 10398200B2.
- [61] F. Gemperle, C. Kasabach, J. Stivoric, M. Bauer, and R. Martin. Design for wearability. In *Digest of Papers. Second International Symposium on Wearable Computers (Cat. No.98EX215)*, pages 116–122. IEEE, 1998.
- [62] J. Walter Lee, Alireza Golgouneh, and Lucy Dunne. Comparative assessment of wearable surface emg electrode configurations for biomechanical applications. 49th International Conference on Environmental Systems, 2019.

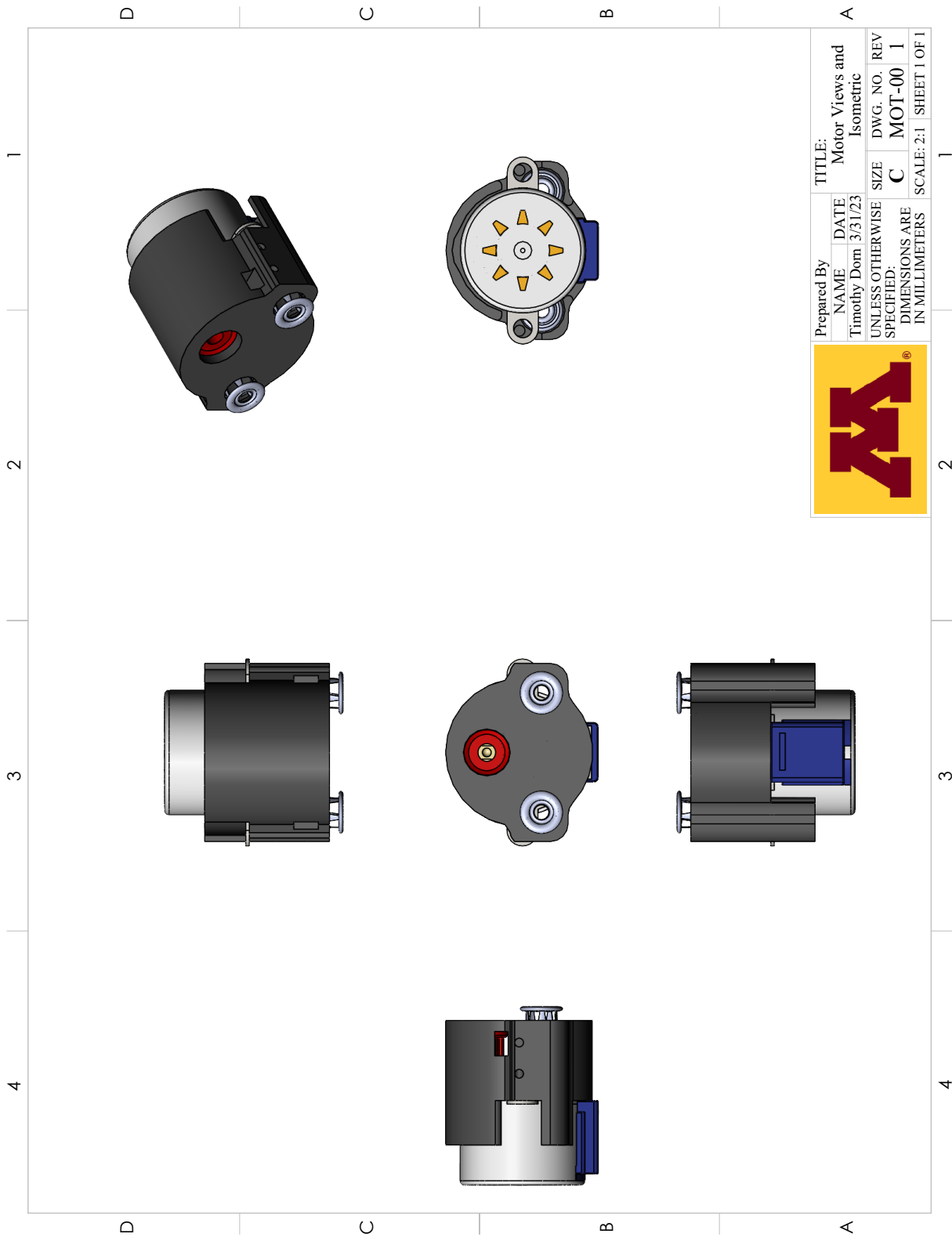
- [63] Artem Dementyev, Tomás Vega Gálvez, and Alex Olwal. Sensorsnaps: Integrating wireless sensor nodes into fabric snap fasteners for textile interfaces. In *Proceedings of the 32nd Annual ACM Symposium on User Interface Software and Technology*, UIST '19, page 17–28, New York, NY, USA, 2019. Association for Computing Machinery.
- [64] Giancarlo Valentin, Joelle Alcaidinho, and Melody Moore Jackson. The challenges of wearable computing for working dogs. UbiComp/ISWC'15 Adjunct, page 1279–1284, New York, NY, USA, 2015. Association for Computing Machinery.
- [65] Tmb electromagnetic brake (torque range: 4 147ft-lbs / 6 200nm), 2021.
- [66] Lisa Eitel. Miniature brakes: Examples of where electromagnetic spring-applied versions excel, May 2020.
- [67] Aksotronik. *Stepper motor 28BYJ-48 12V Datasheet*, 2023.
- [68] Energizer - Western European Region. *Industrial (6LR61) Product Datasheet*, 2023.
- [69] Steven B Heymsfield, Allison Martin-Nguyen, Tung M Fong, Dympna Gallagher, and Angelo Pietrobelli. Body circumferences: clinical implications emerging from a new geometric model. *Nutrition & metabolism*, 5(1):24–24, 2008.
- [70] Antonis Polymeris, Peter D. Papapetrou, and Georgios Katsoulis. An average body circumference can be a substitute for body mass index in women. *Advances in medicine*, 2014:592642–6, 2014.
- [71] Paul K. Whelton, Robert M. Carey, Wilbert S. Aronow, Donald E. Casey, Karen J. Collins, Cheryl Dennison Himmelfarb, Sondra M. DePalma, Samuel Gidding, Kenneth A. Jamerson, Daniel W. Jones, Eric J. MacLaughlin, Paul Muntner, Bruce Ovbiagele, Sidney C. Smith, Crystal C. Spencer, Randall S. Stafford, Sandra J. Taler, Randal J. Thomas, Kim A. Williams, Jeff D. Williamson, and Jackson T. Wright. 2017 acc/aha/aapa/abc/acpm/ags/apha/ash/aspc/nma/pcna guideline for the prevention, detection, evaluation, and management of high blood pressure in adults. *Journal of the American College of Cardiology*, 71(19):e127–e248, 2018, <https://www.jacc.org/doi/pdf/10.1016/j.jacc.2017.11.006>.

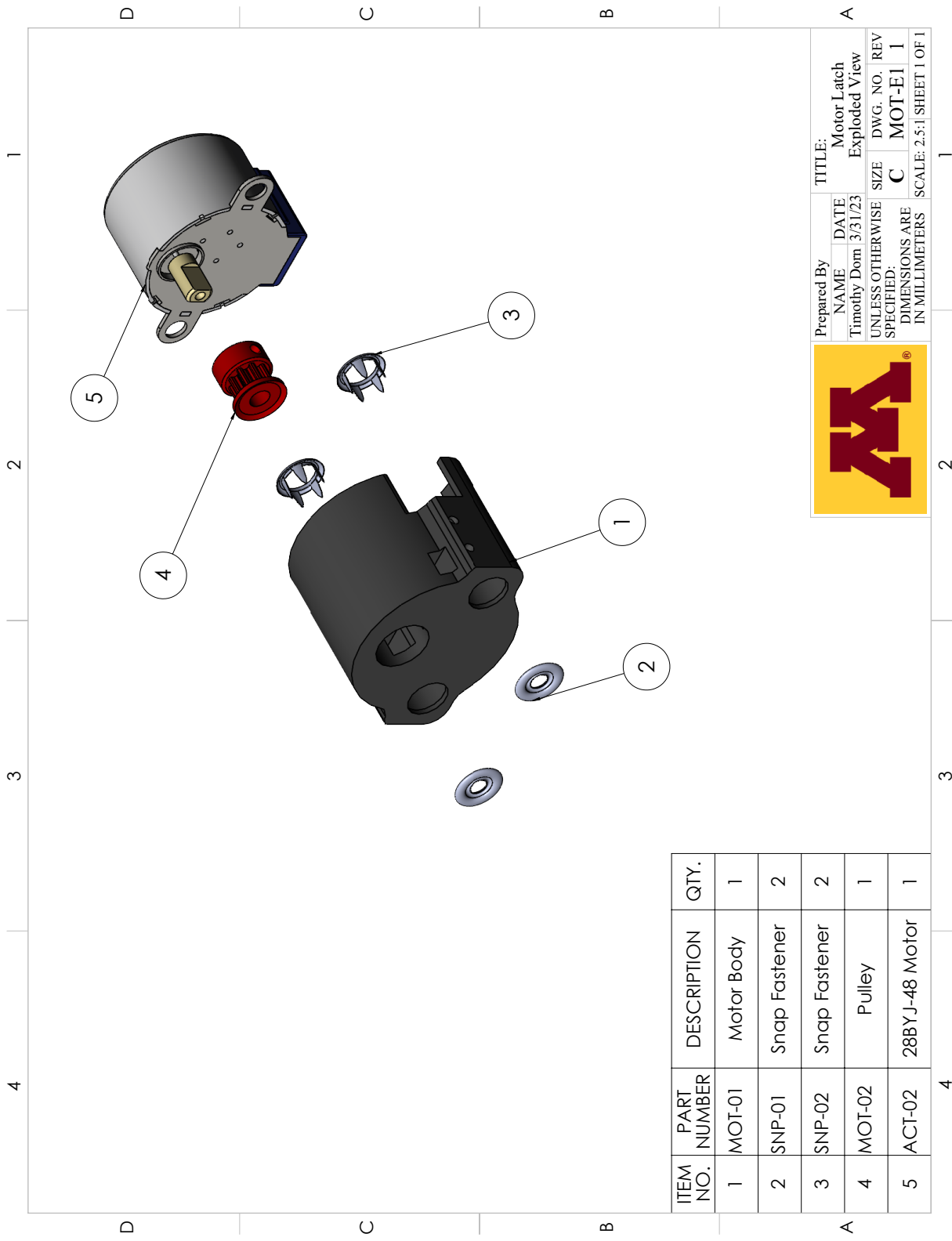
- [72] Shawn Khan, Adam Mosa, Adam Clayton, and Steven McCabe. Hand and wrist injuries associated with application of physical restraints: A systematic review. *Hand (New York, N.Y.)*, pages 155894472211055–15589447221105548, 2022.

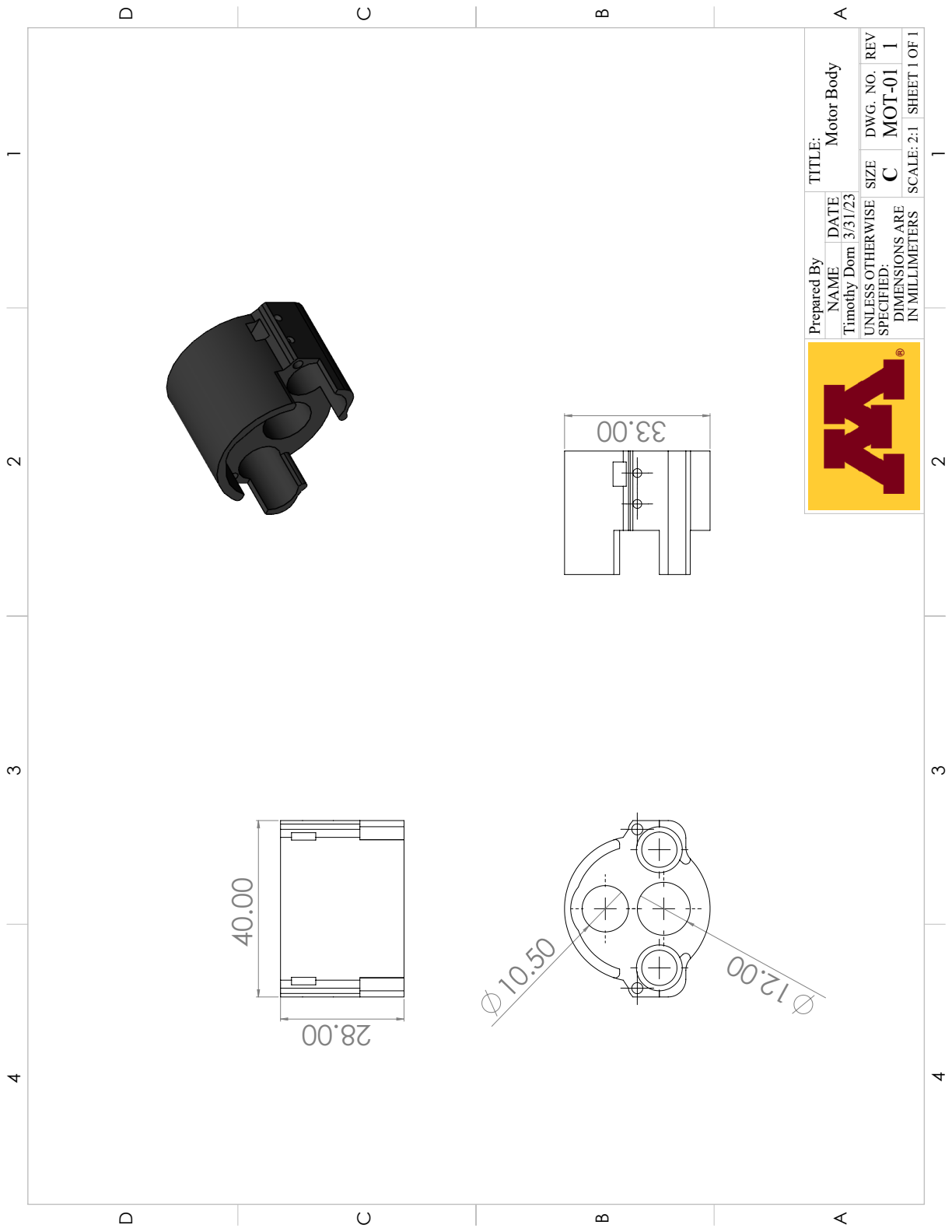
Appendix A

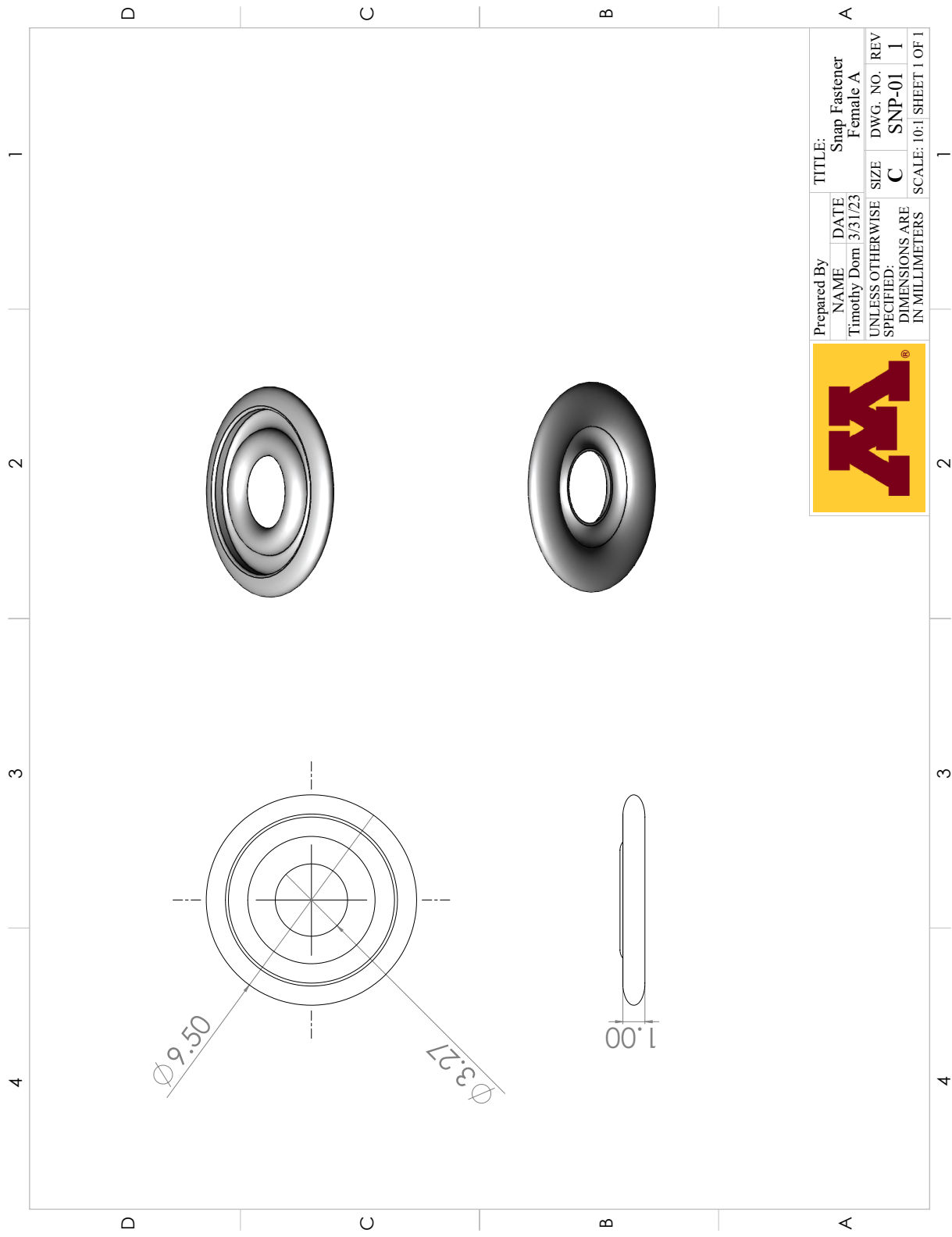
Motor Latch Design Schematics

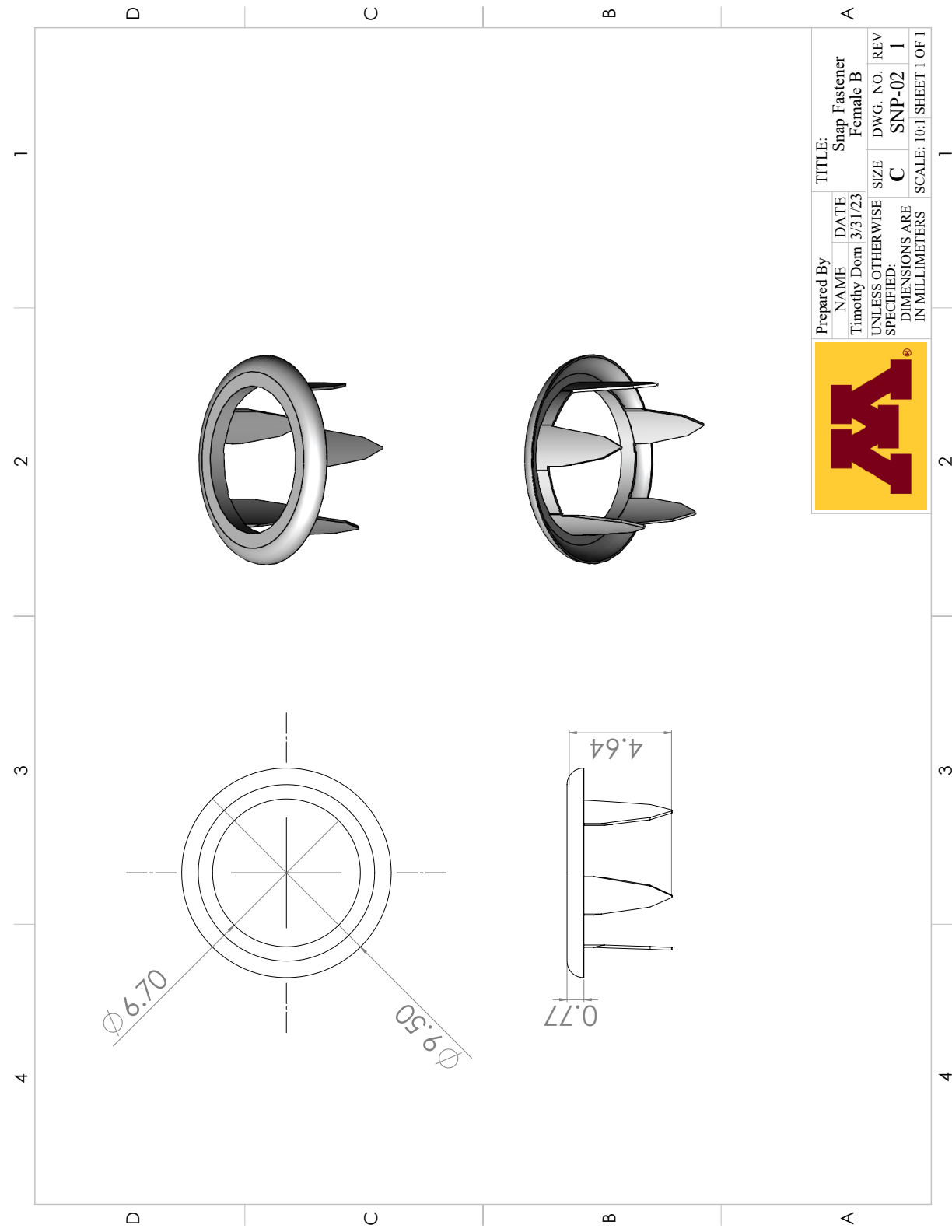
Schematics and drawings for the motor latch design are shown below.

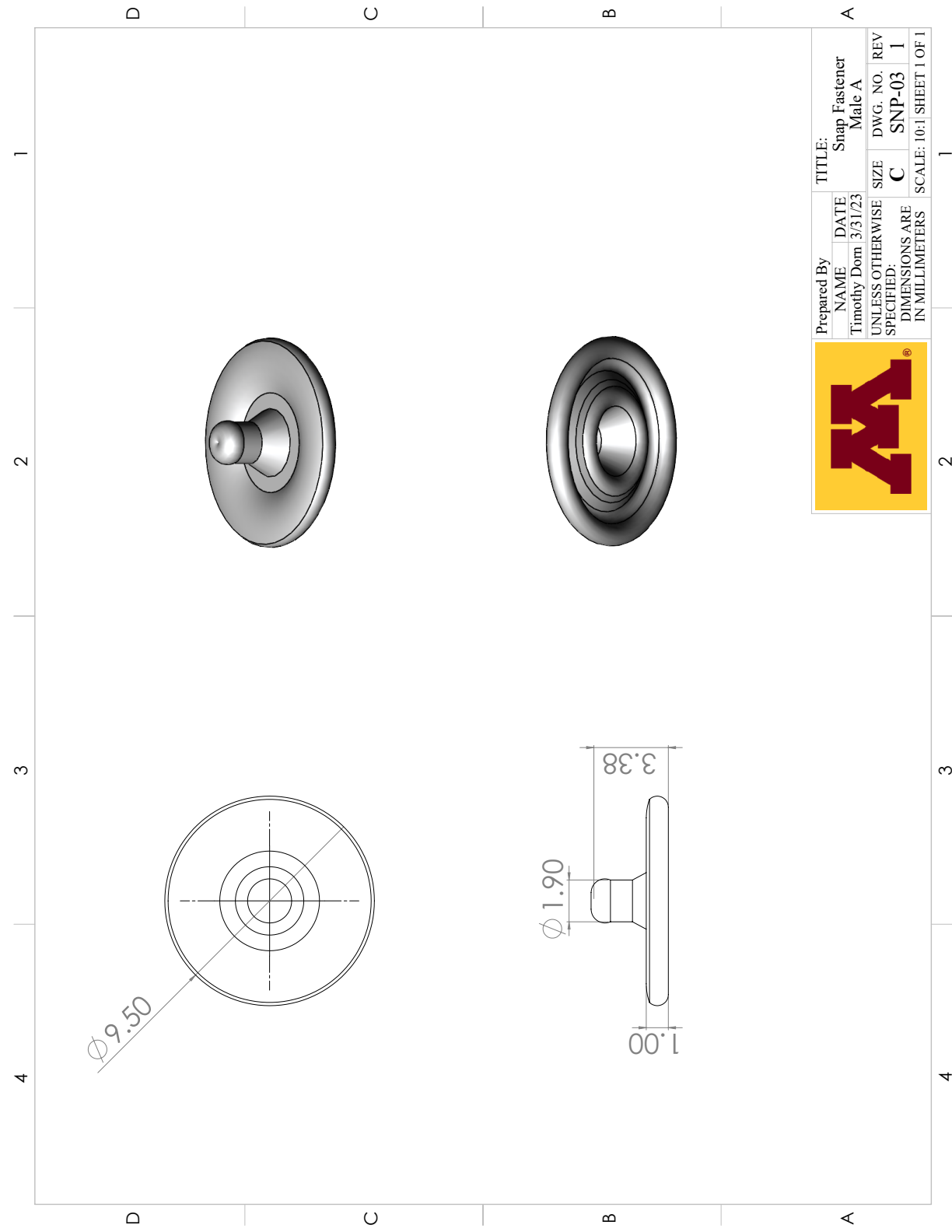


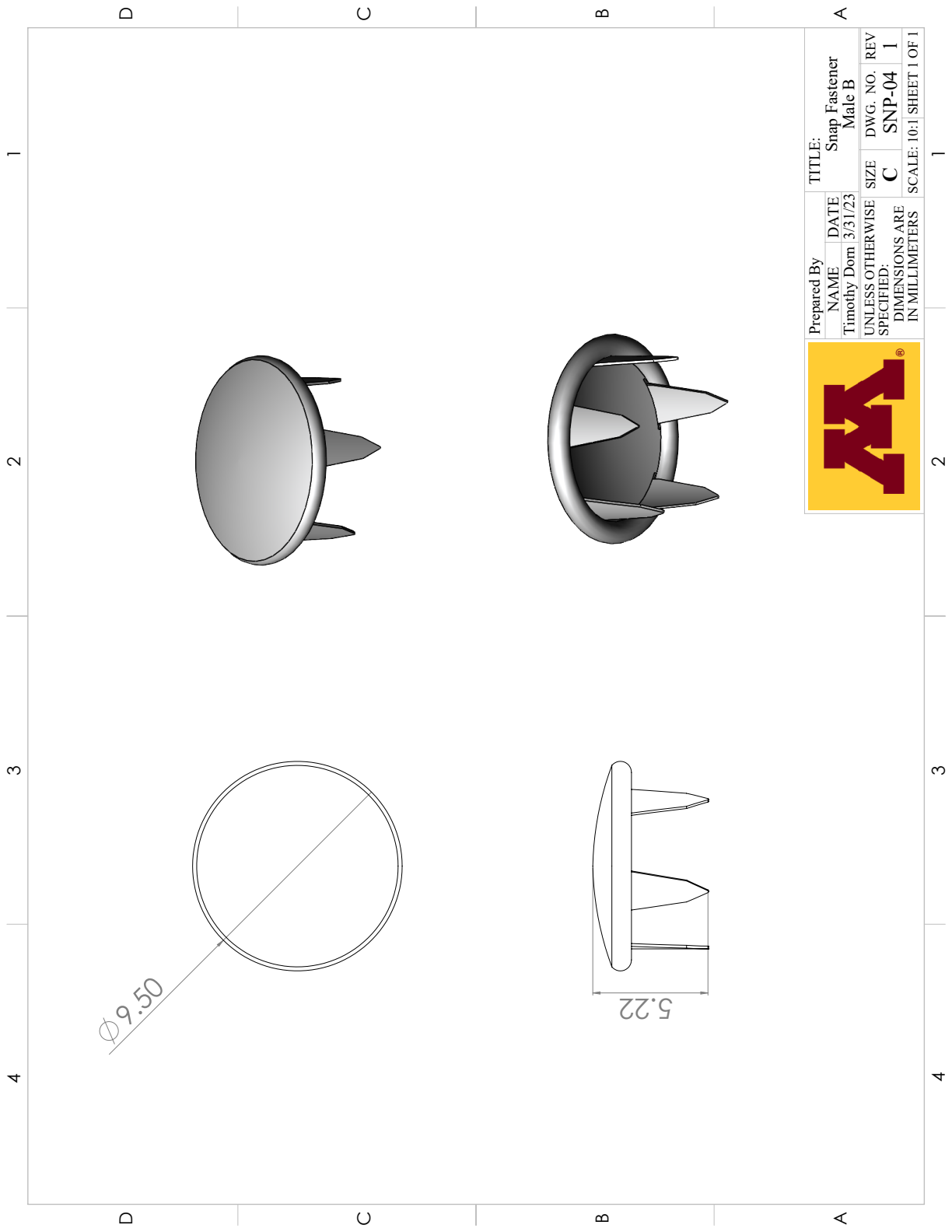


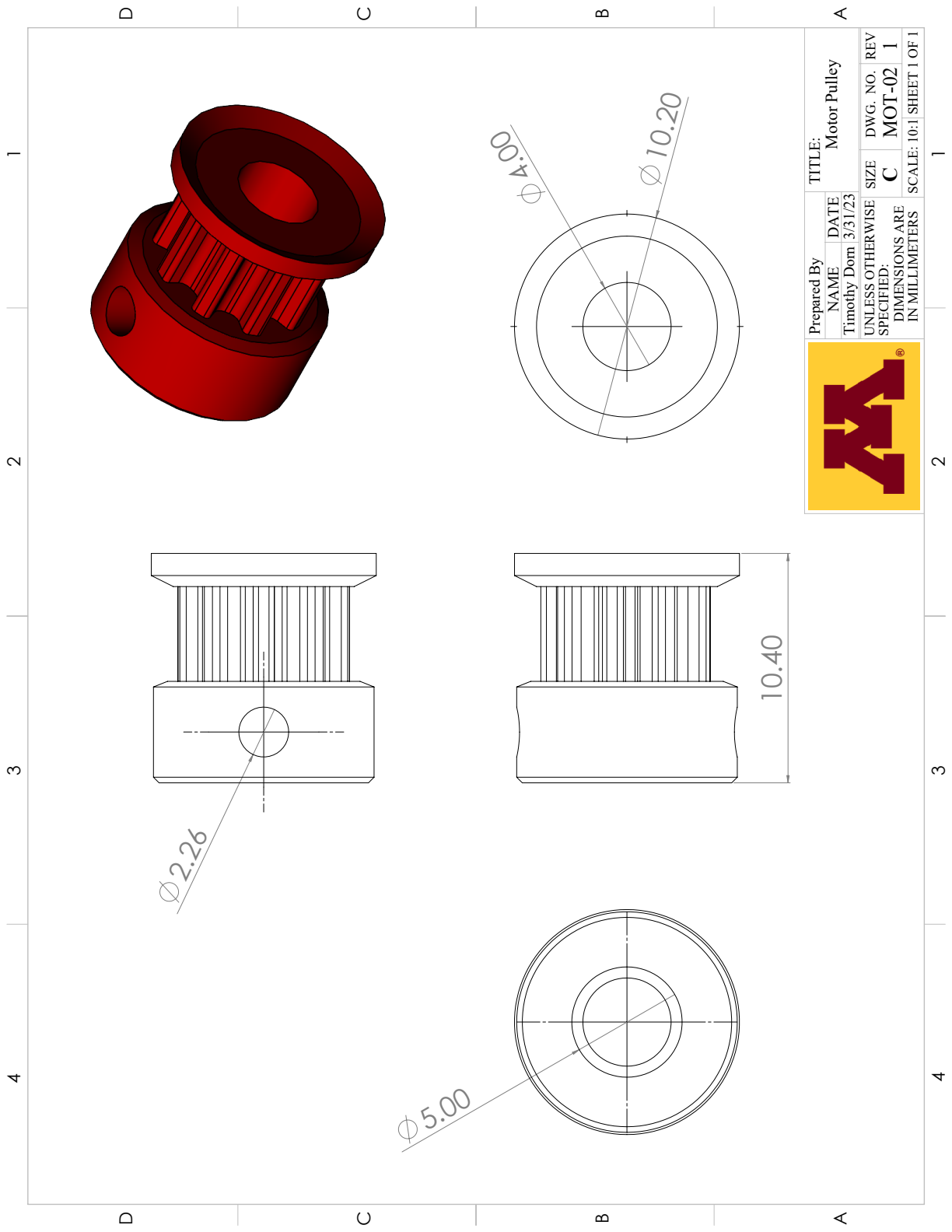


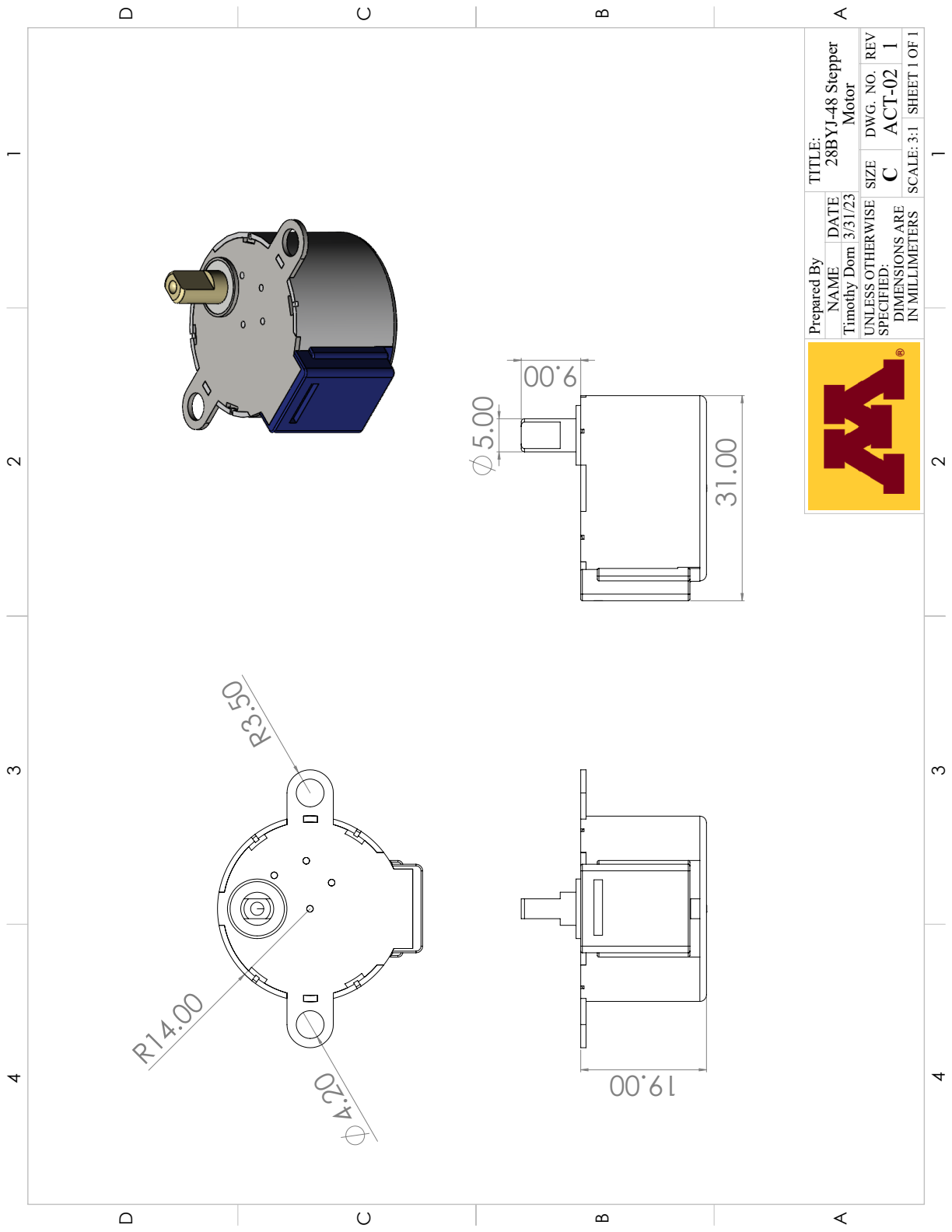








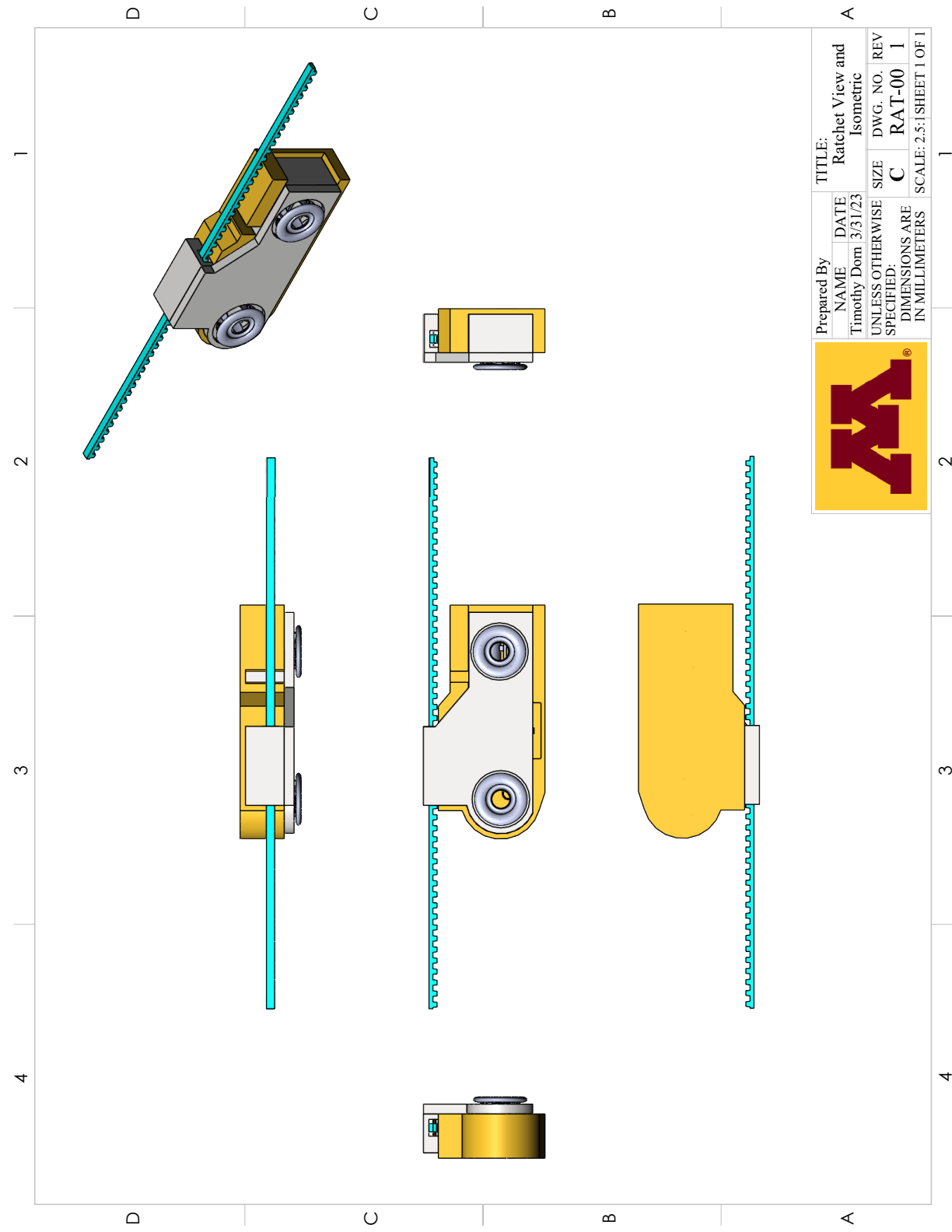


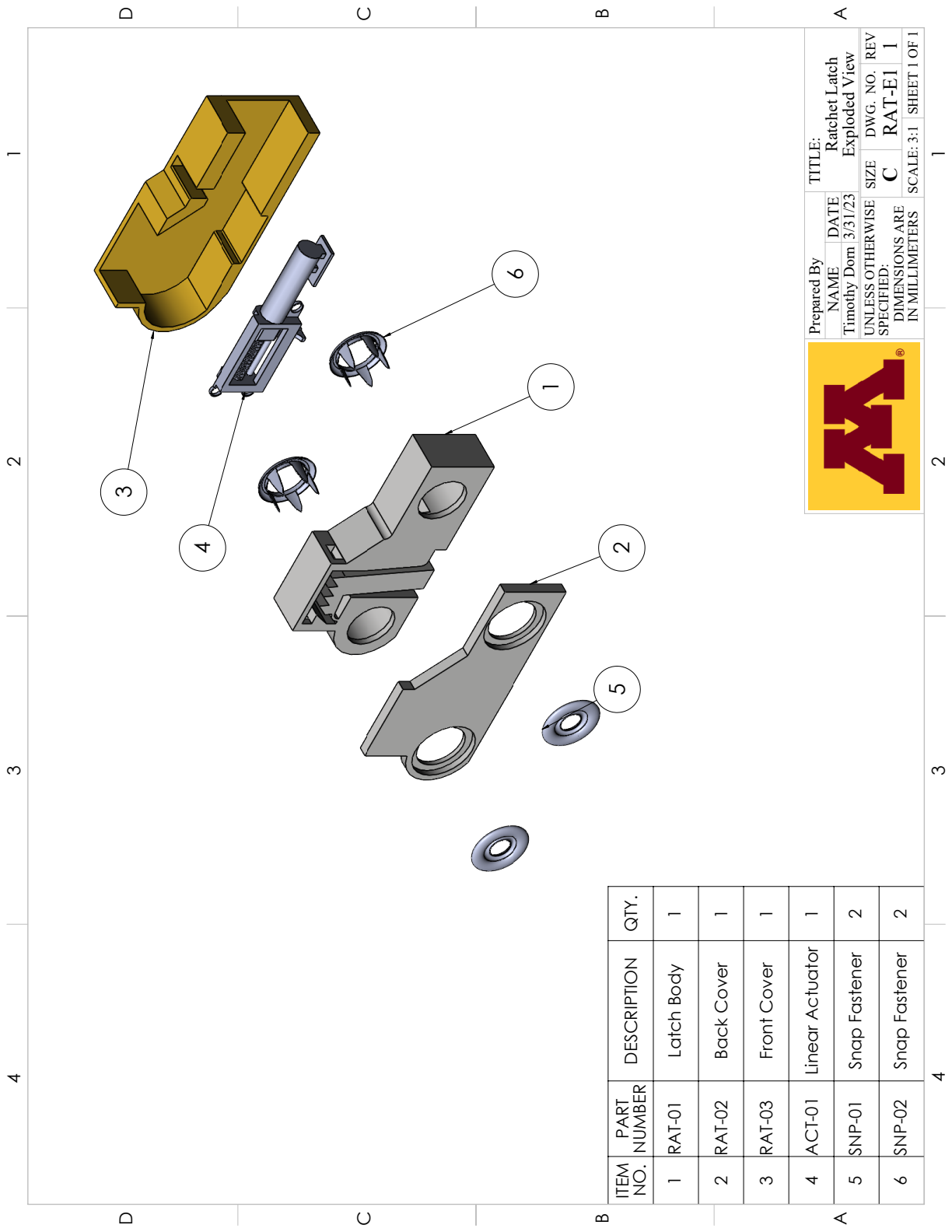


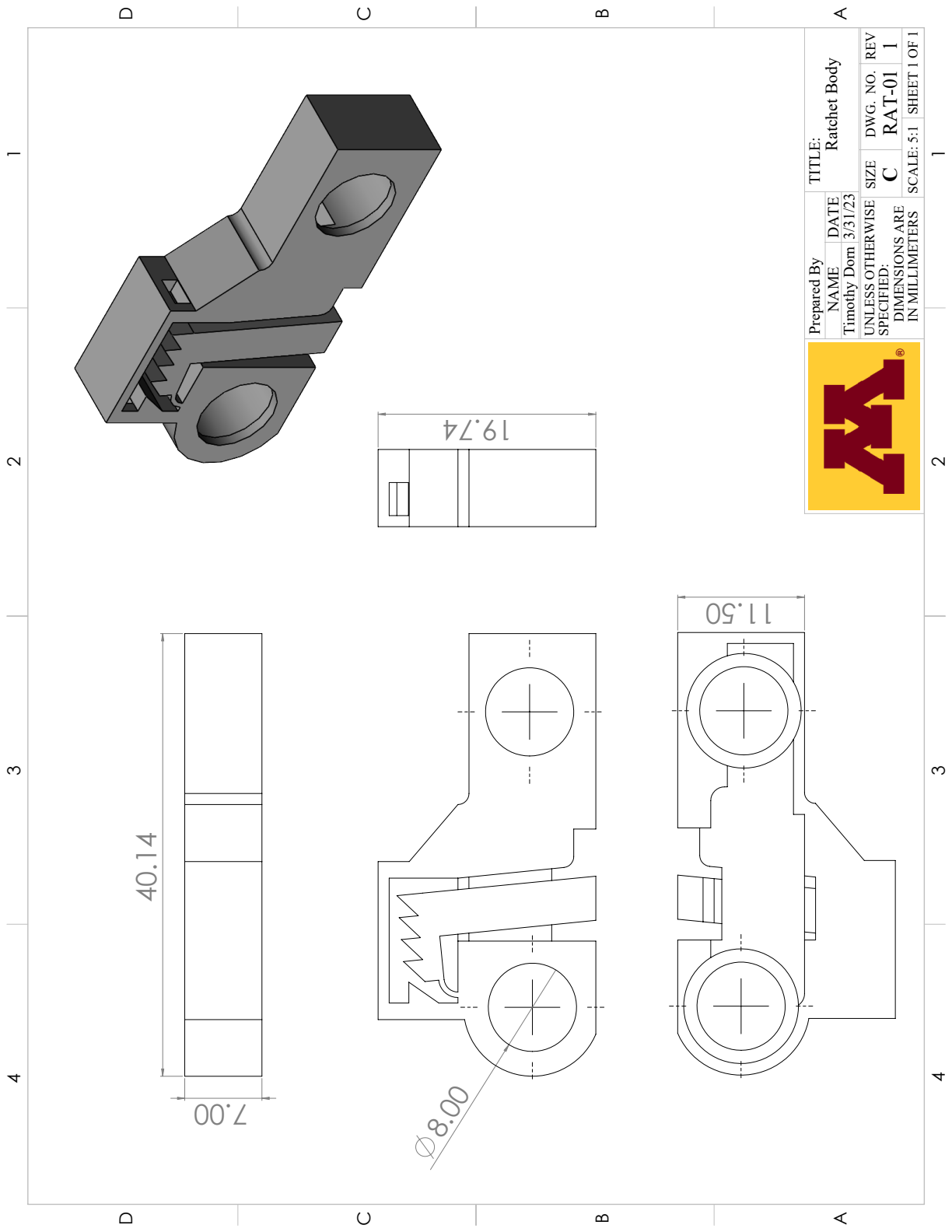
Appendix B

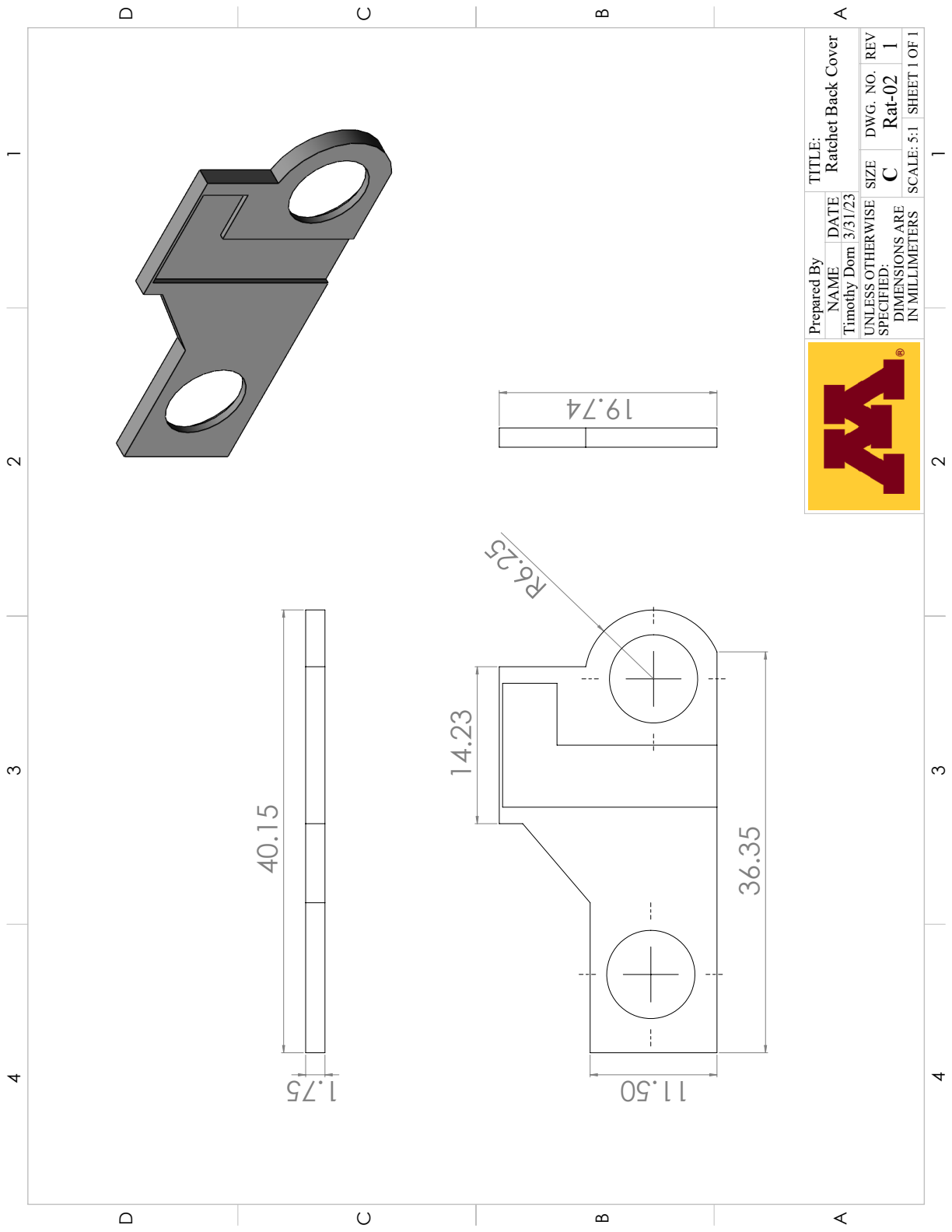
Ratchet Latch Design Schematics

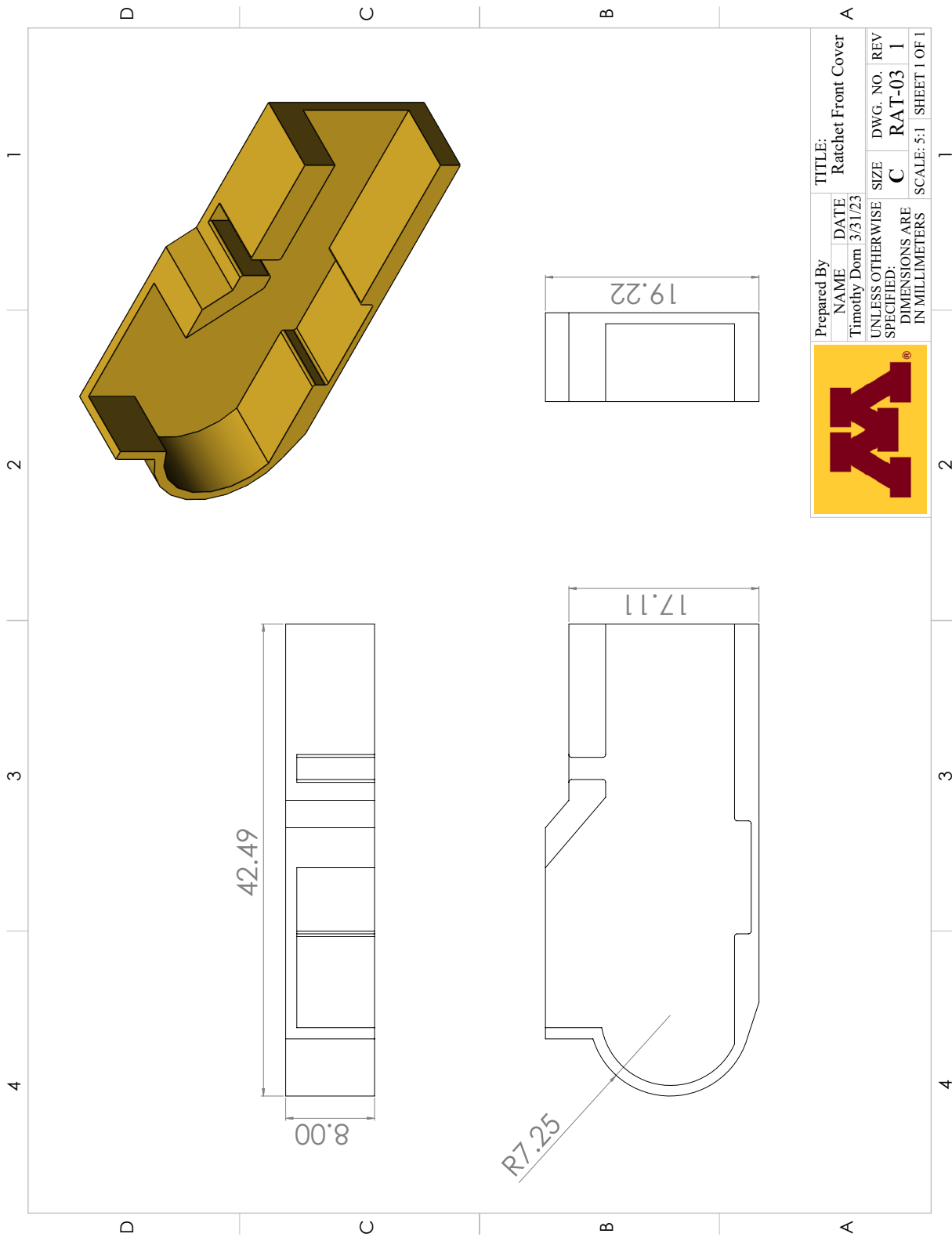
Schematics and drawings for the ratchet latch design are shown below.

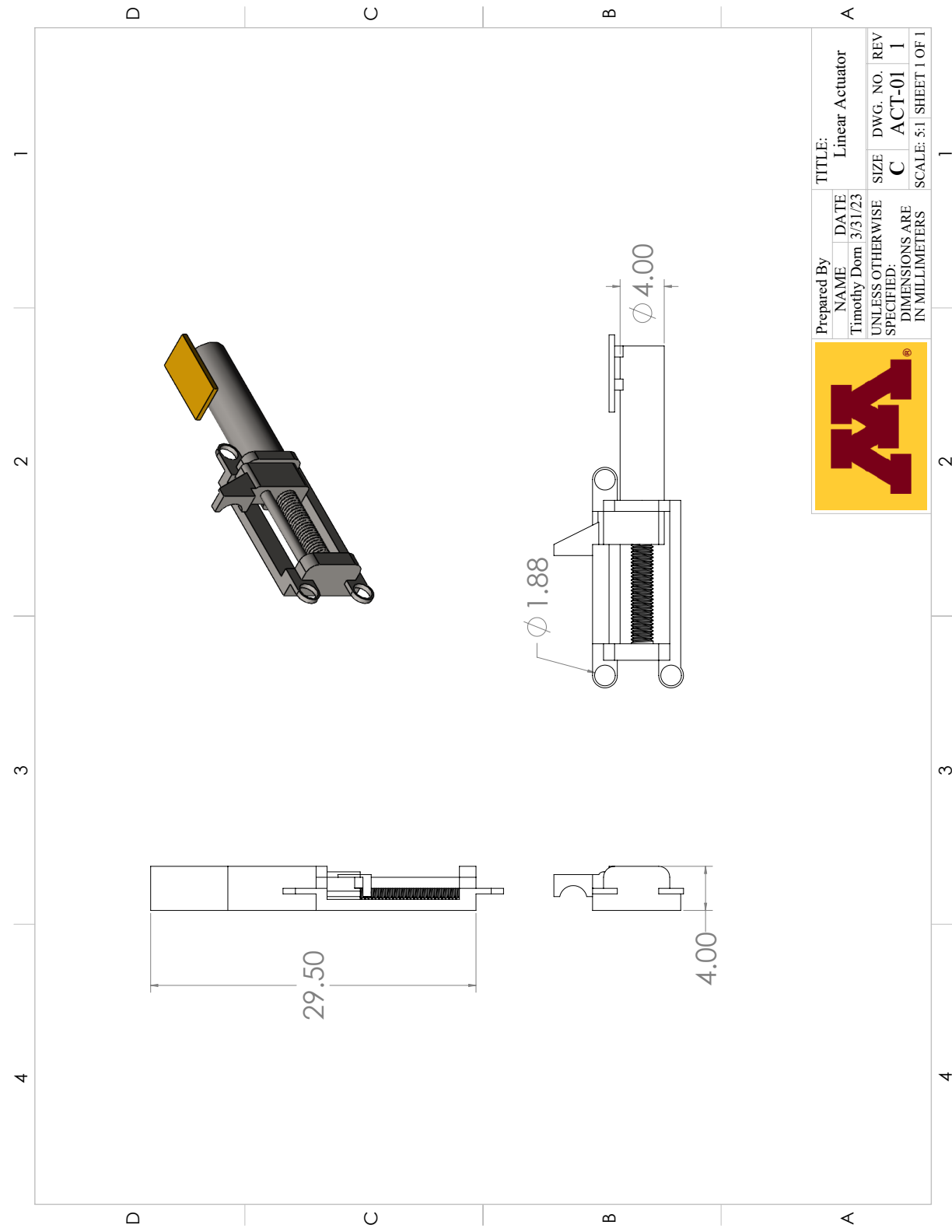












Appendix C

Cam Latch Design Schematics

Schematics and drawings for the cam latch design are shown below.

